Design of a stiff suction grasper for Minimally Invasive Surgery

An explorative design study by

Lars van Loo

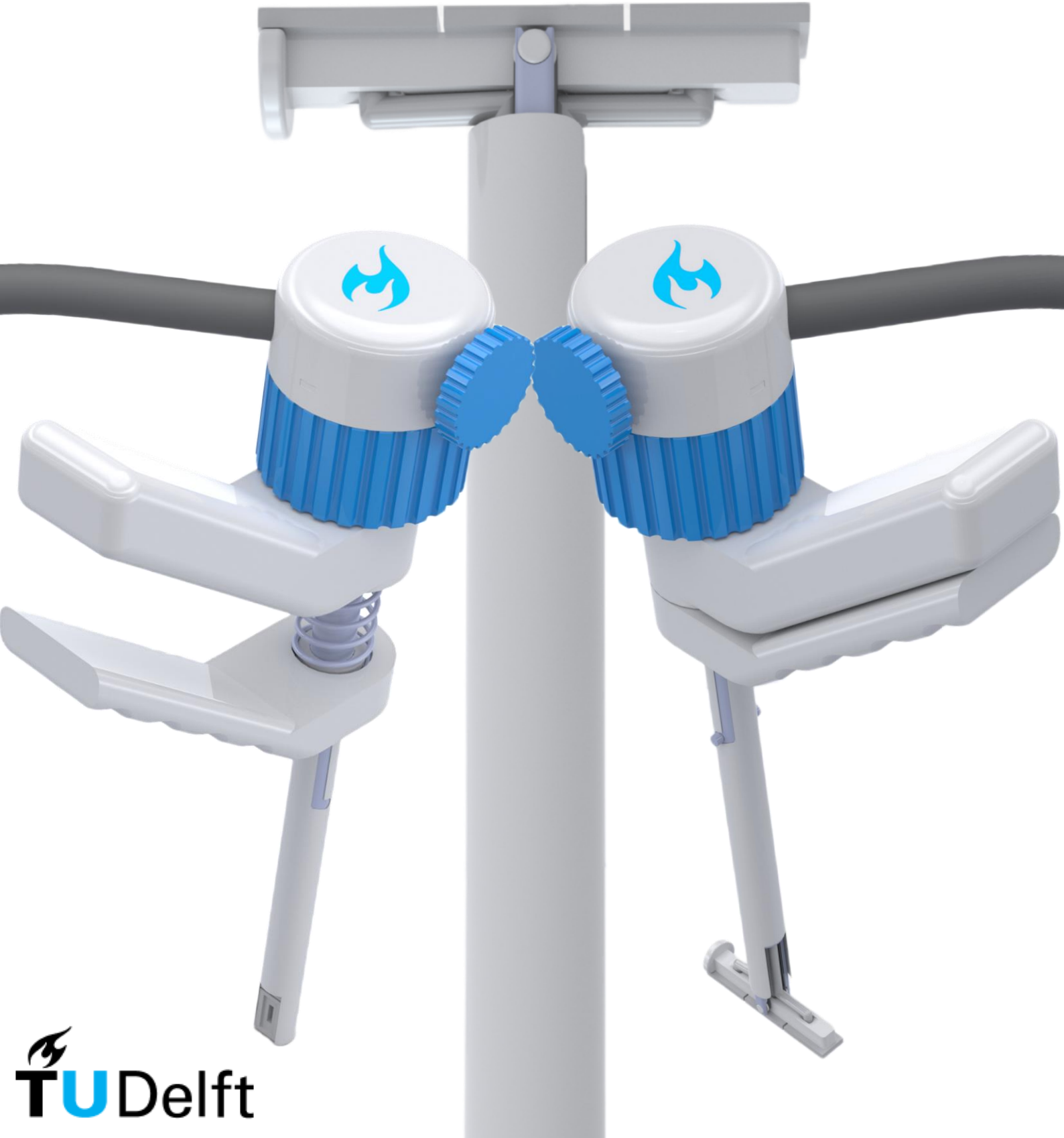

TU Delft

Design of a stiff suction grasper for Minimally Invasive Surgery

An explorative design study

Lars van Loo
Student number: 4970195

Thesis supervisors:
Prof. Dr. Ir. P. Breedveld
Dr. Ir. A. Sakes
Ir. V. Kortman

Thesis committee:
Prof. Dr. Ir. P. Breedveld
Dr. Ir. Aimée Sakes
Dr. J. Jovanova
Ir. V. Kortman

To obtain the degree of

Master of Science
in Biomedical Engineering
At the Technical University of Delft

Faculty of Mechanical, Maritime and Materials Engineering
Delft University of Technology
The Netherlands
Date of presentation: January 25, 2023

Contents

Design of a stiff suction grasper for Minimally Invasive Surgery - An explorative design study

Lars van Loo

Abstract

During Minimally Invasive Surgery human tissue typically is grasped with a grasper relying on clamping forces. Because human tissue is slippery and the surgeon lacks haptic feedback grasping becomes challenging, resulting in excessive peak forces or tissue loss. To overcome these challenges, a suction-based grasper is proposed. Earlier studies designed a suction grasper using a flexible suction surface that was able to expand its suction surface. This however resulted in leakage and tissue loss due to inward slip and air leaking into the suction chamber. For that reason, the design in this thesis consists of a solid suction surface that can fit through a ⌀10 mm trocar opening and can expand its suction surface while inside the patient's body. The solid suction surface can be rotated using two cables looped and tensioned around two axes. Because a solid suction surface is not able to adapt its shape to the surface of the grasped tissue, multiple suction chambers attached to multiple silicone suction tips are used to prevent tissue loss when leakage occurs. Experimental validation showed a significantly higher attachment force using 3 or 4 suction chambers than only 1. However, suction surface performance shows a maximum attachment force of 3,12± 0,27N when using 4 suction tips on a ⌀200 mm curved substrate with 5 kPa stiffness. Premature detachment on the outer suction tips in combination with tissue covering the suction tube outlet showed to be one of the main reasons for not achieving the required 5N suction force. This proposed design provides a base for a stiff suction surface grasper using multiple suction chambers for MIS.

Keywords: Grasper, MIS, Suction, Human tissue, Vacuum

1. Introduction

1.1. Background

In open surgery, large incisions are made to gain access to the patient's body using surgical instruments. These incisions result in a large quantity of blood loss, tissue damage and a long recovery time for the patient. To shorten this recovery time and minimize damage or blood loss, a smaller incision is used. Procedures like laparoscopy, endoscopy or arthroscopy, that use these smaller or even no incisions have an umbrella term which is 'Minimally Invasive Surgery' (MIS). These incisions are typically 5 or 10 millimetres in length and are created at specific locations to reach the targeted tissue efficiently. After this, a trocar is placed through the incision. A trocar is a hollow tube that functions as a portal where laparoscopic instruments can enter the body [1]. With laparoscopy the surgeon enters the abdomen with an instrument with a long shaft To grasp, typically a forceps is used (Figure 1). This

Figure 1: A common laparoscopic grasper which can grasp human tissue.

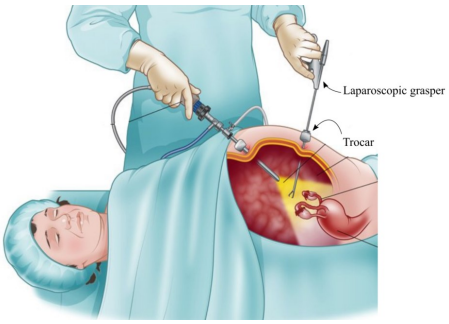

Figure 2: Schematic overview of the use of a trocar in combination with laparoscopic instruments. The trocar is anchored through the abdomen. Through the trocar, laparoscopic devices can be inserted into the body.

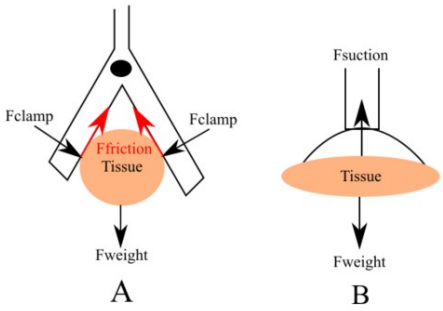

Figure 3: Clamping tissue with a laparoscopic grasper versus grasping tissue with a suction-based grasper. A: The laparoscopic grasper exerts a clamping force onto the grasped tissue. Since tissue is slippery, occasionally not enough friction can be generated in order to grasp the tissue sufficiently. B: When suction is used, these clamping forces in combination with friction are not required.

enables the surgeon to perform manipulations using instruments that are controlled from outside the patient's body (Figure 2). To overcome these issues, a grasper is required that does not rely on clamping forces. Studies show great potential for the use of vacuum grasping during surgery [2] [3]. The compressing clamping forces are replaced by a single suction force which can be controlled by vacuum pressure. This makes the use of this instrument accessible for less experienced surgeons since the suction force will be easier to regulate compared to clamping forces which results in less tissue damage. Using suction forces allow positioning or manipulation of larger organs where a conventional gripper is not able to clamp larger-sized materials between the gripping parts.

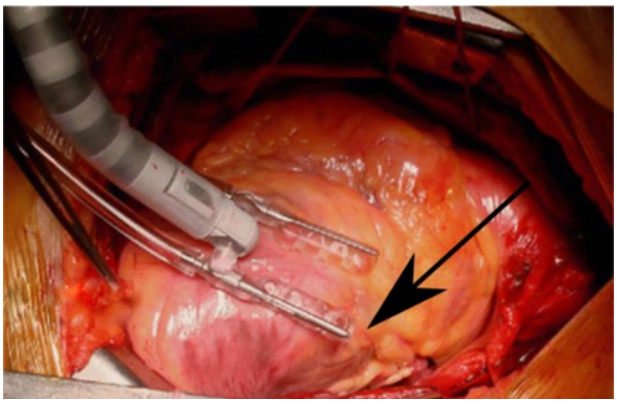

Figure 4: Octopus^{TM} leakage at one of the suction tips. This results in leakage in the right paddle.

1.2. State of the Art

A number of suction-based graspers designed for its use during surgery on human tissue are currently on the market (Appendix A). One of the most used stabilizers on the current market is the Octopus^{TM} Heart Stabilizer. This instrument stabilizes the heart during an open-heart coronary bypass surgery (Figure 4) [4]. The instrument has two suction surfaces (the two arms) each with four suction tips (the suction outlets on each arm) connected to one vacuum source. However, the instrument is vulnerable to leakage at one of the suction tips [5]. This is due to the fact that the suction surfaces do not fully deform to the heart tissue. When this occurs, vacuum pressure in the suction surface will be lost since air molecules are able to stabilize the vacuum pressure that is used. This is called leakage [6] and results in tissue loss or continuous sucking of the vacuum source. A detailed elaboration on vacuum pressure and leakage can be found in Appendix B. None of these commercial suction graspers on the current market are available for MIS. In literature, suction graspers designed for MIS can be found (Appendix C). However, these designs show leakage between tissue and suction tips due to insufficient sealing.

Vonck et al. [3], developed a suction-based grasper for the manipulation of bowel tissue during laparoscopy (Figure 5). This grasper has a diameter of 10 mm and a suction hole with a diameter of 8 mm at the most distal end. Because of this, the instrument can be inserted

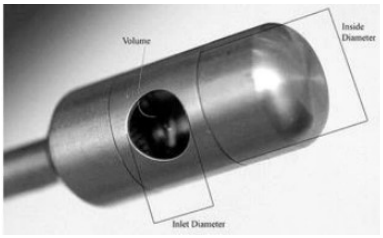

Figure 5: Distal end of the suction grasper designed by Vonck [3]. This grasper has a suction opening at the distal side of the device to grasp bowel tissue.

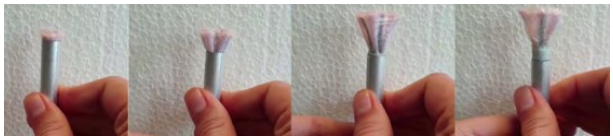

Figure 6: The unfolding suction tip of Kortman [7]. It unfolds when it slides out of the trocar into the patient's body. This is due to pre-bend structures inside the walls of the suction tip. It is a fully flexible suction tip made from silicon

through a trocar with an inner diameter of 10 mm. A negative pressure (in this thesis also called vacuum pressure) of 60kPa is manually actuated by actuating a piston on the other proximal end of the grasper. The suction tip of Vonck is theoretically able to generate a suction force of 4N. However, Vonck states that 5N is a minimum required suction force to be able to grasp human tissue sufficiently [2]. So this requirement was not fulfilled. Furthermore, Vonck [3] tested if suction grasping negatively impacts the human tissue. These tests were performed on bowel tissue. A vacuum pressure with a range between 50 and 97 kPa was used to grasp the tissue. From these tests, Vonck concluded that suction grasping is safe and promising for tissue manipulation during surgery.

Hereafter, Kortman [7] designed a MIS suction grasper with a larger flexible suction surface in order to increase the suction force (Figure 6). The suction surface can be insterted through a trocar with a diameter of 10 mm [8] but is able to expand its suction surface to a diameter of 20 mm after entering the abdomen. Theoretically, this should be large enough to generate the required 5N suction force [9] [3]. However, experimental validation

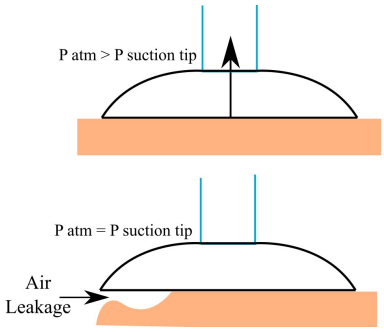

Figure 7: A schematic representation of leakage. In the upper figure, no leakage occurs. When air molecules get sucked away from the suction tip, the pressure in the suction tip will decrease and the atmospheric pressure will be higher. This results in a suction force onto the tissue. When leakage occurs at a suction tip, both pressures equalize and the suction force will be lost.

showed a lower suction force.

1.3. Problem Analysis

As stated in Section 1.2, the flexible suction surface of Kortman is not able to generate the required suction force of 5N. The reason for that is because the suction surface is prone to leakage which results in a maximum suction force of 3.3N. Also, when air leaks into the sealed space of the suction surface, tissue loss occurs inevitably. Leakage is still one of the most common reasons for tissue loss

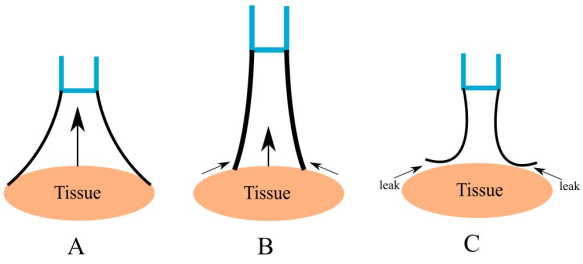

Figure 8: Depiction of inward slip of a flexible suction tip. A: The suction tip is flexible and able to form to the shape of the tissue. B: When a force pulls at the suction tip, the contact surface slips inwards. This causes a decrease of the effective suction area which decreases the suction force. C: Adding to this, the suction tip deforms due to the negative pressure and the lack of stiffness. It deforms inwards and causes leakage.

using suction-based graspers [3] [7] [10] [11]. Leakage occurs when the suction tip and the tissue do not seal completely and air molecules are able to move into the space that should be sealed, which is the suction chamber (Figure 4 and Figure 7). Because of this, the negative pressure of the vacuum equalizes atmospheric pressure. This means that no vacuum and thus no suction force can be generated. The main cause of leakage in flexible suction tips is that the suction surface of the tip slips inwards when negative pressure is built inside (Figure 8B) [12] [13]. Adding to this, a fully flexible suction tip deforms when pushing or pulling tissue. This causes deformations in the sealing which will lead to leakage (Figure 8C) [14]. To summarize, a number of challenges can be encountered while designing a suction-based grasper for MIS. When increasing the suction surface in order to generate a sufficient suction force using a flexible tip, leakage due to suction surface deformations seems one of the most occurring problems. Therefore, this study focuses on the use of a stiff suction surface instead of a fully flexible tip to counter the problems mentioned above.

1.4. Goal of the study

Based on the challenges of current suction-based graspers, the goal of this research is defined as follows:

Goal: *Design of a suction grasper for MIS that is able to enlarge its stiff suction surface and minimize tissue loss due to leakage.*

For a suction grasper, it is desirable that leakage does not occur. However, it is unlikely to fully prevent leakage each time the grasper is used. Because of this, the focus in this study is to minimize tissue loss due to leakage. The paper is structured as follows. At first, the goal of this research is defined by the requirements. The design requirements follow from the problem analysis and design challenges. Subsequently, the design phase is structured according to the two main functions of the instrument. Expanding the suction surface while inside the patient's body and minimizing the consequence of leakage. From this, a final design follows from which the prototype will validate its features by an experimental set-up. Subsequently, the results, the design- and experiment limitations and recommendations are discussed. Lastly, the report finalizes with a conclusion.

2. Requirements

2.1. Design challenges

- **Effective suction area:**
  As mentoined in the Section 1.3, the the suction area must be able to fit through a trocar with a diameter of 10 mm (**R1**). According to Vonck [2], 5N is a safe suction force to grasp and manipulate human tissue. This is high enough to lift the tissue, but does not damage the surface of the tissue. With this suction force, the same tissue manipulations can be performed as with a conventional grasper [15]. In combination with this suction force, a vacuum pressure of 50 kPa is used. The use of a vacuum pressure of 50 kPa on human tissue is broadly tested on safety [5] [4] [16]. When a suction surface of ⌀10 mm is used with a negative pressure of 50 kPa, the corresponding suction force can be calculated using the equation that defines the force that is the result of a pressure difference (compared to atmospheric pres-

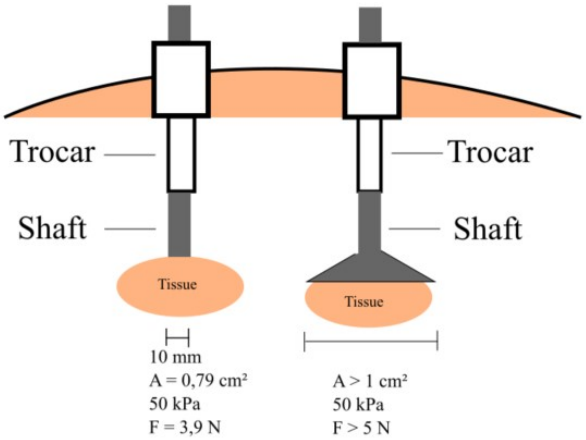

Figure 9: Once the suction grasper is inserted through a trocar with an inner diameter of 10 mm, the suction surface grasps tissue. Once the suction surface is not increased (left) not enough suction force can be generated to sufficiently grasp tissue. When the suction surface is increased to a suction surface of 1 cm^2, a suction force of 5N is reached.

sure) over a certain surface area (Equation 1):

$$F = \Delta p \cdot A \tag{1}$$

Where;

- F is the suction force normal to the surface [N]
- Δp is the pressure difference of the pressure of the sealed space compared to atmospheric pressure)[N/m^2]
- A is the contact surface area [m^2]

This results in a suction force of 3,9 N, which according to Vonck [2] is not high enough (Figure 9). This emphasizes the necessity to enlarge the suction surface while inside the patient's body to increase the suction force. According to Equation 1, a minimal suction area of 1 cm^2 is required as a minimal boundary to provide 5N suction force with 50 kPa vacuum pressure (Figure 9). Since these three values (the suction force, the vacuum pressure and the required suction surface) are linear dependent (Equation 1) these three are stated as one requirement (**R3**). As stated in the Problem Analysis (Section 1.3), the suction surface should be stiff. It is hypothesized that this prevents the problems encountered while using a flexible suction surface. The stiffness of the suction surface should be stiff enough to prevent the surface from bending while pulling and pushing tissue during surgery (**R4**).

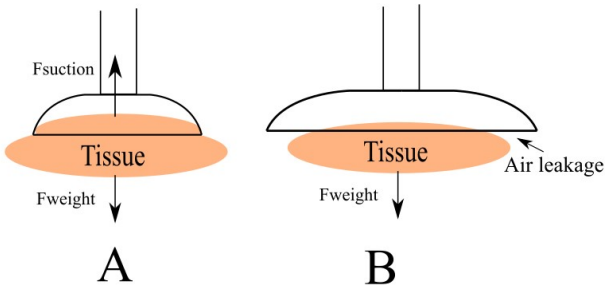

Figure 10: A: The tissue seals the suction tip correctly which results in a partial vacuum when air is sucked away from this sealed space. B: When the dimensions of the grasped tissue do not match the dimensions of the suction tip, a correct seal is not possible. This results in air leaking into the suction tip and no vacuum can be created.

- **Minimize consequence leakage:**
  However, by increasing the suction surface, the risks on leakage will only increase (Figure 10). This is also visible at the Octopus^{TM} (Figure 4). Since tissue curvature plays an important role in a correct sealing between tissue and suction tip [5] (Figure 10), it is hypothesized that leakage occurs most frequent at the most lateral parts of the suction tip. This can also be seen in the design of Kortman [7] and the Octopus^{TM} [5]. These instruments lose total vacuum pressure when leakage occurs. This emphasizes the necessity of a design that maintains its vacuum pressure even when leakage occurs (**R5**). Human tissue that can be grasped during MIS has a wide variety of dimensions and stiffness. During MIS, organs are targeted in the abdominal area. The stiffness from these organs range from 5 to 50 kPa [17]. The surface of the kidney ranges from 5 to 10 kPa while the intestines range from 20 to 50 kPa. (**R6**).

- **Minimizing tissue damage:**
  Earlier this section, the optimal values of Equation 1 are described (R1, R2, R3). These values are based on a trade off between performance and possible

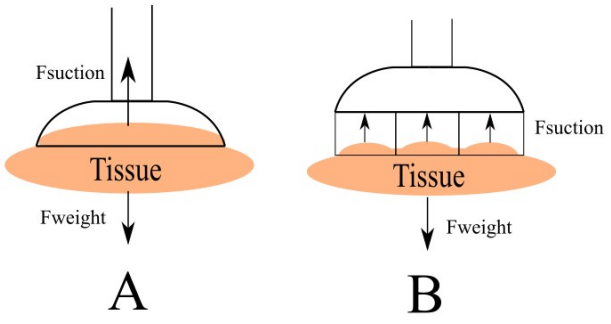

Figure 11: A: When tissue is grasped using suction, the surface of the tissue gets sucked into the suction tip which results in deformation of the tissue's surface. When high pressure is used, this causes high stress on the tissue surface which increases the chance on damage. B: If the suction tip consists of multiple contacts points across the surface of the grasped tissue, the suction force gets distributed over this surface which decreases the peak stress and thus deformation of the surface of the tissue.

tissue damage. However, tissue damage can further be prevented. When one large suction tip is used, the tissue is slightly getting sucked inwards (Figure 11 A). By splitting the surface area into multiple smaller suction areas (**R7**), the suction force is distributed over the surface area (Figure 11 B). This causes less stress in the tissue. The Octopus™ Heart Stabilizer uses multiple suction tips connected to one suction chamber to distribute the stress on the tissue. The Octopus is extensively studied on safety [18], which ensures this technique improves safety. Furthermore, the instrument should not leave any damage inside the patients body. During laparoscopy, the surgeon does not have a clear vision of the insertion of the instrument into the patients body. Occasionally, entry of the instrument causes vessel or organ damage [19]. For that reason, it is important that the instrument does not leave any damage while inside the patients body (**R7**). To prevent this, any sharp edges on the instrument must be prevented.

During laparoscopy, a pneumoperitoneum is created in this cavity [20]. This means that the abdomen are inflated with carbon-dioxide to create separation between organs and increase internal workspace for manipulation with surgical instruments. However, the compliance of the abdominal wall is limited due to its elasticity [21]. Ott [21] states that the amount of inflated carbon-dioxide and thus the pressure should be as low as possible to still accomplish the surgical task. Pressures larger than 12mmHg should be avoided since this is defined as intra-abdominal hypertension which could lead to tissue damage [22]. This results in patients with a smaller intra-abdominal volume offer a smaller workspace for the surgeon. For this reason, the mechanism that increases the suction surface and the dimensions of the suction surface should not be larger than necessary in order to complete the surgical task. Therefore, the mean dimensions of the conventional tissue grasper for MIS on the current market are kept as boundaries of the maximal dimensions of the new developed suction grasper. The mean length of the jaw of these graspers are 32 mm [23] and are able to open 45 degrees (Figure 12). Because of this, the span of the grasper inside the human body is 45 mm. For that reason, the suction surface has a maximum length of 45 mm (**R2**).

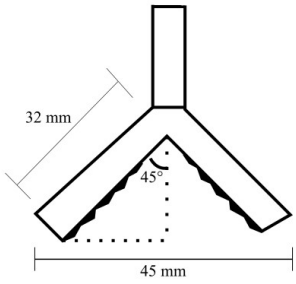

Figure 12: The depiction of the span width of a conventional laparoscopic grasper. The mean jaw length is 32 mm and the jaw can open in a 45 degree angle resulting in a total width of 45 mm.

- **Usability:** Surgery time of laparoscopy is on average shorter compared to open surgery [24], which is an advantage. For this reason, the instruments used for laparoscopy should not delay this process. Handling of the designed grasper should be as easy and as fast as possible. According to Supe [25], surgeons perform laparoscopic surgery using an instrument in each hand (Figure 2). For that reason, it is required that placing, controlling and holding is possible using one hand during surgery (**R9**).

2.2. Design requirements

Dimensions:

- **R1, Trocar dimension:** The surface area of the suction grasper should fit through a trocar with a diameter of 10 mm.
- **R2, Suction surface dimensions:** The span of the jaws of conventional tissue graspers on the current market are used which are able to open 45 degrees. This results in a span and thus a total length for the suction surface of 45 mm.

Performance:

- **R3, Suction generation:** the optimal suction force to manipulate human tissue is 5N [3]. Combining

this with a vacuum pressure of 50 kPa, this results in a required surface area of 1 cm^2.

- **R4, Suction surface stiffness:** The suction surface should be stiff enough to prevent bending while a force of 5N is applied.
- **R5, Maintaining vacuum pressure:** The grasper is designed to maintain total vacuum pressure, even when leakage occurs.
- **R6, Tissue stiffness:** The suction grasper is able to grasp tissue with a stiffness ranging from 5 to 50 kPa
- **R7, Force distribution:** The instrument consists of multiple contact surfaces that distribute the suction force over the grasped tissue. This will lead to less stress on the grasped tissue.
- **R8, Damage risk:** The suction grasper does not leave any damage whilst inside the patients body. Sharp edges or points must be prevented while designing the instrument.
- **R9, Handling:** The instrument should allow for placement, grasping and retracting using one hand.

3. Ideation

3.1. Design structuring

From the problem analysis and design challenges can be concluded that the design of this study has two main design directions. Firstly, a mechanism must be designed that is able to expand the stiff suction surface to a sufficient suction area of at least 1 cm^2 while inside the patient's body. This is elaborated in Subsection 3.2 and is called Design phase: Foldability mechanism. This chosen concept serves as a base for the second design phase described in Subsection 3.3 called Design phase: Leakage reduction. This phase focuses on a design that minimizes the chances of tissue loss due to leakage. The conceptual designs proposed in this section result in a final conceptual design that serves as the base for the final design (Section 4). To schematically represent each concept, the starting shape of the designed instrument is the vacuum grasper of Vonck [3] (Figure 13). Features are added concerning the solutions of each design phase.

Figure 13: The suction grasper designed by Vonck [3]. This grasper has one suction outlet at the distal tip.

3.2. Design phase 1: Foldability mechanism

3.2.1. Concept direction

Since a stiff suction surface is used to counter the disadvantages of a compliant suction surface. In order to maintain the stiffness while unfolding or rotating, also stiff elements are required. These stiff elements are connected with hinges. This conceptual phase is structured based on the number of hinges used in each concept. Concept 1 focuses on the rotation around a single hinge. Concept 2 uses multiple hinges in order to rotate the solid elements to create the suction area.

3.2.2. Concept 1: Use of a single hinge

This concept is based on the principle of using only a single suction surface that can rotate in one sagittal plane. The suction surface can be rotated around one single axis which is located in the middle of the suction surface. When in closed form, the suction surface is located inside the shaft of the suction grasper (Figure 14). The suction surface can be rotated around the single axis in order to rotate to a horizontal position. The length of the shaft is used to cover the suction surface while it is inserted into the patient's body. This way, the length of the suction surface does not lengthen the whole grasper. Another advantage of using one centered hinge is that once the suction surface adheres to the tissue successfully, the resultant force is also centered (Figure 15). Since the small dimensions of the instrument, the hinges also

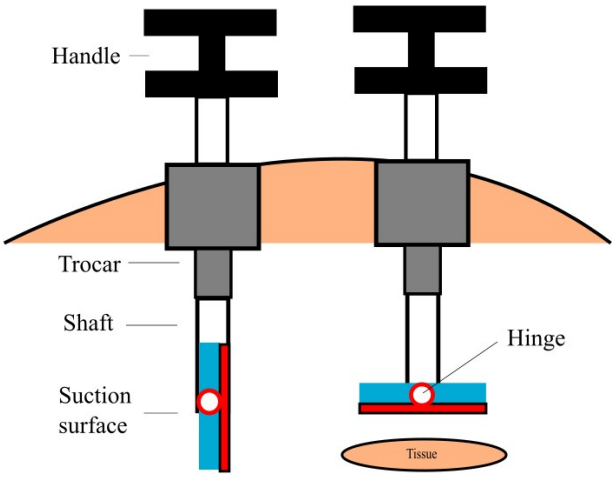

Figure 14: First concept based on one single hinge that rotates the suction surface. The hinge is located in the middle of this surface.

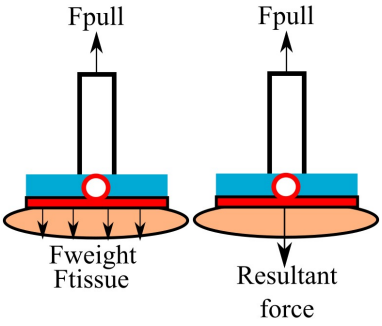

Figure 15: When tissue is pulled and the suction surface adheres to tissue, the resisting forces of the tissue are distributed over the suction surface, because of this, the resultant force is exerted through the axis of the hinge which balances the suction surface and does not result in a moment on the hinge.

become small and fragile.

However, the use of a single hinge means that the suction surface can only rotate in one direction. When the suction surface is rotated to a vertical position (Figure 14 left), the width of the suction surface becomes limited to the inner diameter of the shaft of the instrument, which is ⌀10 mm. This beam can only be lengthened in order to further increase its suction surface. The stiff surface properties prevent suction surface deformations and inwards slip (Figure 8). However, using a stiff suction surface that is only hinged centrally is not able to wrap around the tissue which makes it prone to leakage.

Positives:

- The shaft has a maximal diameter of ⌀10 mm which limits the space to work with. When using only hinge instead of multiple, a larger hinge can be used. This reduces the chance on hinge failure.
- Suction, pulling or pushing forces do not rotate the beam to a closed from. This is due to the location of the hinge, which is in centered at the grasper (Figure 15).

Downsides:

- The stiff suction surface can only expand in one direction since it rotates around one hinge. To reach a larger maximum suction force, the suction surface must be lengthened.
- Limited to the stiff straight surface. Not able to 'wrap' around tissue. Since only a single straight stiff surface is used, the suction surface is not able to wrap around the tissue. When tissue is stiff and not completely able to deform to the suction surface, the edges of the suction surface are prone to leakage.

3.2.3. Concept 2: Use of multiple hinges

The second conceptual design uses multiple hinges to rotate multiple suction surfaces (Figure 16). The red dots in Figure 16 depict the location of each hinge. In this Figure, 4 hinges at the distal end of the shaft are used. A suction surface is connected to each hinge. Because of the use of multiple hinges and suction surfaces, the combined suction surface is now able to shape in different shape configurations. In this example, seen from below, the shape of an cross is formed. However, when more or less hinges are used, different shapes can be formed. Adding to this, the suction surface can open partly, which enable the suction surfaces to adapt to the curvature of the grasped tissue.

However, by adding more hinges, the hinges become smaller since the dimensions are restricted which

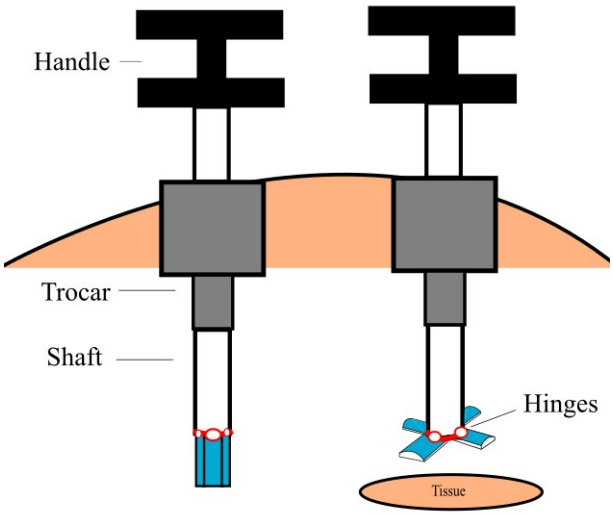

Figure 16: Second concept based on multiple hinges. 4 suction surfaces are depicted in blue and are connected to the hinges that are depicted as red circles at the distal end of the shaft. The suction surfaces are able to rotate around that hinge in order to open.

complicates the production of these hinges. Adding to the manufacturability of the hinges, the mechanical properties of these hinges become an issue. Once the tissue is grasped, a vacuum is generated and tissue is pulled by the surgeon, a moment is applied onto these hinges. Because of this, once the surgeon pulls the suction surface tends to rotate to a closed form (Figure 17). This can be prevented by a system that provides a lock to the orientation of the suction surface and disables the rotation. However, once the orientation is locked, these forces will apply a moment onto the hinges. According to the requirements, a pulling force of 5N is the targeted force.

Positives:

- Suction surface increases in multiple directions.
- Suction surfaces can party be opened to adjust to the surface of the tissue. This enables the suction surface to seal curved tissue.

Downsides:

- Manufacturability. Since the instrument should fit through a shaft of ⌀10 mm, the hinges and the suction surfaces become small.

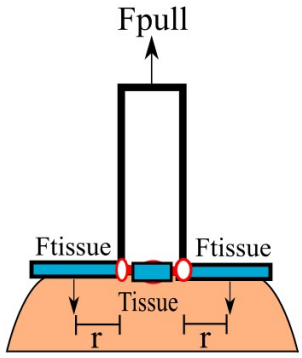

Figure 17: Once the surgeon grasps tissue and pulls the instrument, the tissue resistance force results in a moment onto the hinges. This is due to the distance r between the centre of the suction surface and the hinges.

- Once the surgeon pulls tissue, the suction surfaces rotate back to a closed stage. This is not desirable since this increases shear forces between the suction surface and the tissue. The suction tips in this thesis are not designed to resist these shear forces. Adding to this, if the instrument contains a feature to lock the suction surface in an open position this force results in a moment onto the hinges. Once tissue is pulled, this moment that is exerted onto the small hinges increase the chance on mechanical failure (Figure 17).

3.2.4. Conclusion phase: Foldability mechanism

From Section 3.2 Concept 1 is chosen as the most favorable. This has two main reasons. The first reason is that because of the small dimensions, hinges are hard to prototype and manufacture. The second reason to choose for this design, is that the hinge is located centrally on the suction surface. Because of this, a resultant suction force will be exerted through the centre of the suction surface and will not exert a moment on the hinges. The third reason implies on the damaging risk requirement (**R8**). Because concept 1 does not lengthen the instrument while inserting it in the patient's body, it limits the chances of damaging tissue while inserting through the trocar. These reasons outweigh the negatives about concept 1 and thus concept 1 will be further elaborated on in Subsection 3.3.

3.3. Design phase 2: Leakage reduction

3.3.1. Concept direction

The proposed design of section 3.2 is the starting point for the second design phase which focuses on minimizing leakage using a stiff suction surface. As stated in Section 1.3, stiff suction surfaces are prone to leakage at their outer regions since the stiffness disables the ability of the suction surface to adapt to the surface of the tissue. Because of this, this design phase focuses on further development to prevent leakage. Blocking the leaking air to the suction chamber is an interesting solution. A suction chamber is a space inside a suction tip where the air molecules are sucked away or where the volume is increased in order to generate a negative pressure. Common suction tips use a single suction chamber to generate a vacuum. However, when leakage occurs, the whole suction tip fails to generate a vacuum. This can be seen during leakage using the Octopus^{TM} stabilizer and the suction grasper of Kortman [7]. To solve this, the Octopus^{TM} stabilizer uses a continuous suction pump to suck air molecules away continuously. This is not possible during MIS because the suction grasper will suck away to CO2 used during the pneumopetherotineum. Another solution by Singh [5] is to fill the leaking gap with fatty tissue. To do this, the fatty tissue must be cut and placed exactly at the leaking suction tips. This technique is not desirable since it requires tissue damage and the location of leakage must be located during grasping which takes valuable time. A more viable technique would be to prevent air from leaking into the suction chamber. To prevent air leaking into the suction chamber while maintaining suction force, multiple suction tips are required. If only one suction tip is used which one is blocked, no suction force can be generated. The use of multiple suction tips also fulfills the requirement that the suction force must be distributed over the grasped tissue (**R6**). Two concepts based on this principle are proposed in this section.

3.3.2. Concept 1: Adaptive suction tips

The first concept is based on the principle that the suction surface contains multiple suction tips that are adaptive and can open or close to prevent air leaking into the suction chamber. This can be achieved in two ways. Firstly, by blocking the suction tips that leak, the suction chamber is still able to generate a negative pressure. Since leakage can not be sensed by the surgeon, an active sensor must measure if leakage occurs. The surgeon is then able to read from the sensor which part of the suction surface leaks and can close it. A mechanical system using sliders can be used to close of the suction openings. This system can be improved by automating it in order to decrease reaction time. A sensor is attached to each suction opening that measures if there is full contact around the suction opening. If there is, the sensor passes the signal to the separate motors that open the sliders and thus open the suction tip. This way, only the correctly sealed suction tips open to the suction chamber. However, sensors in soft actuators in recent literature state dimensional limitations and are not produced on such small scales yet [26] [27]. Another way to prevent air leaking into the suction chamber using adaptive suction tips is to only open the suction tips when they have full contact with the surface of the tissue. The mechanical contact force opens the suction tip passively, so no sensors are required. However, a compliant mechanism that can open and close the suction tips must be implemented inside

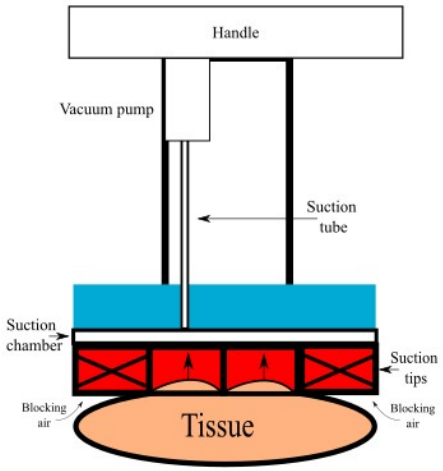

Figure 18: Block air leaking into the suction chamber via the suction tips by closing the suction tip that leaks or only open the suction tips that do seal correctly. The suction chamber is represented as the white area above the red suction tips. A suction tube is connected to this suction chamber which is attached to a vacuum pump. This vacuum pump sucks the air away in this suction chamber and thus the suction tips. By blocking the suction tips that are not fully sealed, air is not able to leak into the suction chamber and thus a negative pressure can be generated.

the suction tips. These mechanisms on this scale are currently not available.

Positives:

- Uses a single suction chamber, which is easier to fit inside the instrument.

Downsides:

- When leakage occurs, reaction time of the surgeon or reaction time of the sensors, the motors and execution time decide how long leakage occurs. Before closing the correct openings air is able to leak in and tissue loss occurs.
- Dimensional limitations of these mechanical sensors inside the suction tips.
- Compliant mechanism that opens the suction surface on contact force are complex to manufacture on such small scales. Also, these mechanisms take redundant space inside these small suction tips.

3.3.3. Concept 2: Seperate suction chambers

Concept 1 uses a single suction chamber (white) that is connected to multiple suction tips. This concept uses multiple suction chambers to generate a negative pressure in multiple suction tips. Figure 19 represents a conceptual and schematic design of this instrument. Each suction tip (red) is connected to a separate suction chamber (white). In these suction chambers air is sucked away by the vacuum pumps. Because of this, if one suction tip fails to seal correctly and air leaks in the suction chamber, it does not affect the other suction chambers and vacuum can be maintained. No actions are required before generating a suction force, since air molecules are not able to transfer from one suction chamber to another.

Positives:

- Air molecules are not able to transfer from one suction chamber to another. This improves the reliability of the suction grasper since leakage in one chamber does not result in total tissue loss.
- The separate suction chambers do not require action from the surgeon or a sensor when leakage occurs, this is automatically blocked.

Downsides:

- Because of the small dimensions of the suction grasper, it is challenging to fit multiple suction cham-

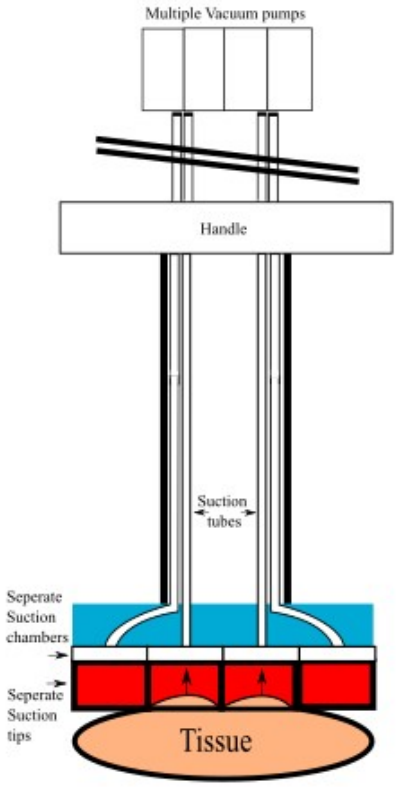

Figure 19: Multiple suction chambers are used to independently actuate a suction force in different suction tips. The suction tubes are attached to the suction chambers and are connected to separate vacuum pumps. Once these pumps suck the air awa in the suction chambers, the pressure in the chambers drop and a suction force is generated. This can only happen when the chamber is sealed correctly. In this case, the outer two suction tips do not seal correctly and air is able to leak into the suction chamber. Because of this, no negative pressure can be generated in these chambers. Because the suction chambers are separated, this does not influence the pressure in the other suction chambers. This results in a suction force, even when leakage occurs at several suction tips. The vacuum pumps are attached to the instrument by tubes and are stationary located in the operating room.

bers inside the instrument. Because of this, the suction chambers are located outside of the suction grasper.

- Multiple suction chambers are actuated by multiple suction chambers. Since these chambers are located outside the instrument small suction tubes are required to connected the suction chambers and the suction tips. Small suction tubes are prone to collapsing when negative pressure is applied inside these tubes.

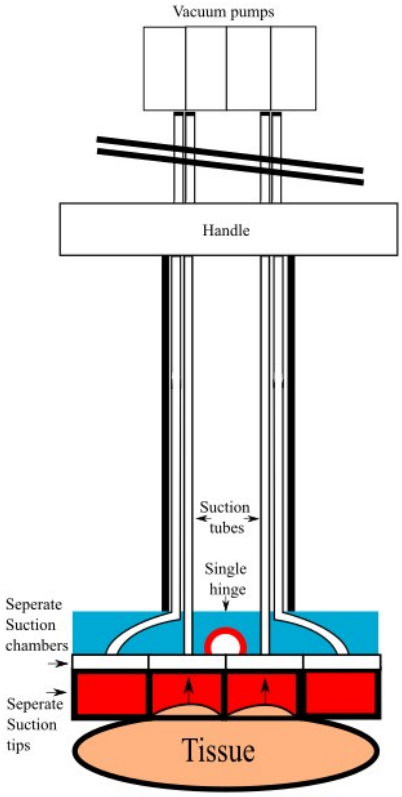

Figure 20: The final conceptual design as a result of the combination of design phase 1 and 2. The design consists of a single stiff suction surface that rotates around one hinge (red dot). Multiple suction chambers are used to generate a separate negative pressure for each used suction tip. The suction chambers and the suction tips are connected with suction tubes (blue).

3.3.4. Conclusion phase: Leakage reduction

Since the dimensions in the suction graspers are small and time in the operating room is limited, simplicity is key. Because of this, concept 2 is chosen as the most promising concept. The main reasons for this choice are that this concept does not require a sensor or mechanical system to measure if a suction tip is leaking or sealing correctly. Also, no mechanical system is required that closes these leaking suction tips. These systems must be placed inside the suction surface, where space is limited. By using multiple suction chambers, the leaking suction tips do not affect the pressure in the other suction chambers because they are not connected. This does not require a sensor or mechanical system. When leakage occurs at one suction tip, it automatically blocks the air from leaking into the other suction chambers and total negative pressure can be maintained. However multiple suction chambers also require extra space, these can be placed outside the instrument and the suction tips and chambers can be connected by longer suction tubes.

3.4. Final conceptual design

The final conceptual design consists of a combination of the chosen concepts of design phase 1 and 2. Figure 20 shows the combination of the two concepts. It uses a fully solid suction surface that rotates around a single hinge (depicted as the red dot) (**R3**). Multiple suction tips are attached to the suction surface to distribute tissue pressure (**R7**) and to be able to generate independent negative pressures within each suction tip (**R4**). Each suction tip is attached to an individual suction chamber that is located outside the shaft of the instrument. This way, space inside the shaft can be used for a mechanism that actuates suction surface rotation and also provide space for the suction tubes that are connected to the vacuum pumps. To summarize, Figure 21 gives a schematic overview of the whole conceptual design process. The green arrows indicate the design choices.

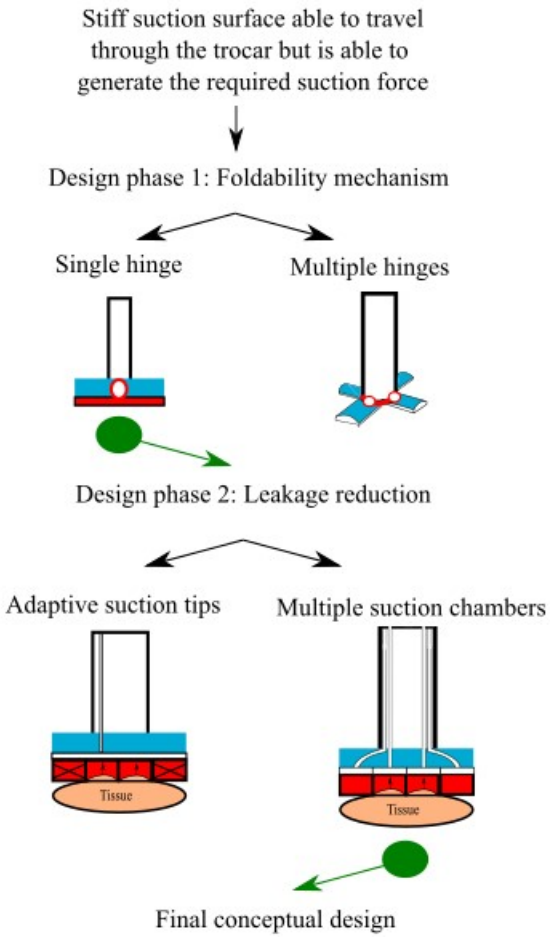

Figure 21: A schematic view of the design phase and choices that lead to the final conceptual design

4. Final design

4.1. Overview of design

In order to optimize the concept to a final design, some adjustments on details are required. Figure 22 shows the design of the final design of the suction grasper. For this thesis, every part in this design is labeled with a unique color to clearly identify the part. However, in the actual design, these colors are not used. Rendered images of the actual final design are shown in Appendix D. An exploded view of the final design is can be found in Figure 23. Here all parts are labeled. According to the requirements, the length of the shaft should be 35 centimeters. The length of the shaft during this thesis is shortened in order to facilitate prototyping using 3D-printers. The shaft will be inserted into the trocar. Once the suction grasper is placed correctly, the surgeon turns the upper axis in order to rotate the suction surface. When the correct orientation is achieved, the surgeon actuates the vacuum pumps and is able to manipulate the tissue. In the following section, the design is elaborated according to the following functions:

- Suction surface rotation
- Cable tension
- Multiple suction chambers
- Ensure patient safety
- Manufacturability

4.2. Enable suction surface rotation

This design uses two cables to actuate the rotation of the suction surface. The cables are looped around two axis. In this design, cables are most optimal since they do not require a lot of space. This space is limited inside the instrument shaft since the diameter is only 1 cm and the suction tubes also are placed inside the shaft. The rotation of the upper axis must be transferred to the distal axis. The distal axis are the extruded parts on the sides of the suction surface (Figure 24). In Figure 24 the suction surface and the inner shaft are shown. The suction surface is clicked into the axis holders of the inner shaft. Because of this, the suction surface is locked in place but it still able to rotate. In order to rotate the suction surface using cables, friction between the axis and the cable is required. There are multiple ways to enhance friction between the cable and the axis. The friction coefficient could be enhanced by changing the material of the axis and the cable. However, since the instrument is used during surgery the friction coefficient will drop since the material will get covered with blood. Another option is to change to shape of the axis to generate more friction. V-shape grooves in the axis show an increase in friction compared to a squared groove [28]. The friction coefficient of a v-shaped groove can be

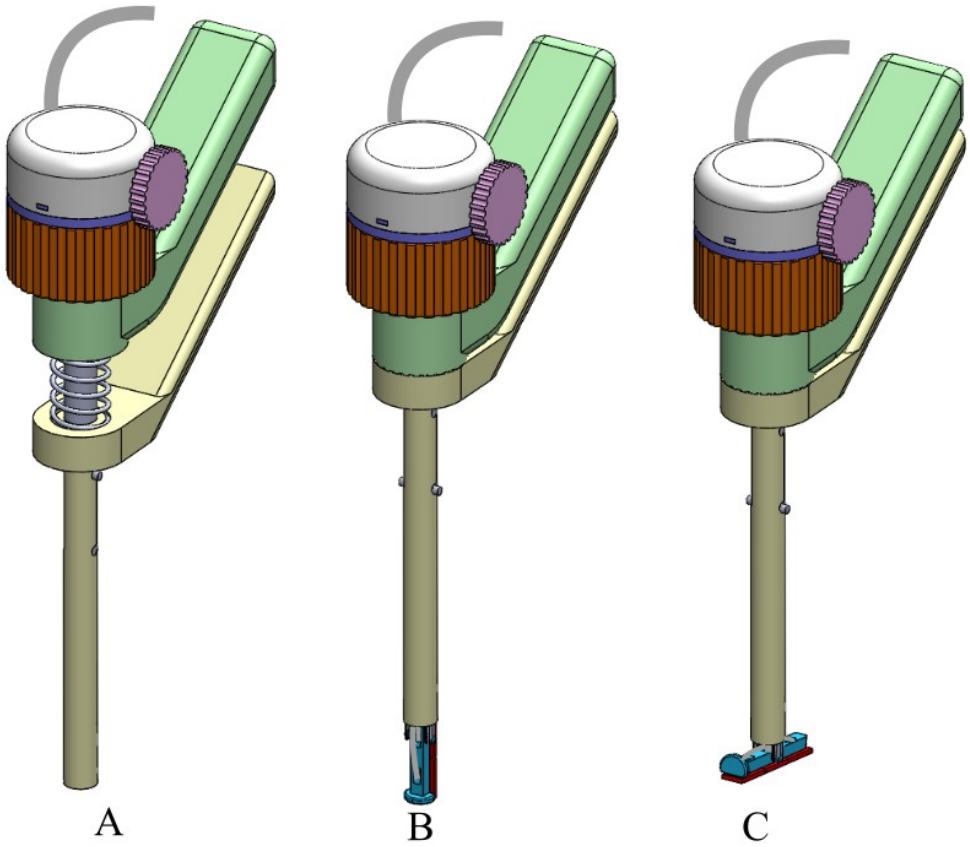

Figure 22: Solidworks model of the final design. Three phases of use are displayed. A: The suction surface is in closed position. This way the suction surface is not able to rotate. In this position, the surgeon inserts the instrument through the trocar. B: Once the instrument reaches to correct location, the suction outer shaft is retracted. This is done by slightly rotating the outer shaft (yellow) counter-clockwise. The extension spring enables an automatic translation of the outer shaft towards the green handle. The suction surface aligns with the cut-outs of the outer shaft and is now able to rotate. C: The surgeon rotates the suction surface to its required position and is now able to actuate vacuum pressure in order to grasp tissue. The suction tubes are depicted in grey. They are placed through the shaft between the cables and leave the instrument on the upper side towards the vacuum pumps that are placed inside the operating room.

determined using the following equation 2:

$$f = \frac{\mu}{sin(\frac{\gamma}{2})} \tag{2}$$

Where γ is the angle of the groove (Figure 25), μ the friction coefficient between the material of the cable and the groove and f the magnitude of the shear force coefficient. Hrabovský [28] states that traction capacity increases with a lower angle of the V-groove , but at the same time, the contact pressure on the contact area between the cable and the groove wall increases. The angle γ must therefore not be less than 32 degrees and it is recommended to choose γ = 40 degrees [28].

Two looped wires are used to transfer the rotational force to the suction tip. A nylon wire is used as this has a small bending radius. A stainless steel wire showed buckling when tensioning (Appendix F). This buckling blocked the transfer of the cable around the axis due to the minimum bending radius of a metal cable. This minimum bending radius depends on the diameter of the

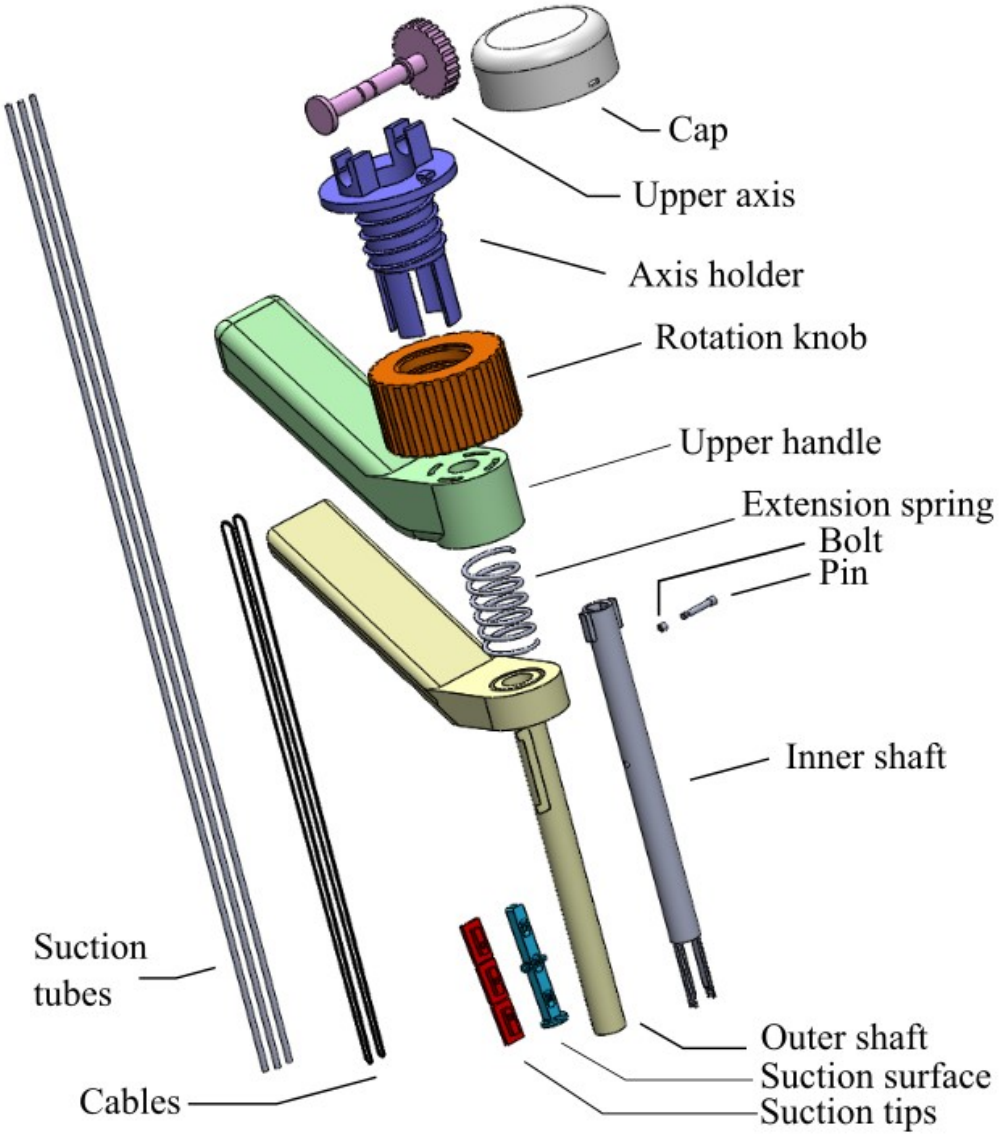

Figure 23: Exploded Solidworks model of the final design. Every part is captioned with a brief name as it can be referred to.

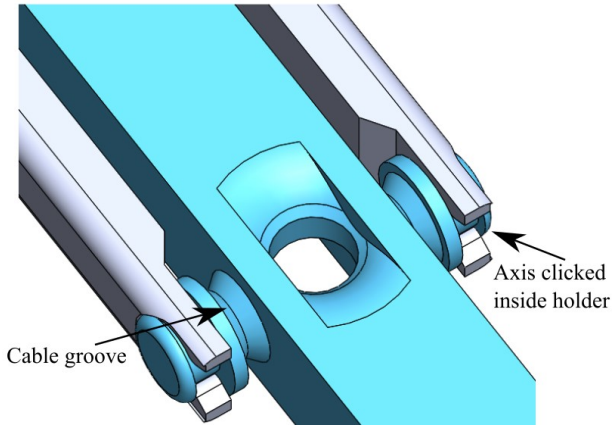

Figure 24: Suction surface clicked into the inner shaft. The V-grooves are visible. The cables are looped around these grooves. Also 1 of the 3 suction tube openings are visible.

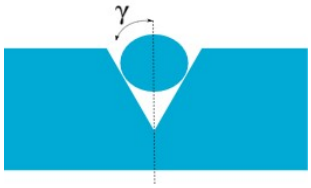

Figure 25: Schematic visualization of the groove angle and how the cable falls into the groove.

cable. The 0.8mm cable needs a minimum bending radius of 16.4 mm [29] to prevent buckling. To successfully use the steel wire, the radius should be decreased. A 0.3 mm steel cable is used (BEADALON 0,3mm), however these small diameter wires started cutting and damaging into the 3D-printed axis when tensioning. Nylon has a small minimum bending radius compared to steel wire and is not prone to buckling. However, it still has high breaking strength of 12 kg and good wear resistance. A 0,8 mm breaded nylon wire is used, which does not cut the 3D-printed axis. The two ends of the wire are

Figure 26: Square knot used to loop the nylon wires.

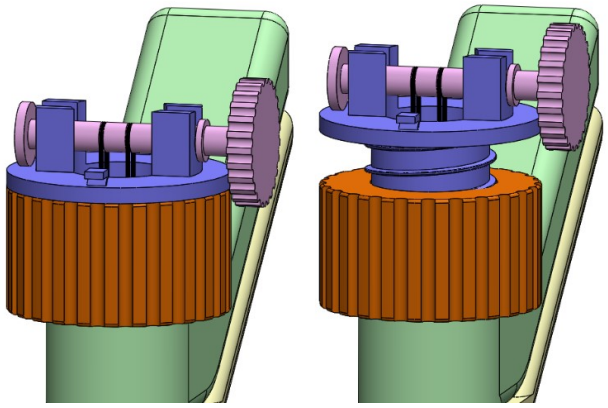

Figure 27: Tension mechanism of the suction grasper. Once the rotation knob (orange) is twisted clockwise, the axis holder (purple) will translate in proximal direction and increases the distance between the lower and upper axis. This means the cables get tensioned.

attached to each other with a knot. In this case, the square flat knot is suitable because it tightens when it is being pulled (Figure 26). Also the knot is small and thin. This is convenient because the knots are located in the inner shaft. The inner shaft is made from stainless steel. The suction surface and the axis are made from biocompatible plastics, like PLA.

4.3. Enable cable tension

In this instrument, it is essential that the two axis are aligned at any time. Otherwise the cable will twist. When the cables are placed around the axis, the cables are not tensioned. However tension is required in order to transfer the forces. To tension the cables when these are placed around the two axis, the shaft of the suction grasper must be lengthened to a length that the cables will be fully tensioned. Furthermore, when the cables are tensioned for a long period of time, creep occurs. This happens for both steel and polymer materials [30]. Creep is the tendency of a material to slowly deform permanently under the influence of a constant force or stress [31]. So over time, slight strain occurs at the cables. In Figure 27 a solution is presented which enables cable tension but keeps alignment between the two axis. To counter creep, cable tension can be increased when necessary. The mechanism contains four moving parts. The axis holder (purple), attached to

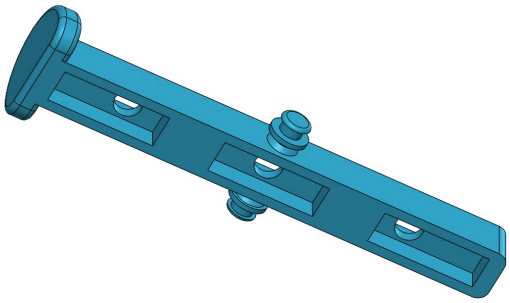

Figure 28: Suction surface including the cut-outs. In these cut-outs the suction tips fit. Through the hole on top the suction tubes are placed and connected with the suction tips using silicone. The suction tips are glued in the cut-outs using glue (BISON). The half-circle extruded part functions as a sealing surface when the suction surface is in closed position and the instrument is being inserted into the patient's body.

the axis holder is the upper axis (pink), the rotation knob (orange) and the rotation lock (green). The rotation lock contains four holes which will fit the extruded parts of the axis holder. These holes constrain the axis holder from rotating and thus maintain alignment between the two axis of the suction grasper. The axis holder contains a thread on the outside that fits the inside thread of the rotation knob. If all parts are locked in place (Figure 27: left) the surgeon can rotate the rotation knob. When the rotation knob is rotated towards the rotation lock, the axis holder will move in a proximal direction because of the thread and its constrain for rotation and tensions the cables (Figure 27: right).

4.4. Leakage reduction

4.4.1. Suction surface

In order to minimize tissue loss due to leakage, multiple suction chambers are used during this thesis. The suction chambers is the location were the volume of this chamber gets enlarged or air gets sucked away in order to generate a negative pressure. In this thesis, multiple suction chambers are used and are located outside the instrument. A suction tube is attached to each suction chamber and is connected to the suction surface (blue). The suction surface is made from bio-compatible resin by the SLA printer. This printer is used in order to enhance precision. The dimensions of the suction surface are determined as follows. The maximum length of the suction surface is 45 mm according to the requirements (**R8**). The width and height of the suction surface are a trade-off between the available space inside the shaft of the instrument. For that reason, the suction surface (minus the axis) has a width and height of 4.5 mm. Using these dimensions, the suction surface is able to fit inside the inner shaft while maintaining enough stiffness. The suction surface contains cut-outs at the bottom part in which the suction tips can be placed (Figure 28).

4.4.2. Suction tips

Inside the cut-outs of the suction surface, corresponding suction tips (red) are placed. These suction tips are made from silicone rubber (SMOOTH ON DRAGONSKIN). Because silicone is soft and flexible, the suction tips are

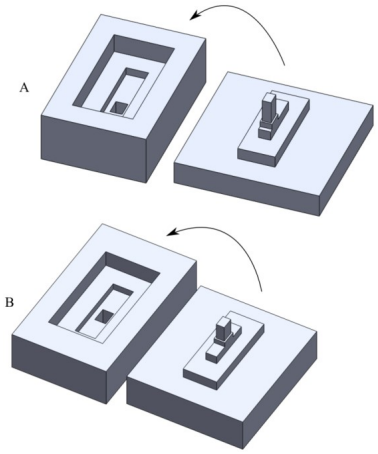

Figure 29: Mold of the lateral suction tip. Once the left part is filled with silicone, the right part gets inserted inside the hole of the left part. The silicone cures and these two parts are parted again.

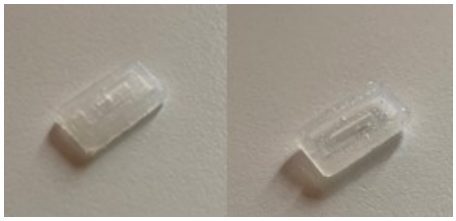

Figure 30: Resulting cured silicone suction tip.

Figure 31: The suction tips placed on the suction surface. The suction tips fit exactly on the cut-outs of the suction surface.

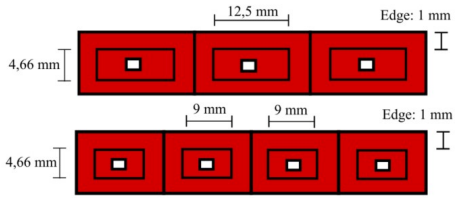

Figure 32: Bottom view of the suction surface with 3 suction tips and 4 suction tips.

able to deform to the surface of the tissue and sealing is enhanced. Molds for the suction tip are printed using the SLA printer (FORMLABS 3B+) (Figure 29). Each mold consisted of a bottom and top part. In the bottom part the silicone is poured, which shapes the outside part of the suction tip. Once the silicone is poured in the bottom part, the top part is placed inside the bottom part. The bottom part compresses the silicone inside the bottom part and shapes the inside of the suction tip. After 8 hours of curing time, the suction tips are removed from the molds (Figure 30). Subsequently, the suction tips are glued inside the cut-outs of the suction surface (Figure 31). Each suction tip has an edge with a thickness of 1 mm (Figure 32). This edge prevents the suction tip from collapsing and air from leaking into the suction tip. A thinner edge than 1 mm collapsed and showed leakage when negative pressure is applied. The silicone that is used is the DragonSkin^{TM} from Smooth-On. This silicone is often used for medical prostheses and has the highest tensile strength and flexibility Smooth-On offers. A tensile test is performed to examine three types of silicone from Smooth-On (Appendix G). The silicone suction tips are placed into the cut-outs in the suction surface and are fixed with strong adhesive glue (BISON). The suction tip and the suction tube are connected with the addition of silicone (SMOOTH-ON SIL-POXY). This prevents air leakage between suction tip and suction tube.

As stated in the Problem Analysis, leakage occurs most frequently on the outer suction sections of a stiff suction surface. Especially if grasped tissue contains a surface curvature and the suction surface is not able to deform to the shape of this surface. For that reason, this design requires minimally one suction tip medially from the two most outer suction tips, which are most prone to leakage. This centrally located suction tip is less prone to leakage and decreases the chances of tissue loss if the outer suction tips leak. This means that 3 is the minimum amount of suction tips that can be used. Each suction tip has a suction surface of 0.58 cm^2. Because three are used, a combined suction surface of 1.74 cm^2 is achieved. This exceeds the minimum suction surface of 1 cm^2 (**R2**). According to Equation 1, this results in a suction force of 2.9N per suction tip. This means that 2 suction tips would be able to generate 5N of suction force (**R2**) and safely manipulate human tissue during MIS. The dimensions of the suction surface allow for using 4 suction tips instead of 3 (Figure 32). Because of this, 4 smaller suction tips can be used which decreases the chance of tissue loss due to more contact points that exert a suction force. However, the use of an extra suction tip decreases the combined suction area of the suction tips since each suction tip is smaller and has an outer edge of 1 mm. The suction area of this suction tip is 0.42 cm ^{2} and thus a minimum of 3 suction tips are required to meet the 1 cm^2. The use of 5 suction tips was not sufficient since the total surface area became less than 1 cm^2 due to the minimum edge thickness of 1 mm. Adding to this, these small suction tips were not manufacturable using the molds. The use of 3 or 4 suction tips and suction chambers are tested in the next Section 5.

4.4.3. Suction chambers

The suction chambers in this thesis are simplified as syringes of 50 ml with a diameter of 3,2 cm. This means that 40 N is required per syringe to generate a negative pressure of 50 kPa according to the requirements

(**R1**). If small suction chambers are placed inside the shaft, they would have a small diameter. This results in a higher required force to compress these suction chambers when manually actuated because of the small surface area (Equation 1) For that reason, the syringes are not attached to the suction grasper directly. These are placed outside the instrument and connected with suction tubes. Suction tubes connect the suction tips to the corresponding suction chambers. The suction tubes leave the shaft as a bundled into one tube through a hole in the cap. This hole is sealed to make it airtight. This suction tubes are made from PTFE. In the final configuration, inside the operating room automated vacuum pumps are attached to the instrument.

4.5. Ensure patient safety

The shaft of the suction grasper consists of two parts (Figure 33). The grey inner shaft is fixed into the green handle. The outer shaft is able to glide over the inner shaft. This outer shaft is made from a thin-walled stainless steel tube of 0,3 mm thickness with an inner diameter of 9,4 mm and functions as a protection and guiding mechanism for the inner shaft, but also as a rotation lock for the suction surface. Part of the outer shaft is a steel handle (yellow) which the surgeon can press to translate

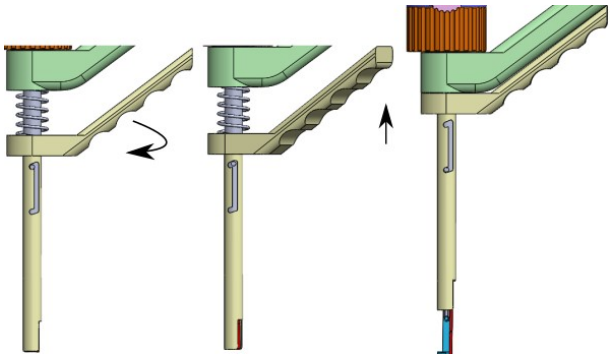

Figure 33: Side view of the shaft of the grasper which demonstrates outer shaft movement. The surgeon is able to push the handle of the outer shaft clockwise with his fingers. Because of this, the pin lines up with the vertical cut-out. The tensioned extension spring pulls the outer shaft towards the handle and the pin falls in the lower slot which aligns the lower cut-out with the suction surface. Now the suction surface is able to rotate. The surgeon now also grasps the handle of the outer shaft together with the main handle to control the instrument.

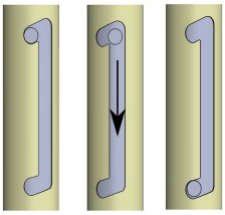

Figure 34: Zoomed depiction of the bracket-shaped pathway on the outer shaft. Because of this pathway, the outer shaft can only move according to these directions.

the outer shaft. The outer shaft consists of two cut-outs on the most distal end. These enable the suction surface to rotate earlier so the distal axis including the cables will not have to be inserted into the patient's body further which limits the chance of tissue damage. Adding to this, the proximal part of the outer shaft also consists of two bracket-shaped cut-outs (Figure 34). These act as a guiding rail and will constrain a movement pathway for the outer shaft. Before the instrument is inserted through the trocar, the pin and bracket are in the most upward position (Figure 33: left). The suction surface is fully retracted and is not able to rotate to an open position. Also, in this position, the shaft is not able to translate upwards which prevents undesired premature translation. Once the surgeon taps the handle of the outer shaft using his index - and middle finger in a clockwise direction, the pin aligns with the vertical trajectory of the bracket (middle of Figure 34 and Figure 33). An extension spring is attached between the outer shaft and the upper handle. Once the outer shaft is in the closed position (Figure 33 left), the extension spring is tensioned. Because of this, the extension spring automatically pulls the outer shaft towards the upper handle when the pin is aligned with the vertical bracket trajectory (Figure 34 middle) and the pin falls in the lower part of the bracket (Figure 34 right). Both handles are now aligned and the surgeon now grasps both handles as a combined handle to control the instrument (Figure 33 right). Also, the suction surface is aligned with the lower cut-out on the outer shaft which enables the surgeon to rotate the suction surface.

Since the instrument is inserted through a trocar, surgeon's visibility inside the abdomen is limited. For that reason, cut-outs are made inside the outer shaft to be

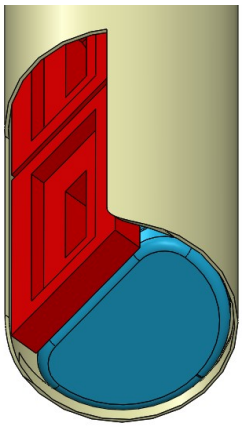

Figure 35: When the suction grasper is in closed position, the distal part of the grasper is sealed with the half-circle-shaped stopper on the suction surface to prevent tissue damage harmed by the edges of the outer shaft.

able to rotate the suction surface earlier. Adding to this, it is not desirable to insert the instrument while the suction surface is fully exposed. The suction tubes or premature rotation could damage tissue. The outer shaft is thin (0,3 mm) and may damage organs or other tissue while it is pointing out and inserted into the patient's body. For that reason, the suction surface consists of a half-circle extruded part at one end. This half-circle shape seals the gap between the outer shaft and prevents the outer shaft from cutting into organs when inserted (Figure 35). This meets the safety requirement (**R7**). Because the suction tips, cables and tubing are covered during insertion, durability is enhanced.

4.6. Ensure manufacturability

To enhance manufacturability, several aspects have been taken into consideration. The device can quickly be assembled manually. First, the suction tubes and suction tips should be connected to the suction surface. The suction tips are attached in the corresponding cut-outs in the suction surface with strong adhesive glue. A quick proof of principle test proved that the use of strong adhesive glue between 3D-printed SLA (Though 1500 resin) and silicone resulted in a 10N attachment force. Hereafter, the suction tubes are placed in the holes of the suction surface and the suction tips. Once placed correctly, they are

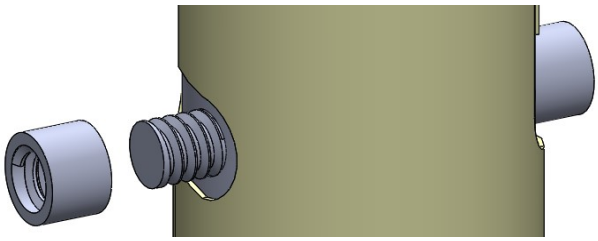

Figure 36: The thread pin which is placed through the holes in the inner shaft and through the cut-outs in the outer shaft. The cap with corresponding thread can be screwed on this thread.

secured with extra silicone (SMOOTH-ON SIL-POXY) which also makes the connection more airtight. Subsequently, the inner shaft (grey) can be inserted into the upper handle (green). The two extruded edges on the inner shaft ensure the inner shaft does not rotate once inside the lock. Adhesive glue (BISON) is used to lock the inner shaft. The rotation knob can now be rotated onto the thread of the axis holder. The 4 extruded pins of the axis holder (purple) should then be placed into the corresponding 4 cut-outs of the upper handle (green) using the extruded rotation locks. The suction surface (blue) and the upper axis (pink) can be clicked onto the inner shaft (grey) and the axis holder (purple). Subsequently, both nylon wires and the suction tubes can be placed through the instrument and around both axis. The wires of 0,8 mm fit inside the grooves of 0,9 mm width. The distal end of the inner shaft is inserted into the outer shaft. Once the inner shaft aligns with the bracket-shaped cut-out of the outer shaft, the 2 mm ⌀thread pin is placed through the hole of the inner shaft (Figure 36). This pin contains a 2mm long thread on the other end. On this thread, a cap with a corresponding thread can be screwed. These off-the-shelf parts fixes the pin to the inner shaft. Also, the pin does not intervene the tensioned cables since the diameter of the pin is smaller compared to the diameter of the two v-grooved axis. Because of this, the pin goes through the space between the cables and will not have contact. The extension spring is glued between two circular cut-outs of both handles. Finally, to be able to rotate the suction surface, the cable must be tensioned using the rotation knob. The instrument is now assembled correctly and is ready to use. The instrument should be compatible for surgery and specifically MIS. This is

dependent on different variables like material choices, dimensions and safety factors. All the parts are made from stainless steel, biocompatible 3D-printed material or silicone which means that all parts are biocompatible and able to be used during surgery. The inner shaft is made from laser-cut stainless steel. The suction surface, rotation knob, axis holder, outer shaft, cap, upper handle and upper axis are 3D-printed using the SLA printer with biocompatible resin to enhance accuracy. Eventually, when production has been upscaled, injection moulding is used to manufacture the plastic parts. The pin and bolt are stainless steel off-the-shelf products and the suction tips are made from silicone. To enhance safety, damage risks of the instrument for the patient's health are minimized (**R7)** during the design of this instrument. Dimensional requirements stated in the requirements are used as maximum boundaries (**R8**).

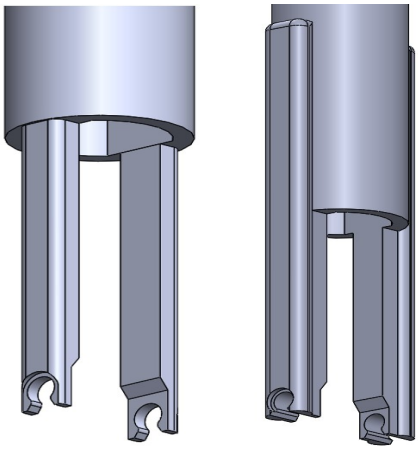

Figure 37: Adjustment of the inner shaft in order to be able to print this prototype. The thickened beam prevents it from bending and breaking when a force is exerted on it

Figure 38: Prototype that is used to test the tensioning mechanism and the rotation of the suction surface. By turning the rotation knob the suction surface can be rotated.

4.7. Prototype

A first prototype was created to test the tensioning mechanism using the thread and the bracket-shaped sliding system. This prototype was created on a 3:1 scale on the FDM-printer (Ultimaker). As shown in Figure 66 in Appendix E, the printed prototype is able to slide and the thread is printed correctly. This prototype functioned as a base for the second prototype. The second prototype is designed on a 1:1 scale. This prototype only focuses on the tensioning and suction surface rotation. In the final model, the inner shaft is made from stainless steel. However, for this prototype, this part is 3D-printed using the Formlabs 3B+ © . Because this material is not as strong as stainless steel and is more likely to break or bend, the beams are thickened to increase stiffness (Figure 37). This thickening disables the ability of the inner shaft to translate through the outer shaft. However, this translation is not tested with this prototype. Figure 38 shows the prototype. This working prototype is able to rotate the suction surface using nylon braided cables. To finalize the design section, the usability of the instrument is represented in Figure 39. This figure shows how the surgeon is able to use the instrument during MIS.

5. Experimental Validation

5.1. Goal

The main goal of this research is described as follows; *Design a suction grasper which is compatible for MIS and minimizes tissue loss due to leakage using a stiff suction surface.* Studies [7] [32] show that a flexible suction surface is able to wrap around the tissue when it deforms or

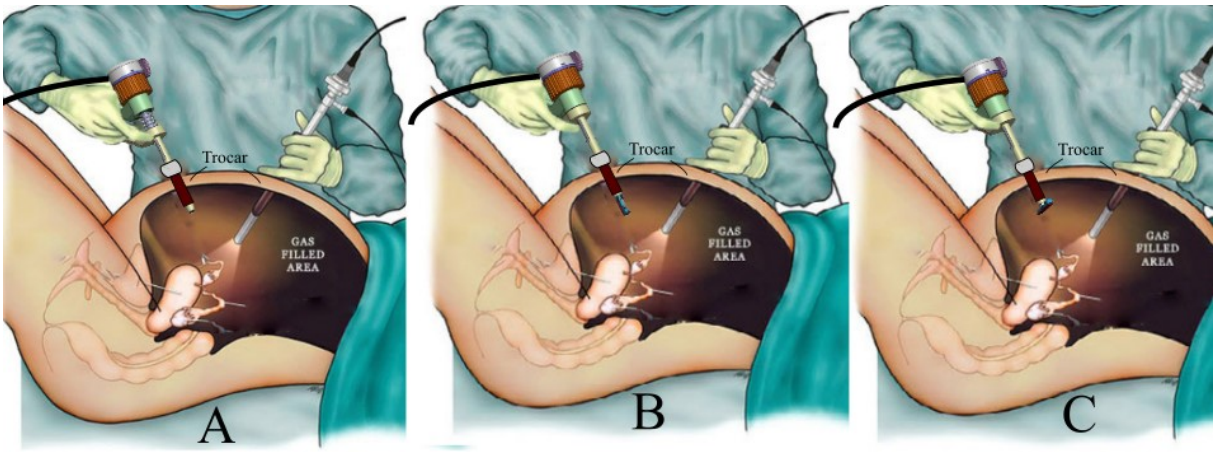

Figure 39: Schematic view of how the surgeon uses the instrument. First a trocar is placed through the abdomen of the patient. Usually multiple trocars are placed. One for the camera (here depicted as the right instrument) and few more for the surgical instruments. Before the suction grasper is inserted through the trocar the cables are tensioned using the rotation knob. Subsequently, the instrument is placed through the trocar while the outer shaft is in the most downward position. Once the correct location is reached, the surgeon twists and pushes the inner shaft downwards from the outer shaft (A). Now the suction surface aligns the cut-outs of the outer shaft and is able to rotate through these. The surgeon rotates the suction surface by turning the upper axis knob (B) and placing the suction surface on the tissue. Now the vacuum pumps are actuated and a negative pressure is generated inside the suction tips.

when the surface contains a surface curvature. Since a stiff suction surface is used in this study, this is not possible. To compensate for this, multiple suction tips connected to separate suction chambers are attached to the stiff suction surface in order to minimize tissue loss due to leakage. The goal of the experiments is to test the attachment performance of the stiff suction surface while grasping curved phantom tissue since it is hypothesized that using a stiff suction surface on a curved substrate decreases sealing performance. For that reason, multiple suction chambers are used to counter that problem. The attachment performance of the suction grasper in these experiments is described as the pulling force which is required to pull the suction surface from the tissue. The tests are performed in series. (1) The assessment of attachment performance of the suction surface on diverse phantom tissue **curvatures**. (2) The assessment of attachment performance of the suction surface on diverse phantom tissue **stiffnesses** on constant surface curvature. The full experimental setup is shown in Figure 41.

5.2. Experimental variables

5.2.1. Independent variables

Tissue curvature:
Since diverse curvatures can be found inside the human body during MIS, only the surfaces of abdominal organs are analyzed. 3D-models of these organs were analyzed to determine a range of surface curvatures that are commonly encountered during MIS (Appendix H). A range between almost flat (infinite diameter) and a diameter of 80 mm can be found. A surface curvature diameter of 80 mm can for example be found on the gallbladder and on the cecum of the bowel. 200 mm can be found on the flatter side of the liver, flat surface of the pancreas and stomach. A surface curvature diameter of 200 mm means that the surface is flatter compared to a surface curvature

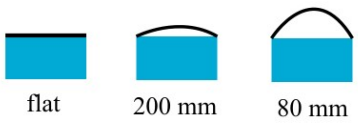

Figure 40: Schematic explanation of tissue curvature diameters. 200 mm means the curvature diameter is flatter compared to 80 mm

of 80 mm (Figure 40).

Tissue stiffness:
Different tissue types can be encountered during MIS. These tissue types have a wide range of mechanical properties. Tissue stiffness varies between 5 and 40 kPa [17] [33]. This wide range of tissue stiffness influences tissue behaviour when a suction force is applied on it. A low stiffness results in a more flexible substrate which is more prone to deformation compared to a stiffer substrate. Therefore, a stiffness of 5, 20 and 35 kPa is used as independent experiment variable.

Number of suction tips with corresponding suction chambers:
According to the requirements (**R8**) the suction surface has a maximum length of 45 mm. However, the number of suction tips can be varied within this length. The final design is designed based on 3 suction tips, although 4 suction tips also fit within this range (Section 4.4.2). The amount of suction tips with corresponding suction chambers is varied during each test to analyze which amount performs most effectively. A suction surface is designed with 3 and 4 suction tips for testing. As a reference, these are compared to a suction surface with 1 suction chamber.

5.2.2. Dependent variables

Attachment force:
The main performance measure of the test protocol is the attachment force of the suction surface on the phantom tissue. This is measured continuously while the linear stage pulls the attached suction surface from the phantom tissue. The maximum attachment force is described as the force that is required to pull all the suction tips from the

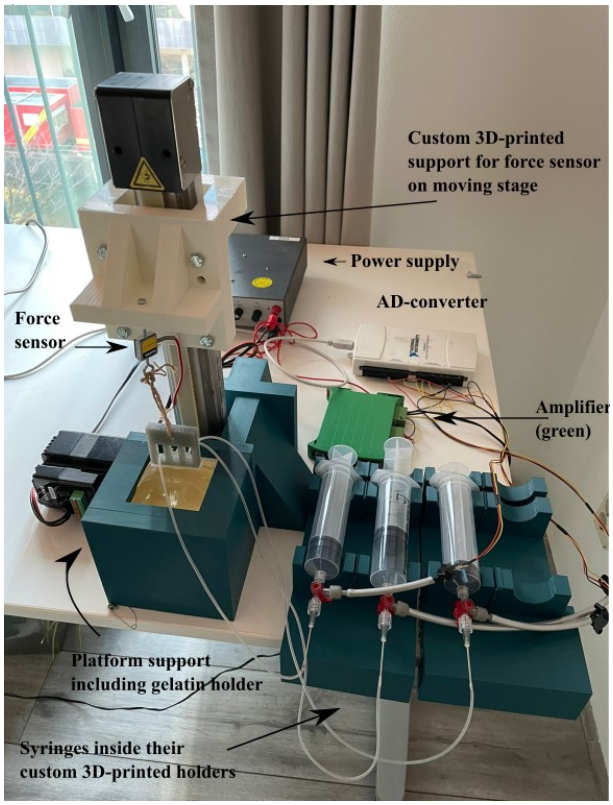

Figure 41: Overview of the complete test setup.

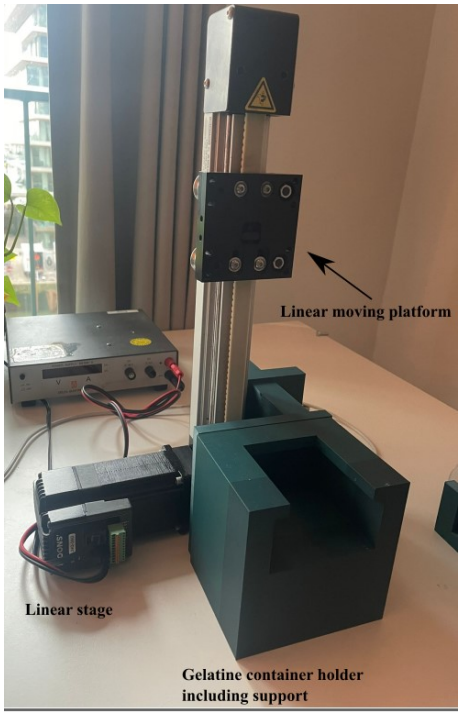

Figure 42: The linear stage including custom 3D-printed support to hold it upright and stabilize it. This support also contains a slot in which the container of the gelatine phantom tissue is placed.

phantom tissue.

5.3. Experimental set-up

5.3.1. Linear stage

An overview of the total set-up is shown in Figure 41. The linear stage (ALMOTION LT50-TR-G8-200) is a platform that is able to translate in one direction (Figure 42). The linear stage is powered by a 30V power supply (DELTA ELEKTRONICA ES030-5). Since this platform is designed for horizontal translation, support is needed to hold the linear stage upright. Once it is upright, the platform is able to translate vertically. The force sensor should be connected to the linear moving platform. For this reason, a base support plate is designed to fit on the square platform and is connected using M5 bolts (Figure 41). The force sensor is attached by an M3 bolt through the central hole in the support plate. These supports are 3D-printed using a FDM-printer (Ultimaker).

5.3.2. Suction surface

During the experimental validation, only the suction surface including the suction tips from the final design are used since only performance is tested. This means that the rotation of the suction surface is not required during testing. For that reason, the suction surface is modified for experimental validation. The axis is removed and a new attachment hole is made in which a wire is attached to the force sensor which is attached to the linear stage. The suction surface is 3D-printed by a SLA-printer (Formlabs 3B) with a layer thickness of 0.1 mm. SLA 3D-printing was chosen because it results in precise and airtight prints, which FDM printing does not guarantee. On the distal side of the suction surface, cut-outs are made in which the suction tips fit. The number of cut-outs corresponds to the number of suction tips that are used. In total 3 suction surfaces are printed; using 1 suction tip, 3 suction tips and 4 suction tips. The exact dimensions can be found in Appendix I (Figure 73,74,75).

5.3.3. Suction tips

The experimental validation consists of 3 different suction surfaces containing different number of suction tips. A suction surface is printed for the use of 1, 3 and 4 suction tips. For these suction tips, different molds are printed. The dimensions of each suction tip can be found in Appendix I (Figure 76, 77, 78).

5.3.4. Suction chambers

4 syringes (INJECTOMAT 50 ML standard) are used as suction chambers during the experimental validation (Figure 43). By pulling the syringes, the volume increases and thus a negative pressure is generated. A silicone suction tube with an inner diameter of 2 mm is attached to the needle of the syringe. This other end of the silicone tube is attached to each hole of the suction surface. An extra silicone layer is placed in this hole to ensure the connection is airtight. The syringes must be mounted on the table in order to be able to pull all 4 syringes simultaneously. This mount and corresponding pulling handles (Appendix I Figure 82, 87) are 3D-printed using FDM printing with an Ultimaker with a line thickness of 0.2mm and an infil of 20%. As a result of the large dimensions of this mount, FDM printing is chosen for its shorter printing time.

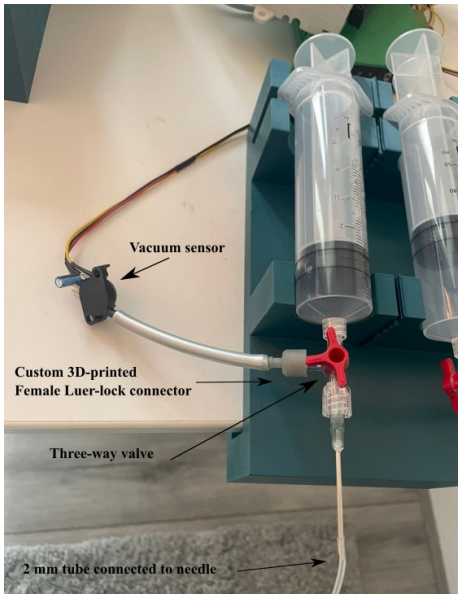

Figure 43: The linear stage including custom 3D-printed support to hold it upright and stabilize it. This support also contains a slot in which the container of the gelatine phantom tissue is placed.

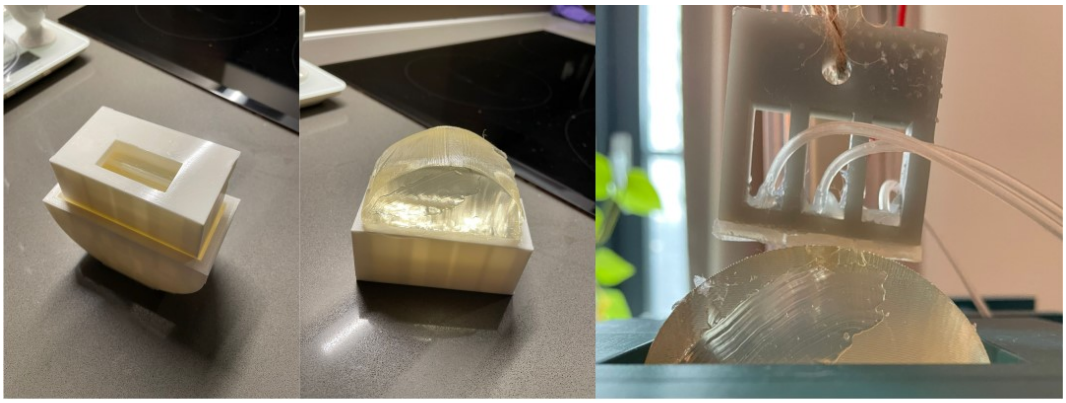

Figure 44: Multiple steps on how the curved gelatine mold is used. A: The top mold is placed into the curved bottom mold. The solved gelatine (in warm water) is poured into the hole in the top mold. Gelatin is placed in the fridge for at least 4 hours. B: The bottom (curved) mold is removed gently by cutting the edges of the gelatine with a knife. C: The gelatine is placed inside the gelatine container slot of the support of the stage.

5.3.5. Data acquisition

Between the linear stage platform and the suction surface, a load cell is placed (FUTEK, model FLLSB200). This load cell measures the pulling force that is required to pull the suction surface from the tissue. The load cell is attached to the linear stage platform with an M3 bolt. On the bottom part of the load cell, an M3 screw hook is connected. A looped wire around this screw hook and the hole in the suction surface connects the load cell and the suction surface. This wire assured that the suction surface could move freely and that the load cell is not rigidly connected to the suction surface. To measure the vacuum pressure in each suction chamber, a pressure sensor with a range of 0-115 kPa is used (NXP, model MPX4115AP). The pressure sensor is connected by 6mm diameter tubing (FESTO PAN-6X1 6mm). However, due to a worldwide semiconductor shortage during this research, only 3 pressure sensors could be collected. Each suction chamber is connected to a three-way valve (Figure 43). This three-way valve connects the pressure sensor and the suction tube to the suction chamber. To be able to connect the pressure sensor to this three-way valve, a connecting Luer lock piece is 3D-printed using the SLA printer (Appendix I). The load cell and the pressure sensors are connected to an analogue signal converter (CPJ RAIL, SCAIME) and a 30 Hz sample rate data acquisition unit (NI USB-6008, National Instruments Corporation)

5.4. Experimental protocol

Gelatine was used as phantom tissue that resembles the stiffness of 3 types of tissues. This gelatine was poured into the gelatine holder which is shown in Appendix I (Figure 81). This 3D-printed gelatine holder contains grooves to prevent the cured gelatine from pulling out during the experiment. This mold only functions for the flat phantom tissue. To cure gelatine in the desired 80 mm diameter curvature and the 200 mm curvature, a top and bottom mold are made (Figure 44A). The bottom molds (Appendix I: Figure 84 and Figure 85) are designed with the correct curvatures. On top of this, a top mold is placed (Appendix I: Figure 86). This mold has a hole in the middle in which the gelatine can be poured. This part also contains grooves to fix the gelatine when this is cured. After curing, the curved bottom mold is removed. The remainder is shown in Figure 44B. This mold is placed into the corresponding slot in the stage support and can now be used for the experiments (Figure 44C).

Since gelatine degrades over time, the used gelatine is created at least one day before testing. The amount of gelatine used depends on the stiffness of the phantom tissue. In the second test, tissue stiffness varied between

Table 1: Tissue stiffness of tissue types that can be encountered during MIS including the corresponding percentages of gelatine solved in water.

Tissue type	Stiffness	Percentage gelatine
Kidney/Brain	5 kPa	5 wt%
Liver/intestine	20 kPa	13 wt%
Skel. muscle/intestine	35 kPa	18 wt%

5 kPa, 20 kPa and 35 kPa. To cure the gelatine with a certain stiffness, the amount of gelatine used per unit of water can be varied. Tabel 1 gives an overview of how much percentage of the total volume should consist of gelatine. The correct gelatine surface is placed into the gelatine holder slot of the support.

After this, the suction surface is connected to the force sensor using a wire. This wire is untensioned at the start of every measurement as this prevents premature tension before measuring. Subsequently, the sensors are calibrated. The vacuum sensors are calibrated on the air pressure of the room the tests are performed. The force sensor is calibrated in a way that the weight of the suction surface and wire are subtracted. The suction tubes of the suction surface are connected to the syringes. This is achieved by sliding the tubes onto the syringe needles. Next, the suction surface is slightly pressed onto the gelatine. While pressing, the syringes are pulled backwards until the desired pressure is achieved (50 kPa) and is kept in place at that point. The air pressure and suction force are monitored live in LabVIEW 2018. Subsequently, the linear stage, which is controlled by a laptop using Q-Programmer software, moves upwards with a constant speed of 800 revolutions per second. Table 2 & 3 give an overview of the performed tests and the different substrate conditions. Every test is performed 5 times. In total, 105 tests are performed.

5.4.1. Data analysis

The experimental data is analyzed as follows. The LabVIEW data is saved and converted into Excel where the data is converted into attachment force versus time graphs and corresponding vacuum pressure versus time graphs. These graphs show behaviour of the vacuum pressure per

Table 2: Test protocol of Experiment 1. These tests are performed on different curved gelatine substrates with a stiffness of 20 kPa. The different curvatures that are used are flat, 200 mm and 80 mm. 5 tests per condition are performed.

1 suction	3 chambers	4 chambers
flat	flat	flat
200 mm	200 mm	200 mm
80 mm	80 mm	80 mm

Table 3: Test protocol of Experiment 2. These tests are performed on a 200 mm diameter curved gelatine surface. The amount of suction tips and gelatine stiffness is varied during these tests. 5 tests per condition are performed.

1 chamber	3 chambers	4 chambers
5 kPa	5 kPa	5 kPa
20 kPa	20 kPa	20 kPa
35 kPa	35 kPa	35 kPa
rigid	rigid	rigid

suction tip during pulling. An example of these graphs is shown in Figure 45. In the upper graph the output of the vacuum sensors are shown over time. The graph starts at a vacuum pressure of 50 kPa. In the graph below the attachment force is plotted over time. First, the wire which is attached to the force sensor tightens and does not influence the attachment force. These graphs can be used to analyze leakage in a certain suction tip. From these graphs, maximum attachment forces are extracted which are reported in a separate excel sheet. The data is analyzed using a one-way ANOVA test to test if there are significant differences in maximum attachment force using different substrate curvatures or stiffness. This test is also used to test the differences when a different amount of suction tips is used for the same curvature or stiffness. The data differs significantly when the p-value is less than 0.05.

5.5. Results

5.5.1. Experiment 1: Varying curvature

The first experiment used different curvature diameters as independent variable with a stiffness of 20 kPa. The results show a higher mean attachment force on flatter

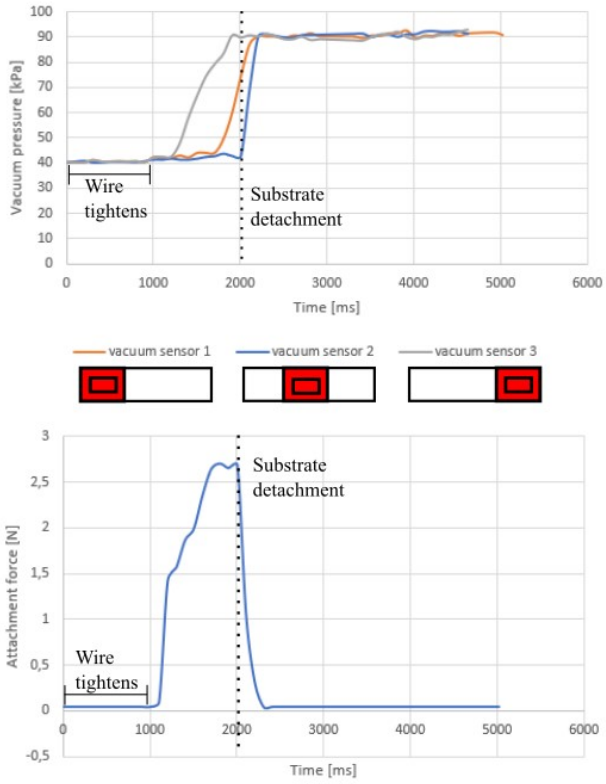

Figure 45: Graphs used when analysing the data from each test. The upper graph is the result of the vacuum pressure sensors. Vacuum sensor 1 and vacuum sensor 3 always represented the two outer suction tips (also when using 4 suction tips). The lower graph represents the attachment force against time. From this graph substrate detachment can registered when substrate detachment occurs.

curvatures with the highest on complete flat. This also means that when the curvature diameter decreases (gets more steep), the mean attachment force decreases. Furthermore, more suction chambers & tips also result in higher mean attachment forces in combination. The mean maximal attachment force are plotted is suction tip in Figure 46.

The average maximum attachment force including standard deviation per curvature is shown in Table 4. A one-way ANOVA test shows the difference between maximum attachment forces on different curved phantom tissue. This test is performed for 1 tip/chamber, 3 tips/chambers

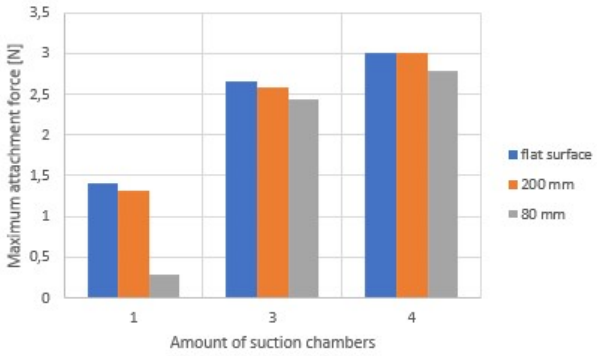

Figure 46: The mean maximal attachment force of a different amount of suction chambers versus different tissue curvature diameters on gelatine of with a stiffness of 20 kPa.

Table 4: Average maximum attachment force including standard deviation in different substrate curvatures with a stiffness of 20 kPa and amount of suction chambers.

	1 chamber	3 chambers	4 chambers
flat	1,4 ± 0,37N	2,7 ± 0,4N	3 ± 0,3N
200 mm	1,3±0,34N	2,6 ± 0,2N	3 ± 0,15N
80 mm	0,28 ± 0.15N	2,44 ± 0,3N	2,78 ± 0,24N

and 4 tips/chambers; [F(2,15)= 32.0584, p=3.83e-6], [F(2,12)=0.646, p=0.5415], [F(2,12)=0.2918, p=0.2918]. This shows that the differences between attachment performance only when using 1 suction tip are significant. When using 3 or 4 suction tips, the maximum attachment force does not differ significantly when changing the tissue curvature (p-value larger than 0.05). Subsequently, another one-way ANOVA is performed to examine if there is a significant difference when a different amount of suction tips is used on the same curved substrate. For respectively flat, 200 mm diameter and 80 mm diameter; [F(2,12)=27,1196, p=0,00003535], [F(2,12)=56,2058, p=8,052e-7], [F(2,12)=194,2111, p=7,244e-10]. This means that using more suction tips on the same curved substrate increased performance significantly.

5.5.2. Experiment 2: varying stiffness

In experiment 2 the gelatine substrate is varied in stiffness. The curvature of this substrate is fixed on 200 mm diameter. Figure 47 gives an overview of the per-

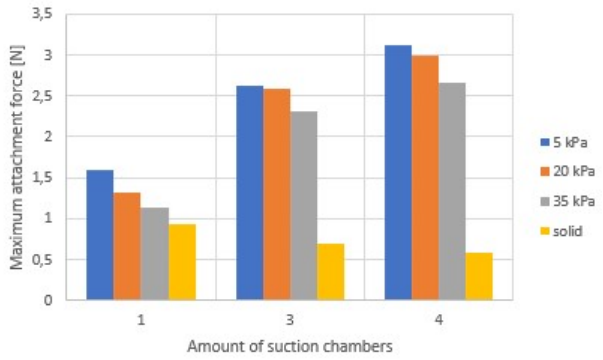

Figure 47: The mean maximal attachment force of a different amount of suction tips & chambers versus different tissue stiffness on gelatine of with a curvature diameter of 200 mm.

Table 5: Average maximum attachment force including standard deviation for different tissue stiffness and amount of suction tips & chambers

	1 chamber	3 chambers	4 chambers
5 kPa	1,6 ± 1,43N	2,62 ± 0,34N	3,12 ± 0,27N
20 kPa	1,32±0,34N	2,58 ± 0,25N	3 ± 0,16N
35 kPa	1,14 ± 0,11N	2,32 ± 0,3N	2,66 ± 0,42N
Rigid	0,94 ± 0,27N	0,7 ± 0,28N	0,58 ± 0,37N

formance of each amount of suction tips/chambers on these different stiffnesses. Table 5 represents the mean of each test with the corresponding standard deviation. A one-way ANOVA test shows if there is a significant difference between different substrate stiffnesses within the same used amount of suction tips/chambers. For respectively 1 suction tip/chamber, 3 suction tips/chambers and 4 suction tips/chambers; [F(3,16)=5,4537, p= 8,9e-4], [F(3,16)=48,8973, p = 2,781e-10], [F(3,16)=68,6732, p=2,35e-10]. This means that within the same amount of suction tips, the results when changing substrate stiffness differ significantly. To see if there is a significant difference using the same substrate stiffness but using a different amount of suction tips, another one-way ANOVA is performed. Using different amounts of suction tips resulted for respectively 5 kPa, 20 kPA, 35 kPa and solid; [F(2,12)=34,0984, p=1,1e-5], [F(2,12)=56,2058, p=8,052e-7], [F(2,12)=33,73, p=1,2e-5], [F(2,12)=1,7379, p=0,2173]. This means that there is a significant difference when using a different amount of suction tips on the same substrate. However, this is not the case when a solid surface is grasped.

6. Discussion

6.1. Performance

This design study resulted in a suction grasper with a stiff suction surface for MIS using multiple suction tips and chambers. The use of a stiff suction surface prevents unwanted deformations like inward slip that result in leakage. After inserting the instrument through a trocar with an inner diameter of 10 mm, the surgeon can rotate the suction surface to enlarge it. Maximum attachment force was the main measurement during experimental validation. Since a solid suction surface is used, it is hypothesized that a stiff suction surface is prone to leakage on the outer sides of the suction surface. This is due to when the surface of the tissue is curved, the surface can not deform and will not be able to correctly seal this surface. Therefore, experiments are performed on different tissue curvatures and different stiffnesses to examine how this suction surface performs. The maximum measured attachment force of the suction surface is 3,12 ± 0,27N. This does not meet the requirement of 5 N (**R2**). While theoretically this requirement should be met, the lower attachment forces can be explained. Since the suction surface is solid it can not deform to the surface of the tissue. To enhance sealing with the tissue, silicone suction tips are used. In order to fit through the shaft of the instrument, the suction tips are shaped like a small rectangle. Because of this, the edges of the suction tips

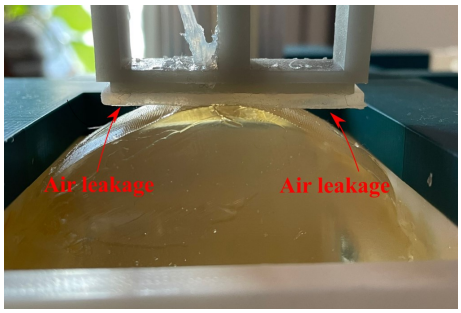

Figure 48: The mean maximal attachment force of a different amount of suction tips & chambers versus different tissue stiffness on gelatine of with a curvature diameter of 200 mm.

are thin (1 mm). These thin edges are prone to leakage since they collapse when compressed which results in leakage. Regardless the centered suction tips seal for a longer period of time compared to the outer suction tips, leakage occurs before full suction tip potential could be reached. However, the results clearly state that using multiple suction chambers compared to using only a single suction chamber with a similar shaped suction tip increase attachment performance significantly. Figure 51 shows the ability of the suction surface on objects with different shapes, sizes and textures.

During experiment 1 it was noticeable that if one suction chamber is used instead of using multiple, the maximum attachment force significantly decreases. This can also be seen when looking at Figure 46 and Table 4. When the suction surface with only 1 suction chamber is pulled from the tissue, the outer edges are quickly exposed which resulted in total vacuum loss. Especially with steeper curvatures like 80 mm diameter, this results a low mean attachment force of 0,28N. When using a steep curvature like 80 mm diameter, the suction surface had to be pressed into the gelatine substrate in order to seal all suction tips. However, the gelatine deformed back to its initial shape quickly after this pressure is released (Figure 48).

The use of one suction chamber resulted in early leakage resulting in a low attachment force. The use of 4 suction chambers compared to the use of 3 suction chambers, resulted in slightly higher attachment forces. During testing, it was noticeable that the most centred suction tips hold their sealing and attachment force longer than the outer suction tips. This can also be seen when looking at the vacuum pressure graphs of the

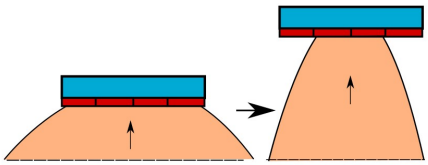

Figure 49: Tissue stretches when being pulled. When tissue reaches maximum elongation, detachment at the outer suction tips occurs. After this, the centered suction tips detach.

suction tips. The suction surface with 4 suction chambers performed better compared to the suction surface with 3 suction chambers (on average 0,3N), although the total effective suction area of the suction surface with 3 suction chambers is larger compared to the suction surface with 4 suction chambers which should lead in a higher total suction force (Equation 1). Two causes can be found in this experiment. Firstly, the transformation of the gelatine back to its initial curvature results in leakage at both of the outside suction tips. This means that only 1 chamber is still effective for the suction surface with 3 chambers and 2 chambers are still effective for the suction surface with 4 suction chambers. This means that, just before detachment, the total suction area using 4 suction tips is larger compared to using 3 suction tips (Figure 32) which results in a larger attachment force. Secondly, the phantom tissue in experiment 1 has a stiffness of 20 kPa. This means that it slightly stretches more compared to the 45 kPa stiffness when it is being pulled. The phantom tissue deformation increases the chance of tissue detachment, especially on the outer suction tips (Figure 49). That 4 suction chambers show higher performance on steep curvatures compared to using only 3 suction chambers can also be seen from the vacuum pressure and force graphs (Figure 50). 4 suction chambers are able to exert an attachment force for a longer time, which results in a higher attachment force.

During the experiment 2, the tissue stiffness was varied to examine if this affects the attachment force when using a solid suction surface. Figure 49 shows how substrate tissue reacts when it is being pulled when it has lower stiffness. Results show that the lower the stiffness, the higher the maximum attachment force (Figure 47 and Table 5). This can be explained by the fact that less stiff tissue stretches more and shapes to the suction tip for better sealing. Using 4 suction chambers significantly increases attachment force compared to using 3 suction chambers. The 2 centered suction tips were able to maintain a longer attachment force compared to the 1 centered suction tip when using 3 suction tips. This can be explained by the fact that there are two central located suction tips that grasp the tissue instead of only one. When one fails, the other central located suction tip can still hold on to the tissue. Adding to this, the two central suction tips combined have a larger surface area

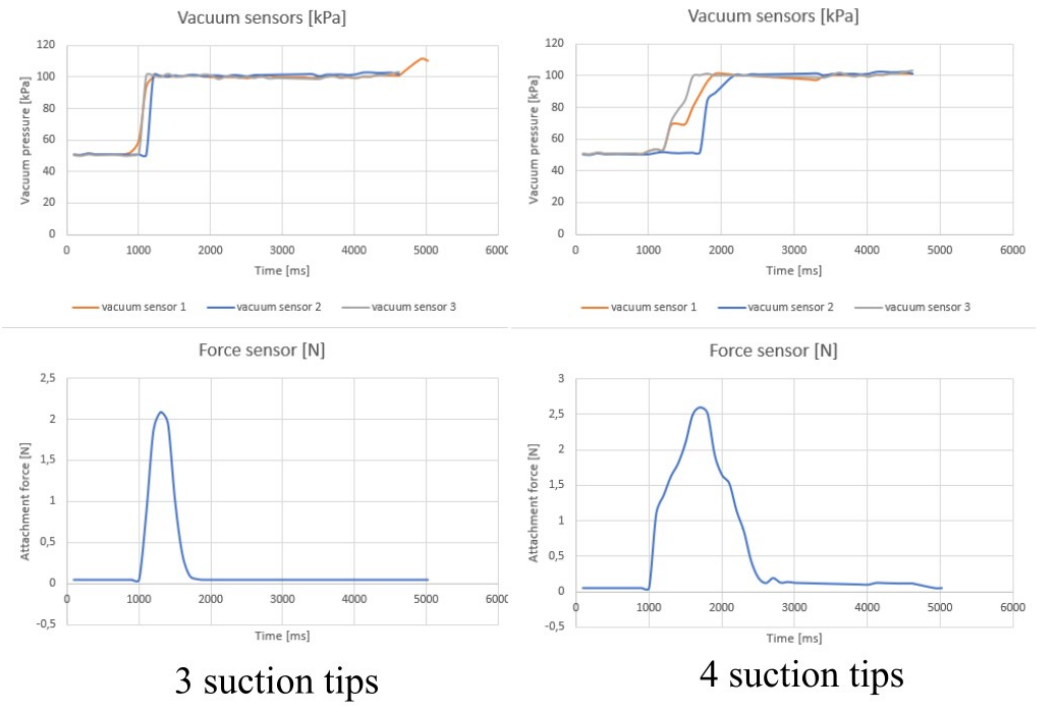

Figure 50: Comparison of 3 suction tips versus 4 suction tips when testing at gelatin tissue of 80 mm curvature and 20 kPa stiffness. Left: suction surface with 3 suction tips and suction chambers. Right: suction surface with 4 suction tips and chambers. The two centered suction tips are able to adhere longer to the substrate which results in a higher attachment force.

compared to the single centered suction tip (Figure 32).

6.2. Limitations

6.2.1. Device limitations

The designed prototype demonstrates the rotating mechanism of the suction grasper. After using the prototype and after testing the suction surface some limitations showed up. The main limitation of the instrument is that despite the v-grooves at the axis, the cable randomly slips when the rotation of the suction surface is resisted. However, the tensioning mechanism increases the friction, the friction between the 3D-printed axis and the nylon wire is not large enough. Adding to this, the device will be used in an environment where it gets lubricated with bodily fluids. This will only decrease the friction coefficient between these two parts.

The instrument is not prototyped with the correct shaft length. This means that the shaft length of the prototype is not tested with a shaft length of 30 cm. Because of the maximum dimensions of the used SLA printer, the prototype is printed with a shaft length of 12 cm. The eventual design consists of a 35 cm shaft. Through this shaft, long and thin-walled suction tubes connect the suction surface and suction chambers. These suction tubes however are prone to buckling. This however can be solved by using thin-walled steel tubes instead of silicone tubes, or 3D-print air channels inside the shaft of the instrument.

6.2.2. Experiment limitations

The experimental validation gave insight into the suction capacity of the instrument. However, several limitations can be noted. Firstly, the number of tests that are used

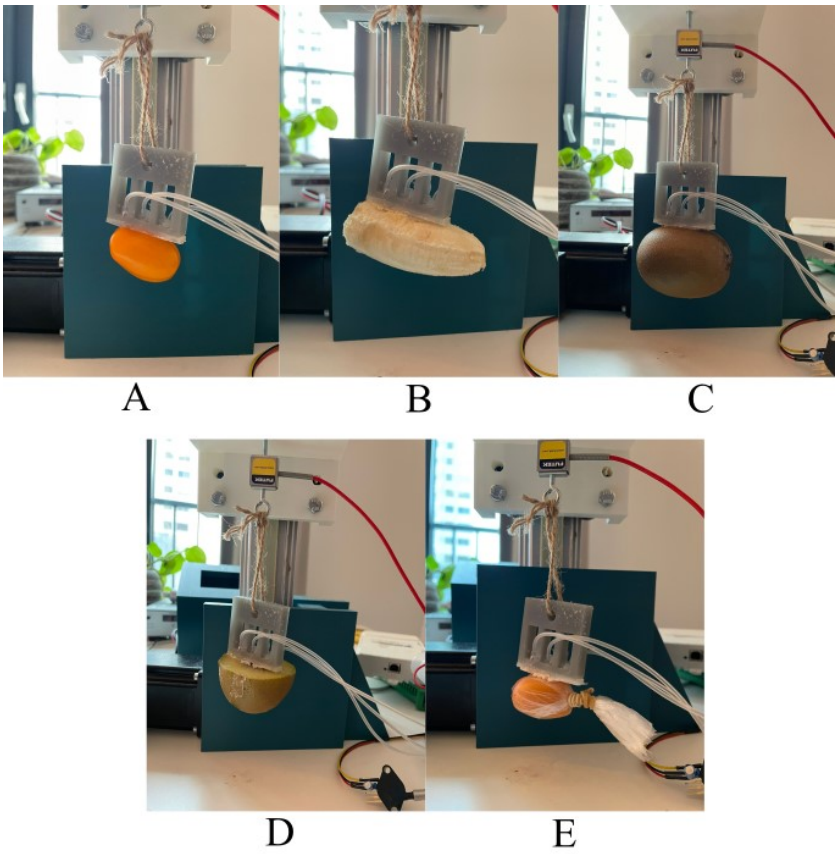

Figure 51: Testing the suction surface on different object characteristics. Texture of the objects are varied. A: Cherry tomato, B: Banana without peel, C: Kiwi, D: inside of a sliced kiwi, E: Cherry tomato wrapped tightly with a sandwich bag to mimic a membrane

to describe the suction capacity of the instrument was restricted. A larger sample size is needed to validate the outcomes to produce more precise conclusions. Another limitation during this experimental validation was the use of syringes as suction chambers. 4 syringes were used at the same time during the validation of the suction surface with 4 suction tips. These syringes are pulled simultaneously to generate a negative pressure. Despite 3D-printed pullers (Appendix I Figure 87) are used to generate a negative pressure, it was not possible to exactly pull each syringe to a negative pressure of 50 kPa simultaneously. Also, not enough vacuum sensors are used to measure when 4 suction chambers are used. Because of a worldwide semiconductor shortage only 3 pressure sensors could be used. Since leakage does occur most often at the outer suction tips, it is chosen to only use 1 pressure sensor in the 2 centered suction tips when using 4 suction tips.

Gelatine substrate is used to mimic human tissue. This is performed by varying the stiffness and curvature diameter between the range of human tissue that can be found during MIS. Despite stiffness and tissue curvature, other variations in tissue surface can be found. For example, bowel tissue contains a membrane that might interact differently with the suction surface compared to gelatine tissue [34]. For that reason, a single test is performed by wrapping a thin plastic sandwich bag over the gelatine substrate to mimic this membrane and around the grasped cherry tomato (Figure 51). This increased

the maximum attachment force compared to grasping gelatine substrate, since the membrane is getting sucked into the suction tip sealing is enhanced. However, more profound testing should give better insights.

The wire that is used to tighten the force sensor and the suction surface during testing is attached to the centered hole of the suction surface. From testing, it became clear that if a suction tip at one side leaks and detaches, the suction surface rotates around the centered hole to the side that still is adhered to the tissue. This results in an increase of shear forces between the suction tip and the gelatine tissue.

6.3. Experiment recommendations

The experimental validation in this thesis solely focused on the attachment performance of the suction surface. Future research should validate the performance of the use of the complete instrument. This will give more profound insights into how the instrument could be used by the surgeon. Furthermore, in future testing, the suction surface should be attached through holes on both ends to prevent surface rotation. Lastly, it would be interesting the test the performance of this suction tip on tissue that mimics real human tissue more precisely than gelatine substrate. However the gelatine substrate did a good job mimicking stiffnesses and curvatures, the different textures of the organs and other human tissue were hard to implement. This will also evaluate how the suction surface performs when in an environment covered with e.g. blood. Also, the suction surface attachment membrane in this test is performed on gelatine and a tomato covered with a thin plastic bag. This recreates the thin layer of the membrane sufficiently but is not as delicate as a real membrane. These additional experiments will further improve the validation of this instrument.

6.4. Design recommendations

6.4.1. Suction surface rotation

For the instrument, a number of development steps are recommended in this section to further increase the performance of this instrument. First, the design of the rotation mechanism must be improved in order to prevent slip while rotating the cables. When slip occurs, the suction surface can not be rotated and the instrument can not be used. In section 6.2.1 it is mentioned that when the cable and instrument are used in lubricated environments, the cable tends to slip. The goal of the designed mechanism is to rotate the suction surface to an open and closed configuration, which works. However, when a moment is applied to the suction surface, the cable does not exert enough friction to counter this moment. To further develop the instrument, this would be a helpful feature when grasping or stabilizing tissue during MIS. Cable slip is prevented by increasing the friction between the cable and the axis. Rubber in combination with a solid material or silver on silver gives high friction coefficients [35] [36]. However, these friction coefficients are based on the fact that both materials are dry. It is not guaranteed both materials will remain dry during surgery. Since the suction surface only rotates on one plane, solid beams can be used to rotate the suction surface. This way slip is not possible. However, solid beams were considered in the designing phase during this thesis, but then dimensional issues were decisive to choose a mechanism based on cables. Appendix J proposes an idea with solid beams attached to hinges

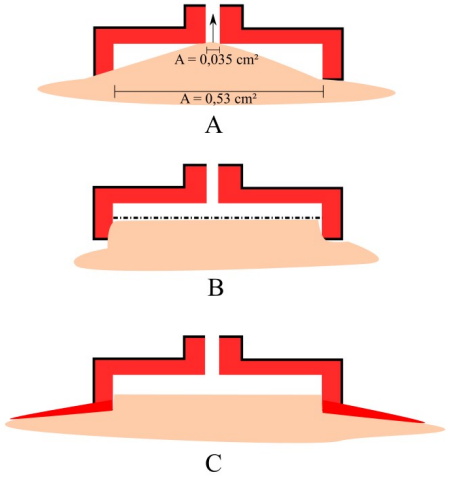

Figure 52: A cross sectional view of the suction tip when it is grasping human tissue. A: The effective suction area and thus the suction force decreases when tissue blocks the suction tube outlet. B: When a mesh is placed between the suction outlet and the suction tip edges, tissue is not able to block the suction outlet. C: Membranes at the suction tip edges improve sealing and block air passages towards the suction chamber.

are used to rotate the suction surface. Lastly, the sliding mechanism using the handles and the spring of the final model is not validated using a prototype. This prototype will give insights into ergonomics and functionality.

6.4.2. Suction tip optimization

During testing it became clear that the suction tips can be improved to further increase performance. Firstly, when tissue consists of a membrane or tissue stiffness is low, it sometimes gets sucked into the suction tip (Figure 52A). This decreases the effective suction area since the membrane seals the suction opening of the suction tube inside the suction tip. This can be prevented by using a mesh that covers the suction outlet of the suction tip (Figure 52B). If the mesh is placed between the suction outlet and the contact surface of the suction tip, the tissue can slightly be sucked into the suction tip (which increases sealing) but is not able to close to decrease the suction area by sealing the suction outlet. Another issue that occurred using these suction tips is that the edge of the suction tip caused leakage not wide enough. The dimensions of the suction tips including the edge thickness were chosen as a trade-off between edge thickness and the suction area within a fixed surface area (Figure 32). Another option to increase sealing is to add thin flexible membranes on the outer edges of the suction tip (Figure 52C). This membrane forms to the surface of the suction surface and decreases the chance of air pathways forming towards the suction chamber [6] [37]. If the membrane is thin and flexible, it does interrupt rotating the device to a closed or open position. Lastly, the suction tips can be improved to prevent shear movement between the tissue and the suction tip. This can be achieved by placing micro-structures on the edges of the suction tip that increase the friction coefficient. These can be found on a variety of fishes or the octopus that are able to clamp themselves on e.g. rocks using biological suction discs [12] [38] [39] [40].

6.4.3. Suction chambers

Furthermore, the suction chambers should be developed. The syringes were used only for experimental validation. Vacuum pressure can be actuated manually or automatically. The advantage of using manual actuation is that the suction chambers can be attached to the instrument, for example using a hand-actuated pump [41]. This means that the instrument itself is not connected to an external pump by suction tubes which enhances the mobility of the surgeon using the instrument. The downside of using manually actuated suction chambers on the instrument is that it takes force to reach a negative pressure of 50 kPa, which destabilizes the instrument while inside the patient's body and is hard for the user to achieve. Because multiple suction chambers are required, the surface area of the suction chamber becomes small which results in a high required force 1). However, a new handle design compared to the KIWI vacuum pump (Appendix A Figure 55) offers a solution. This instrument enables the surgeon to squeeze the handle multiple times using silicone valves to build up negative pressure using a one-way air outlet. The suction tubes can also be attached to an automated vacuum system which is placed in the operating room. The vacuum pump automatically sucks air away until a sufficient amount of suction tips are sealed and reach a negative pressure of 50 kPa. Appendix K elaborates on different vacuum generation systems. However, these automated vacuum systems can not be used for MIS since it sucks air and gasses away from the peritoneum. Appendix K also proposes a schematic design of an automated plunger system to generate a negative pressure in a closed system in which air can not transfer to the atmosphere. Lastly, an additional design process is required for tissue detachment of the suction tips. It should be examined if equalizing the vacuum pressure with the environmental pressure is enough to detach the tissue correctly before retracting the instrument from the patient's body.

7. Conclusion

The goal of this thesis was to design a suction-based grasper for MIS using a stiff suction surface while minimizing the consequences of leakage. The suction surface of the instrument is able to fit through a trocar of 10 mm but must be able to increase its suction surface once it is inside the patient's body. To achieve this, a single central-located rotational hinge is used to rotate the stiff suction surface. Multiple suction chambers connected to multiple suction tips are used to minimize the chance of tissue loss when leakage occurs. The silicone suction tips are attached to the rotational suction surface which

increases sealing between the suction tip and the tissue. To ensure patient safety, the suction surface is covered by an outer shaft while inserting the instrument into the patient's body. To provide insights into the performance of the suction surface using a different number of chambers and substrate characteristics, experiments are performed. Since a stiff suction surface is used, it is hypothesized that varying tissue stiffness and tissue curvature influence sealing. This experimental validation showed a maximum attachment force of 3,12 ±0,27N using 4 suction tips on a gelatine substrate with a stiffness of 5 kPa. The use of multiple smaller suction tips connected to multiple suction chambers significantly increases attachment performance compared to one larger suction tip connected to one suction chamber. To conclude, this design introduces a base for future research in developing a multiple-suction chamber grasper using a stiff suction surface.

References

[1] Chapelle et al. "Trocar types in laparoscopy". In: *Cochrane Database of Systematic Reviews* 12 (2015). Publisher: John Wiley & Sons, Ltd. ISSN: 1465-1858. DOI: 10.1002/14651858.CD009814.pub2.

[2] D. Vonck. "The feasibility of vacuum technique in minimal invasive surgery: Improving the patient safety through instrument design". In: (2013).

[3] D. Vonck et al. "Vacuum grasping as a manipulation technique for minimally invasive surgery". In: *Surgical Endoscopy* 24.10 (2010), pp. 2418–2423. ISSN: 0930-2794. DOI: 10.1007/s00464-010-0967-4.

[4] E. W. L. Jansen et al. "Coronary artery bypass grafting without cardiopulmonary bypass using the octopus method: results in the first one hundred patients". In: *The Journal of Thoracic and Cardiovascular Surgery* 116.1 (July 1998), pp. 60–67. ISSN: 0022-5223. DOI: 10.1016/S0022-5223(98)70243-0.

[5] Singh et al. "Making octopus tissue stabilizer more effective, a valuable technique". en. In: *Indian Journal of Thoracic and Cardiovascular Surgery* 29.1 (2013), pp. 52–54. ISSN: 0973-7723. DOI: 10.1007/s12055-013-0189-1.

[6] A. Tiwari and B. N. J. Persson. "Physics of suction cups". In: *Soft Matter* 15.46 (Nov. 2019). Publisher: The Royal Society of Chemistry, pp. 9482–9499. ISSN: 1744-6848. DOI: 10.1039/C9SM01679A.

[7] V. Kortman. "A Suction Based Tissue Gripper for Minimally Invasive Surgery". In: (2021). URL: https://repository.tudelft.nl/islandora/object/uuid:ce4849d5-0dc7-4f0c-9491-d81c87ee7161?collection=education.

[8] T. Limperg et al. "Laparoscopic Trocar Dimensions: Marketed Versus True Dimensions – a Descriptive Study". In: *Journal of Minimally Invasive Gynecology* 28 (Nov. 2021), S79. DOI: 10.1016/j.jmig.2021.09.509.

[9] Chang Yeon Jung et al. "Trocar Size Selection for Trans-Trocar Appendix Removal in Laparoscopic Appendectomy". In: *Journal of Minimally Invasive Surgery* 17.1 (2014), pp. 1–4. DOI: 10.7602/jmis.2014.17.1.1.

[10] M. Osaki et al. "Transformable lung positioner for thoracoscopic surgery". In: *2011 IEEE/SICE International Symposium on System Integration (SII)*. Dec. 2011, pp. 138–143. DOI: 10.1109/SII.2011.6147434.

[11] T. Takayama, K. Kuroda, and T. Omata. "3P1-C02 Suction Hand for Grasping Large Internal Organs for Laparoscopic Surgery(Medical Robotics and Mechatronics (2))". In: *The Proceedings of JSME annual Conference on Robotics and Mechatronics (Robomec)* 2014 (May 2014), _3P1–C02_1. DOI: 10.1299/jsmermd.2014._3P1-C02_1.

[12] D. K. Wainwright et al. "Stick tight: suction adhesion on irregular surfaces in the northern clingfish". In: *Biology Letters* 9.3 (June 2013). Publisher: Royal Society, p. 20130234. DOI: 10.1098/rsbl.2013.0234.

[13] Y. Chuang et al. “Climbing upstream: Multi-scale structural characterization and underwater adhesion of the Pulin river loach (Sinogastromyzon puliensis)”. en. In: *Journal of the Mechanical Behavior of Biomedical Materials*. Biological Articulated Structures and Protective Designs 73 (Sept. 2017), pp. 76–85. ISSN: 1751-6161. DOI: 10.1016/j.jmbbm.2017.01.029.

[14] L. Briones, P. Bustamante, and M. A. Serna. “Robicen: A wall-climbing pneumatic robot for inspection in nuclear power plants”. en. In: *Robotics and Computer-Integrated Manufacturing* 11.4 (Dec. 1994), pp. 287–292. ISSN: 0736-5845. DOI: 10.1016/0736-5845(95)00005-4.

[15] H. de Visser et al. “Forces and displacements in colon surgery”. eng. In: *Surgical Endoscopy* 16.10 (Oct. 2002), pp. 1426–1430. ISSN: 1432-2218. DOI: 10.1007/s00464-002-9003-7.

[16] N. A. Scott et al. “Systematic review of beating heart surgery with the Octopus Tissue Stabilizer”. eng. In: *European Journal of Cardio-Thoracic Surgery: Official Journal of the European Association for Cardio-Thoracic Surgery* 21.5 (May 2002), pp. 804–817. ISSN: 1010-7940. DOI: 10.1016/s1010-7940(02)00075-1.

[17] A. Handorf et al. “Tissue Stiffness Dictates Development, Homeostasis, and Disease Progression”. In: *Organogenesis* 11 (Jan. 2015), pp. 1–15. DOI: 10.1080/15476278.2015.1019687.

[18] U. Kappert et al. “The application of the Octopus stabilizing system for the treatment of high risk patients with coronary artery disease”. eng. In: *European Journal of Cardio-Thoracic Surgery: Official Journal of the European Association for Cardio-Thoracic Surgery* 16 Suppl 2 (Nov. 1999), S7–9. ISSN: 1010-7940.

[19] I Alkatout. “Complications of Laparoscopy in Connection with Entry Techniques”. In: *Journal of Gynecologic Surgery* 33.3 (June 2017), pp. 81–91. ISSN: 1042-4067. DOI: 10.1089/gyn.2016.0111.

[20] H. J. Bonjer et al. “Open versus closed establishment of pneumoperitoneum in laparoscopic surgery”. en. In: *BJS (British Journal of Surgery)* 84.5 (1997), pp. 599–602. ISSN: 1365-2168. DOI: 10.1046/j.1365-2168.1997.d01-1355.x.

[21] D. E. Ott. “Abdominal Compliance and Laparoscopy: A Review”. In: *JSLS : Journal of the Society of Laparoendoscopic Surgeons* 23.1 (2019), e2018.00080. ISSN: 1086-8089. DOI: 10.4293/JSLS.2018.00080.

[22] O. H. M. Hypólito et al. “Creation of pneumoperitoneum: noninvasive monitoring of clinical effects of elevated intraperitoneal pressure for the insertion of the first trocar”. eng. In: *Surgical Endoscopy* 24.7 (July 2010), pp. 1663–1669. ISSN: 1432-2218. DOI: 10.1007/s00464-009-0827-2.

[23] S. V. Jackman and J. T. Bishoff. “Laparoscopic Instrumentation and Equipment”. In: *Minimally Invasive Urological Surgery*. Num Pages: 27. CRC Press, 2005. ISBN: 978-0-429-22105-7.

[24] V. Velanovich. “Laparoscopic vs open surgery: a preliminary comparison of quality-of-life outcomes”. eng. In: *Surgical Endoscopy* 14.1 (Jan. 2000), pp. 16–21. ISSN: 1432-2218. DOI: 10.1007/s004649900003.

[25] A. N. Supe, G. V. Kulkarni, and P. A. Supe. “Ergonomics in laparoscopic surgery”. In: *Journal of Minimal Access Surgery* 6.2 (2010), pp. 31–36. ISSN: 0972-9941. DOI: 10.4103/0972-9941.65161.

[26] M. Li et al. “Soft actuators for real-world applications”. en. In: *Nature Reviews Materials* 7.3 (Mar. 2022), pp. 235–249. ISSN: 2058-8437. DOI: 10.1038/s41578-021-00389-7.

[27] Y. Yang and Y. Chen. “Innovative Design of Embedded Pressure and Position Sensors for Soft Actuators”. In: *IEEE Robotics and Automation Letters* 3.2 (Apr. 2018). Conference Name: IEEE Robotics and Automation Letters, pp. 656–663. ISSN: 2377-3766. DOI: 10.1109/LRA.2017.2779542.

[28] L. Hrabovský et al. “Determination of the Coefficient of Friction in a Pulley Groove by the Indirect Method”. en. In: *Coatings* 12.5 (May 2022). Number: 5 Publisher: Multidisciplinary Digital Publishing Institute, p. 606. ISSN: 2079-6412. DOI: 10.3390/coatings12050606.

[29] O. M. Ikumapayi et al. “A Brief Overview of Bending Operation in Sheet Metal Forming”. en. In: *Advances in Manufacturing Engineering*. Lecture Notes in Mechanical Engineering. Singapore: Springer, 2020, pp. 149–159. ISBN: 9789811557538. DOI: 10.1007/978-981-15-5753-8_14.

[30] B Beake. “Modelling indentation creep of polymers: a phenomenological approach”. en. In: *Journal of Physics D: Applied Physics* 39.20 (Sept. 2006), p. 4478. ISSN: 0022-3727. DOI: 10.1088/0022-3727/39/20/027.

[31] E. Catsiff, T. Alfrey, and M.T. O’Shaughnessy. “Generalized Creep Curves for Nylon”. In: *Textile Research Journal* 23.11 (Nov. 1953). Publisher: SAGE Publications Ltd STM, pp. 808–820. ISSN: 0040-5175. DOI: 10.1177/004051755302301109.

[32] B. Mazzolai et al. “Octopus-Inspired Soft Arm with Suction Cups for Enhanced Grasping Tasks in Confined Environments”. en. In: *Advanced Intelligent Systems* 1.6 (2019), p. 1900041. ISSN: 2640-4567. DOI: 10.1002/aisy.201900041.

[33] M. Makhsous et al. “Investigation of Soft-Tissue Stiffness Alteration in Denervated Human Tissue Using an Ultrasound Indentation System”. In: *The Journal of Spinal Cord Medicine* 31.1 (Jan. 2008). Publisher: Taylor & Francis _eprint: https://doi.org/10.1080/10790268.2008.11753987, pp. 88–96. ISSN: 1079-0268. DOI: 10.1080/10790268.2008.11753987.

[34] T. Ranzani et al. “A soft suction-based end effector for endoluminal tissue manipulation”. In: *The Hamlyn Symposium on Medical Robotics* (June 2016).

[35] J. Plagge and R. Hentschke. “Numerical solution of the adhesive rubber-solid contact problem and friction coefficients using a scale-splitting approach”. en. In: *Tribology International* 173 (Sept. 2022), p. 107622. ISSN: 0301-679X. DOI: 10.1016/j.triboint.2022.107622.

[36] D. Kaneko et al. “Friction Coefficient between Rubber and Solid Substrate –Effect of Rubber Thickness–”. In: *Journal of the Physical Society of Japan* 76.4 (Apr. 2007). Publisher: The Physical Society of Japan, p. 043601. ISSN: 0031-9015. DOI: 10.1143/JPSJ.76.043601.

[37] S. Song et al. “Adaptive Self-Sealing Suction-Based Soft Robotic Gripper”. en. In: *Advanced Science* 8.17 (2021), p. 2100641. ISSN: 2198-3844. DOI: 10.1002/advs.202100641.

[38] M. Tietbohl. “Fishes that suck: comparison of the adhesive discs of three fishes of the Pacific Northwest”. en_US. In: (July 2014). Accepted: 2014-11-08T00:04:07Z Publisher: Friday Harbor Laboratories.

[39] P. Ditsche, D. K. Wainwright, and A. P. Summers. “Attachment to challenging substrates – fouling, roughness and limits of adhesion in the northern clingfish (Gobiesox maeandricus)”. In: *Journal of Experimental Biology* 217.14 (July 2014), pp. 2548–2554. ISSN: 0022-0949. DOI: 10.1242/jeb.100149.

[40] F. Tramacere et al. “Hairy suckers: the surface microstructure and its possible functional significance in the Octopus vulgaris sucker”. In: *Beilstein Journal of Nanotechnology* 5 (2014), pp. 561–565. ISSN: 2190-4286. DOI: 10.3762/bjnano.5.66.

[41] K. Groom et al. “A prospective randomised controlled trial of the Kiwi Omnicup versus conventional ventouse cups for vacuum-assisted vaginal delivery”. en. In: *BJOG: An International Journal of Obstetrics & Gynaecology* 113.2 (2006), pp. 183–189. ISSN: 1471-0528. DOI: 10.1111/j.1471-0528.2005.00834.x.

[42] M. C. Williams. “Vacuum-Assisted Delivery”. en. In: *Clinics in Perinatology*. Complicated Labor and Delivery I 22.4 (Dec. 1995), pp. 933–952. ISSN: 0095-5108. DOI: 10.1016/S0095-5108(18)30263-X.

[43] M. Deutchman. “Vacuum Extraction: A Necessary Skill”. en-US. In: *American Family Physician* 62.6 (Sept. 2000), pp. 1269–1276.

[44] F. White. *Fluid Mechanics*. English. 8th edition. New York, NY: McGraw-Hill Education, Jan. 2015. ISBN: 978-0-07-339827-3.

[45] C Pellerin. “Vacuum basics”. In: *Industrial Robot: An International Journal* 22.4 (Jan. 1995). Publisher: MCB UP Ltd, pp. 27–28. ISSN: 0143-991X. DOI: 10.1108/01439919510098434.

[46] N. S. Harris. *Modern Vacuum Practice*. English. 0 edition. London ; New York: McGraw-Hill, Mar. 1990. ISBN: 978-0-07-707099-1.

Appendices

A: Commercially available suction grippers for grasping human tissue

Several suction based grippers to grasp human tissue are currently on the market. However, none of these suction grippers are used for MIS. For that reason, suction grippers that are used to adhere to human tissue during surgery are mentioned in this section. Medtronic, one of the current market leaders in medical innovation and technology, designed the Octopus^{TM} Heart Stabilizer to stabilize the beating heart during an open-heart coronary bypass surgery (Figure 53) [16]. This surgery restores blood flow to the heart muscle by redirecting blood around a section of a blocked artery. Due to cardiac motion, the suturing of the anastomosis is jeopardized. For that reason stabilization is key. The instrument has a flexible, but stable shaft that can be positioned to approach the tissue from every angle. When the required position is acquired, the arm can be locked into this position. The suction head is split into two arms. These arms consist of four or five suction tips with an internal diameter of 6mm [4]. The arms are attached to two separate suction tubes which are connected to a vacuum pump. These two suction hoses enable the two arms to use separate vacuums to grasp tissue.Suction is activated and the suction tips are able to generate a negative pressure of 53 kPa [4]. This means that each suction tip generates a suction force of 1.5N under perfect conditions. However, sometimes the devices fails to maintain vacuum pressure with the tissue at one of the suction tips [5]. This is due to the fact that the suction tips do not fully enclose the heart tissue (Figure 4). When this occurs, vacuum pressure in the other suction tips will be lost since the same suction chamber is used. To compensate for this, the surgeons in this research, used continuous sucking of the vacuum pump. However, this results in continuous sucking of the heart tissue and tissue or blood surrounding this leaking suction tip. This is not desirable. The instrument by Medtronic is currently the market for open-heart surgery. Estech [**bertolero˙tissue˙2006**] and Terumo [**sharrow˙devices˙2004**] also designed comparable suction graspers with the same function.

In combination with the Octopus^{TM} Heart Stabilizer, Medtronic offers the Starfish^{TM} Heart Positioner (Figure 54) to further improve beating heart surgery. This device uses the same suction technology but is able to position and hold the beating heart in an orientation which is beneficial for the surgeon. After positioning the heart with the Starfish^{TM}, the Octopus^{TM} can be placed at the location of the targeted artery. The suction tip of the Starfish^{TM} is made from flexible silicon and is shaped to the apex of the heart to create sufficient sealing. Only a single suction surface is used. Because of the large suction surface, the suction force can be distributed.

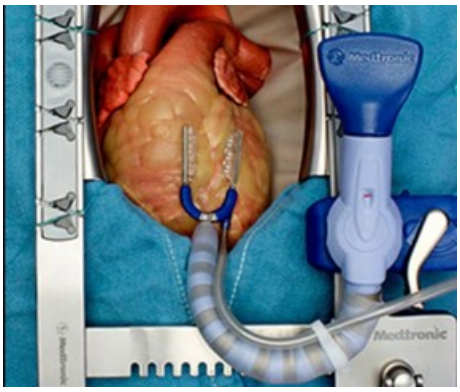

Figure 53: Octopus^{TM} provides stabilization of the heart during an open-heart surgery

Figure 54: Starfish^{TM} provides stabilization of the heart during an open-heart surgery and is able to assist the Octopus^{TM} with a larger suction force.

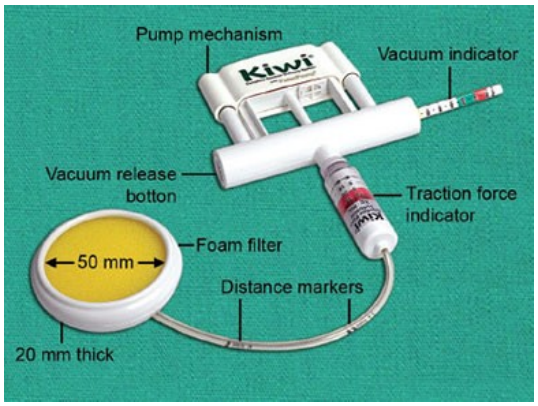

Figure 55: The Kiwi^{TM} [41] Vacuum Delivery System

The Kiwi^{TM} Vacuum Delivery System [41] (Figure 55) is a suction tip that used to help guide the baby out of the birth canal. The suction tip is placed between the anterior and posterior fontanelle, which is called the flexion point. Because the baby's head is still soft, it deforms slightly due to the pressure it receives during vaginal birth. When a vacuum extractor is used, the head also deforms slightly due to negative pressure and gets slightly sucked into the suction tip. This is called Chignon [42] and improves the sealing. This is, to a certain extent, not harmful for the baby [43]. The device is able to create a vacuum up to 0.8 bar (80 kPa), which is an optimal balance between damaging consequences of Chignon and generating suction force. Combining this with a large suction surface of 50mm creates a large suction force up to 245 N. The suction tip itself is made from hard plastic and relies on the chignon effect to create sufficient sealing. The inside of the suction tip is a soft and spongy material. The suction force is generated manually. This can be done by pressing down the pump mechanism with the palm of the hand. Air is stored in the handle and is pushed out by a piston when the handle is pressed down. Because the in contains a one-way valve, air molecules can only be pushed out. This way, a vacuum can be created.

All these instruments consist of a single suction tip or multiple that are actuated by a single vacuum source. Once the suction tip fails to create vacuum or leakage occurs, the device fails to grasp the tissue.

B:Working principle of vacuum

Vacuum, also called negative pressure, is a space with less air molecules compared to the atmospheric pressure. Atmospheric pressure typically has a value of 100 kPa or 1 bar [44]. The air molecules of the closed space are sucked away using a vacuum pump. Figure 56 explains how the pressure of this space decreases. When an airtight container is sealed, there is a certain amount of air molecules inside that container which are in relation to the atmospheric pressure (Figure 56A). These air molecules collide with each other and with the wall of the container which result in a force perpendicular to the inner surface of the closed container.

Subsequently, air molecules are sucked away from container B. This decreases the collisions of the air molecules with each other and thus the resultant force on the inside walls. If the atmospheric pressure stays the same, a pressure difference (Δ p) occurs between containers A and B. In this case, the air molecules exert a smaller force on the inside wall compared to the atmospheric air molecules on the outside wall [45]. According to equation 1, when the pressure difference increases and the surface area stays constant, the suction force also increases. Figure 57 describes the

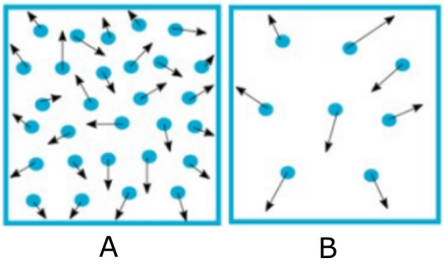

Figure 56: Schematic overview of the air molecules in container A (left) compared to container B (right). The air molecules are figured as blue dots. The direction in which the air molecules are moving are depicted as black arrows. The size of both containers A and B are the same.

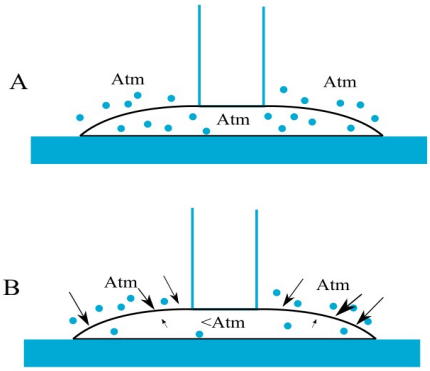

Figure 57: Working principle of a suction tip. The air molecules are depicted as blue dots and move in random directions. (A) The atmospheric pressure (Atm) and the pressure inside the suction tip are equal, therefore the situation is in balance and no resultant forces are exerted. (B) The air inside the suction tip is sucked away and thus the inside of the suction tip has a lower pressure compared to atmospheric pressure. Because of this the air molecules of the atmosphere press onto the suction tip (the black arrows) and generates a suction force.

working principle of a suction tip. In Figure 57A the suction tip is fully sealed with airtight material (blue). The air pressure inside the suction tip is equal to the atmospheric pressure, so there is no force difference on the outside and

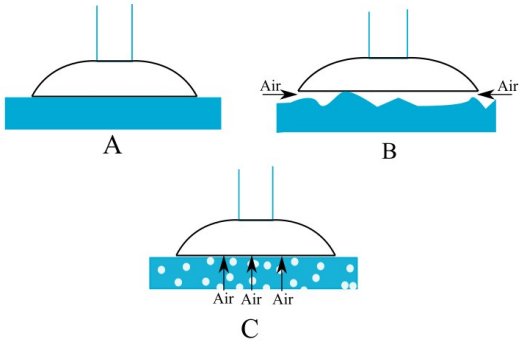

Figure 58: Different surfaces of grasped materials. Left: A level smooth suction surface has good sealing capability and maintains vacuum. Middle: An uneven surface causes an incorrect seal of the suction tip. Right: The grasped material is porous. When the suction tip sucks air, it sucks through the pores of the material which causes flow of atmospheric air inside the vacuum.

inside walls of the suction tip. Subsequently, the air is pumped out of the suction tip (Figure 57B), creating a drop in absolute pressure of the remaining air inside the suction tip which is called a partial vacuum (a perfect vacuum that contains no particles at all can only be achieved theoretically) [44]. Because the outside pressure is still the same (atmospheric pressure) this pressure difference results in a resultant force onto the suction tip [6]. This explains the adhesive function of the suction tip. An essential part of using a suction tip is that it seals the suction chamber of the cup perfectly, otherwise leakage occurs. Molecules always move from areas with a high concentration to an area containing a lower concentration in order to equalize this concentration difference. When the suction chamber of the suction tip in Figure 4B contains almost no air molecules, the atmospheric air molecules tend to flow inside. The flow of atmospheric air molecules through openings in the sealing of the suction chamber is called leakage [6]. Because of leakage, the pressure inside the suction chamber equalizes the atmospheric pressure and no pressure difference can be maintained [46]. The type of surface of the object which needs to be grasped has a large influence on the sealing (Figure 58).

If the surface is uneven and the suction tip is not flexible enough to compensate for this, there is an increased risk that air openings will form in the sealing of the suction tip and atmospheric air molecules equalize the air pressure inside the suction chamber. To seal the pressure in the suction chamber, the walls of the suction chamber and the grasped tissue must be airtight. When material is grasped which is porous like spongy or skeletal materials, atmospheric air molecules move through air passages inside the grasped materials' surface (Figure 58) [46]. This will also result in leakage and a reduction in pressure difference. When the grasped material does not cause leakage as depicted in Figure 58, shear movement between the suction tip and the grasped tissue is the main cause for leakage [12], [13]. When the tissue is pulled, the suction tip slips inwards. The slip decreases the contact surface of the suction tip and also deforms the suction tip which increases the chance of formation of air passages in the sealing, which will cause leakage [14].

Leakage is a highly important aspect of maintaining vacuum pressure. This is especially important for grippers that rely on consistency like the suction grippers used during surgery [3]. To ensure the desired suction force is generated and maintained to grasp human tissue, leakage should be prevented or compensated.

C: Suction graspers designed for MIS from literature

Because suction instruments in Appendix A are not designed for MIS, this enables the instruments to have large suction tips which are able to generate large suction forces. However, when focusing on MIS, these are not usable. On the current market, no suction grippers suitable for MIS can be found. This identifies the development of suction grasper designed for MIS as a promising market gap. In literature however, transformable suction tips designed to grasp human tissue can be found.

Osaki et al. [10] designed a transformable lung positioner for thoracoscopic surgery that is able to transform into a triangle while inside the thoracic cavity (Figure 59). The initial form of the instrument is a tube with a diameter of 12 mm in order to fit through trocars with a comparable inner diameter. The part that is inserted into the patient's body (pictured in yellow) is made of three rigid links with three revolute joints that can rotate 70°. Each link has a suction opening that can generate vacuum separately of each other. A cable (pictured in red) is placed through the shaft towards the most distal joint. This cable can be pulled and due to the revolute joints and the location of attachment, the links transform into a triangle shape.

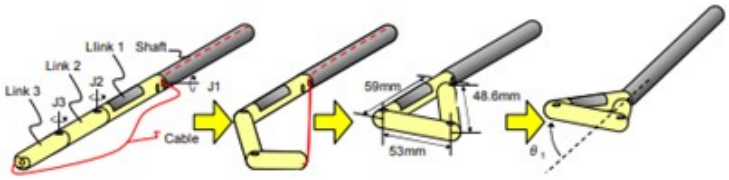

Figure 59: The transformable device of Osaki et al.[10] It is able to bend like a finger by tensioning cables

Each link contains its own suction tip (Figure 60). These suction tips are connected to separate pneumatic tubes. These tubes are connected to a vacuum pump. Osaki et al. [10] thought of a configuration where the final link is only connected to the associated pneumatic tube when in triangle form (Figure 7c). A silicon rubber film seals the connecting area of the final flow path connection. Osaki et al. [10] performed experiments to evaluate the gripping capability of the suction device. Each sucker is compared to a sucker that is directly connected to a pneumatic tube. A weight is attached to each sucker and 40 kPa is applied. Measured suction forces of suckers 1,2 and 3 were 2.75 N, 2.8 N and 2.75 N in perfect conditions. This means that the suction tips were directly attached to vacuum pump without the instrument. However, leakage using the instrument is not measured. The device is designed to grasp a single lung, which requires 4.9N of suction force to pull it up. When pork meat was used as tissue, the three suckers were able to generate an average suction force of 1.91 N. This loss of suction force is caused by a lot of leakage at the suction tips.

Another laparoscopic suction device, designed by Takayama et al. [11], uses cables to transform the finger-like suction tips into the desired position (Figure 61). The device consists of a three finger-like parts that function as suction tips. The suction tips are attached to three separate cables. In order to fit the suction tips through the trocar, they are lined up in series (Figure 61a). The device is inserted in the trocar (Figure 61b). When the main unit passes the trocar the suction tips start to hang (Figure 61c). Subsequently, the cables are tightened by a pulley and the suction tips line up as in Figure 61d. The cable tension is locked and the suction tips are transformed to a firm surface. To dismiss the device from the patient's body, the cable tension is released. This causes the suction tips to hang loose again. When the cables are shortened, the suction tips are able to move through through the trocar one by one (Figure

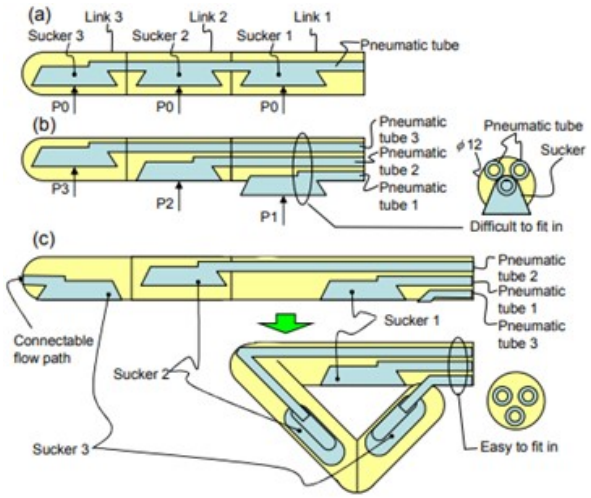

Figure 60: The transformable device of Osaki et al. [10] It is able to bend like a finger by tensioning cables

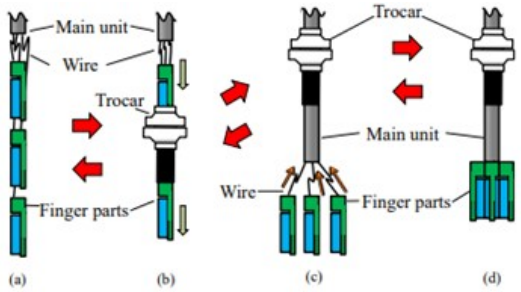

Figure 61: The transformable device of Takayama et al.[11] It uses loosely finger like suction tips that can be re-arranged by tensioning the cables while inside the human body

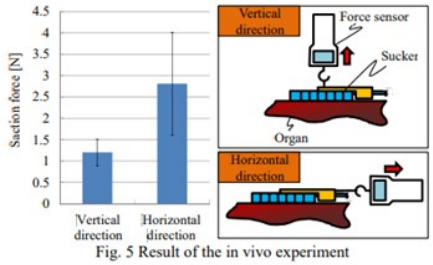

Figure 62: Results of suction force measurements of the transformable device of Takayama et al. [11]

61a).

Takayama et al. [11] conducted an experiment where the suction force can be determined per finger part (Figure 62). A negative pressure of 41 kPa is used to grasp pig liver. The suction force in vertical and horizontal direction was measured. The mean suction force over 5 experiments was 1.2N for the vertical direction and 2.8N for the horizontal direction (Figure 62).

However, the working mechanism described in Figure 61 will cause problems when using it during surgery. The device is inserted into the human abdomen where there is not much space. Also it is uncertain that the suction tips will line up perfectly each time in this surgical environment. These wires can get entangled with each other or get stuck in tissue which it may damage. For that reason, loose wires are not preferred inside the human body for this thesis. The patents of Osaki [10] and Takayama [11] are designed for usage in MIS. However, the working principle of these concepts seem not ideal during surgery. Leakage, safety and use of loose parts are the main disadvantages of these concepts and should be taken into account designing a novel suction grasper.

D: Rendered images of final design

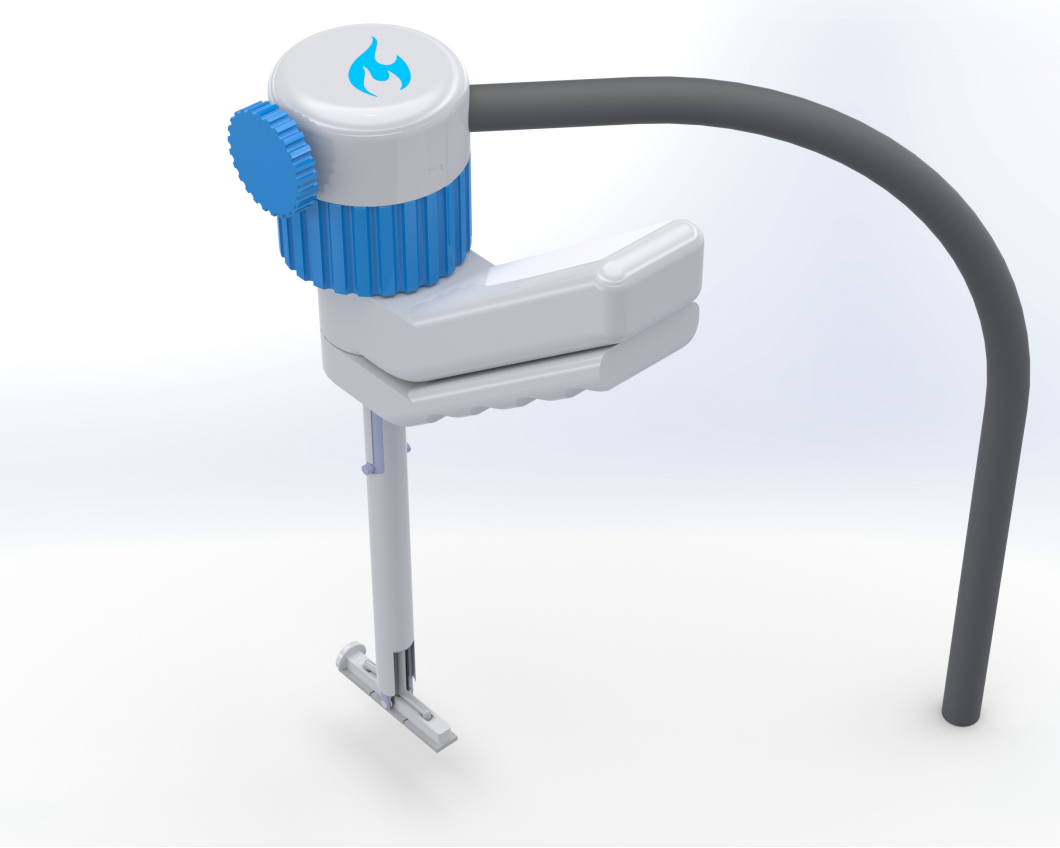

Figure 63: Render of the final design with the non-label colors. The outer suction tube to the vacuum pump bundles the three suction tubes from the suction surface.

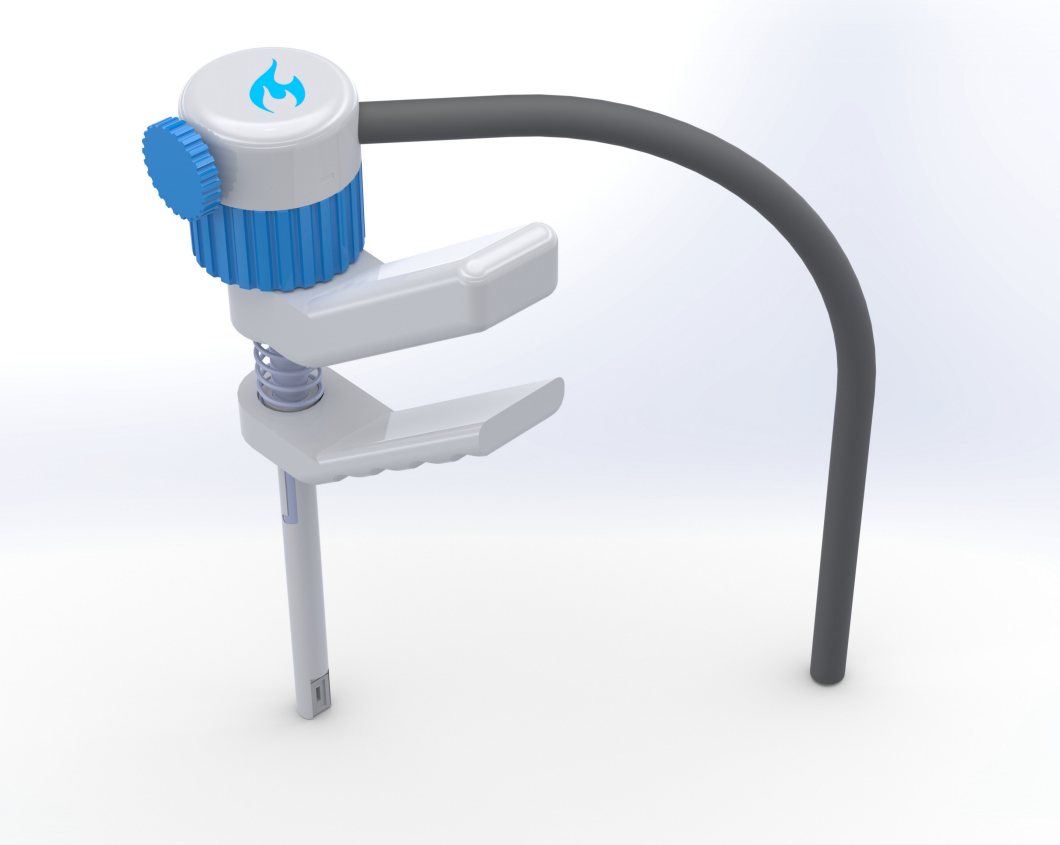

Figure 64: Render of the final design with the non-label colors.

Figure 65: Zoomed render of the suction surface and the shaft.

E: Testing the push - pull and the tensioning mechanism

In this figure the push and pull mechanism can be demonstrated. Once the user twists the upper part of the instrument, the pin in the railing bracket alligns with the vertical section (middle figure). Now the user can press the upper part into the shaft (right).

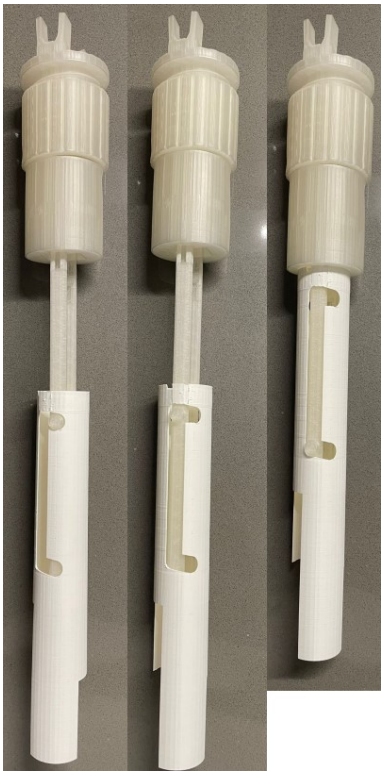

Figure 66: The 3D-printed proof of principle for the push - pull mechanism and the tensioning mechanism.

F: Cable buckling

Figure 67: Cable buckling after tensioning using the prototype. The buckling prevented the cable from moving around the axis.

G: Tensile test of metal thread in silicone mold

Different kind of silicone are tested on tensile force until it fails or until the steel wire slips out of the silicone. This is an essential part of Concept 1 since this concept depends on the connection between the steel wire and the silicone. Molds were printed using the Ultimaker. In these molds silicone is poured. After this, the steel wire is placed in the correct depth. When the silicone is hardened, the tensile tests can be performed 68. The results of the tensile test are noted in figure 69.

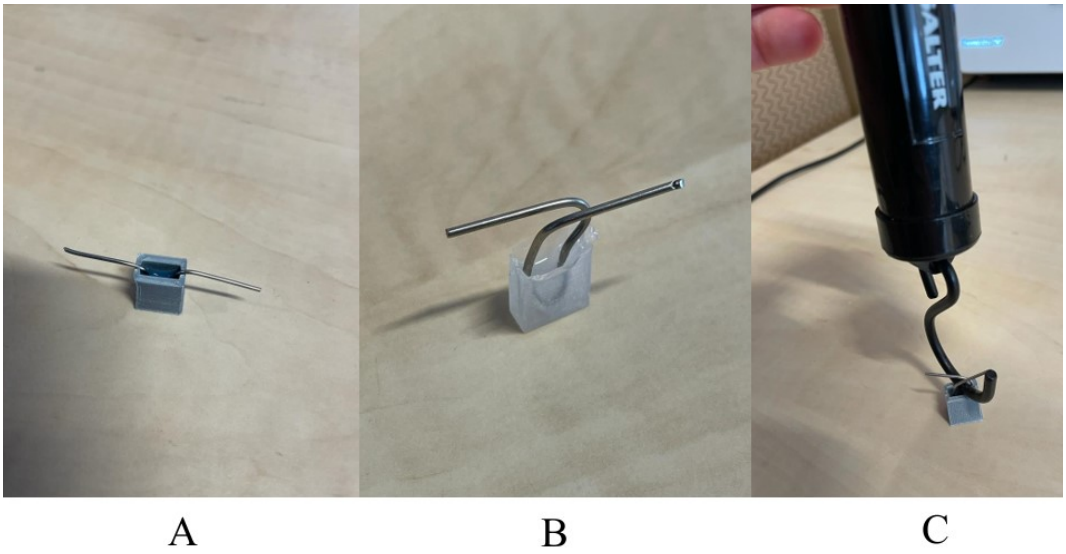

Figure 68: A: The steel wire placed into silicone. B: The silicone is hardened with the steel wire in it. C: A spring scale is placed around the steel wire. The mold is fixed and the tensile force is measured and noted.

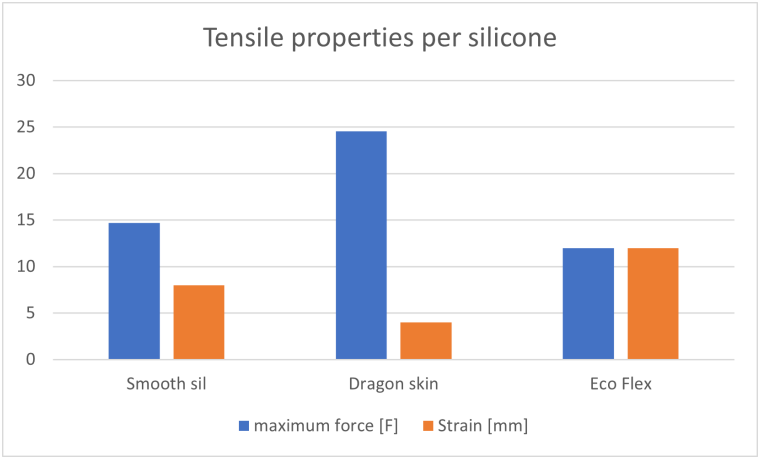

Figure 69: Graph of the tensile test on different kinds of silicone of Smooth On.

H: Determination of tissue curvatures using 3D-models

To assess the diameter of the circle that is similar to the curvature of organs that can be found in the human body during MIS 3D-models are used. This technique is used since data of these curvature diameters are not found in literature. The 3D-organ models are downloaded from several websites and are rated on precision on dimensions which can be found in literature. After this, the surface

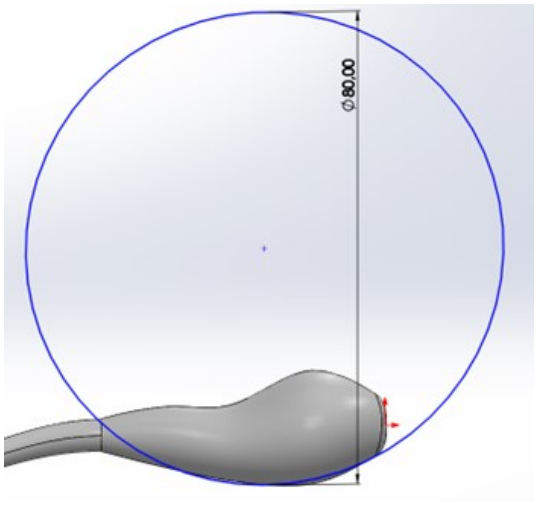

Figure 70: Diameter of the curvature of the gallbladder

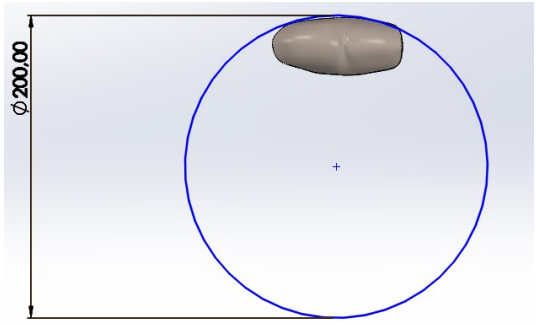

Figure 71: Diameter of the curvature of the liver viewed from the top.

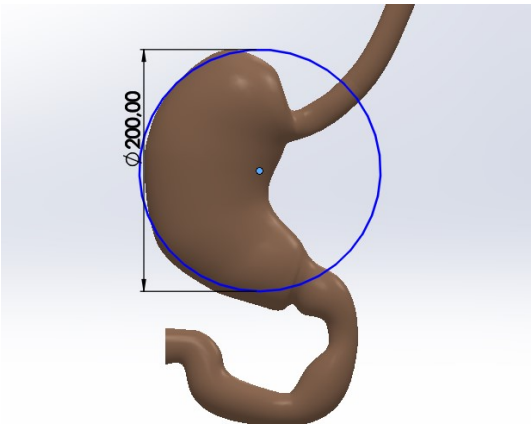

Figure 72: Diameter of the curvature of the stomach

I: Technical drawings

In this appendix the following techincal drawings are presented:

- Suction surface (1 tip) for testing
- Suction surface (3 tips) for testing
- Suction surface (4 tips) for testing
- Suction tip (for single tip surface)
- Suction tip (for 3 tips surface)
- Suction tip (for 4 tips surface)
- Support stage
- Stage connector
- Gelatine container
- Syringe holder
- Connector Luerlock to 4mm tube
- Mold for 80mm diameter curvature
- Mold for 200mm diameter curvature
- Top part for curvature molds
- Syringe puller

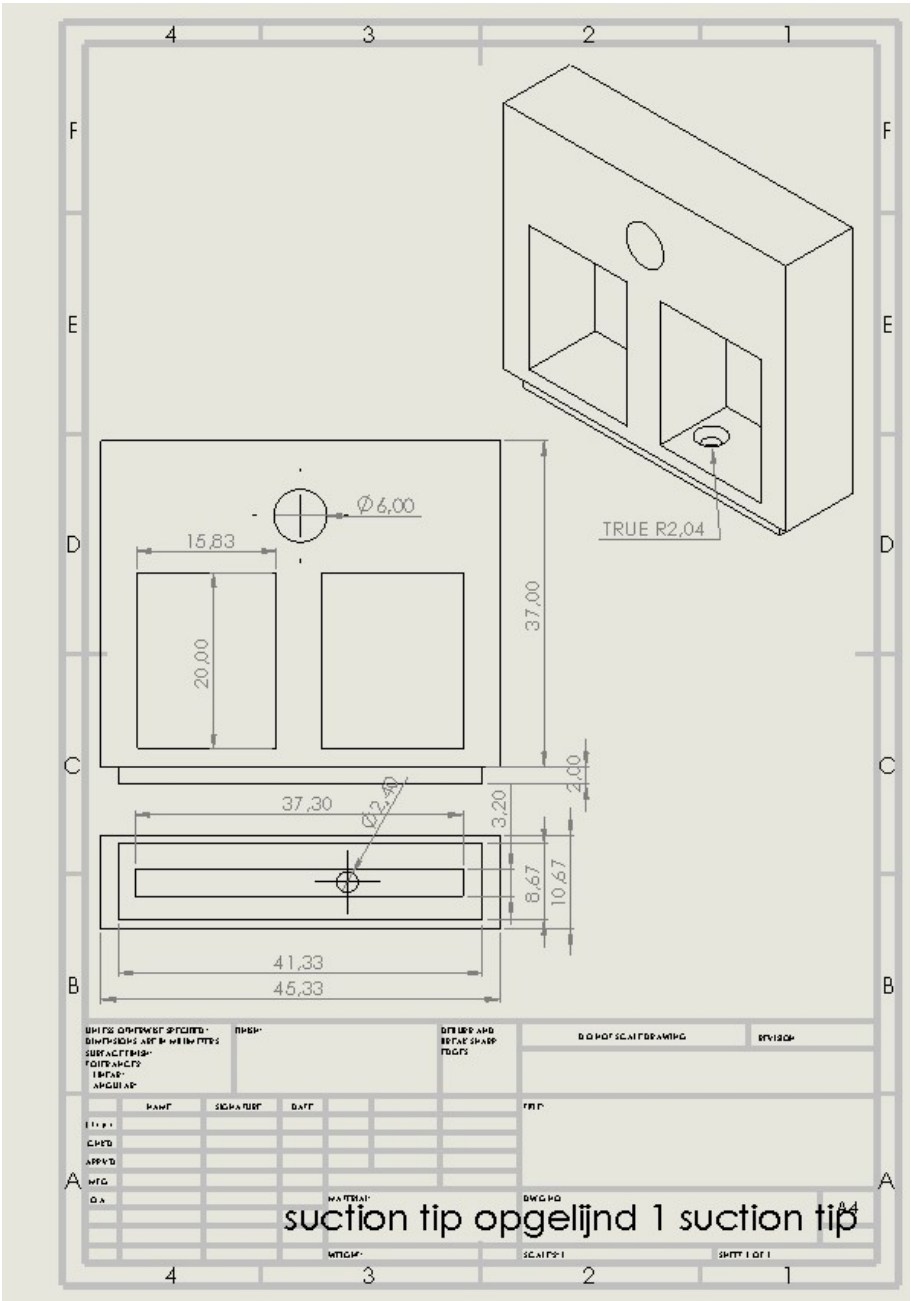

Figure 73: Suction surface designed for experimental testing designed for 1 suction tip

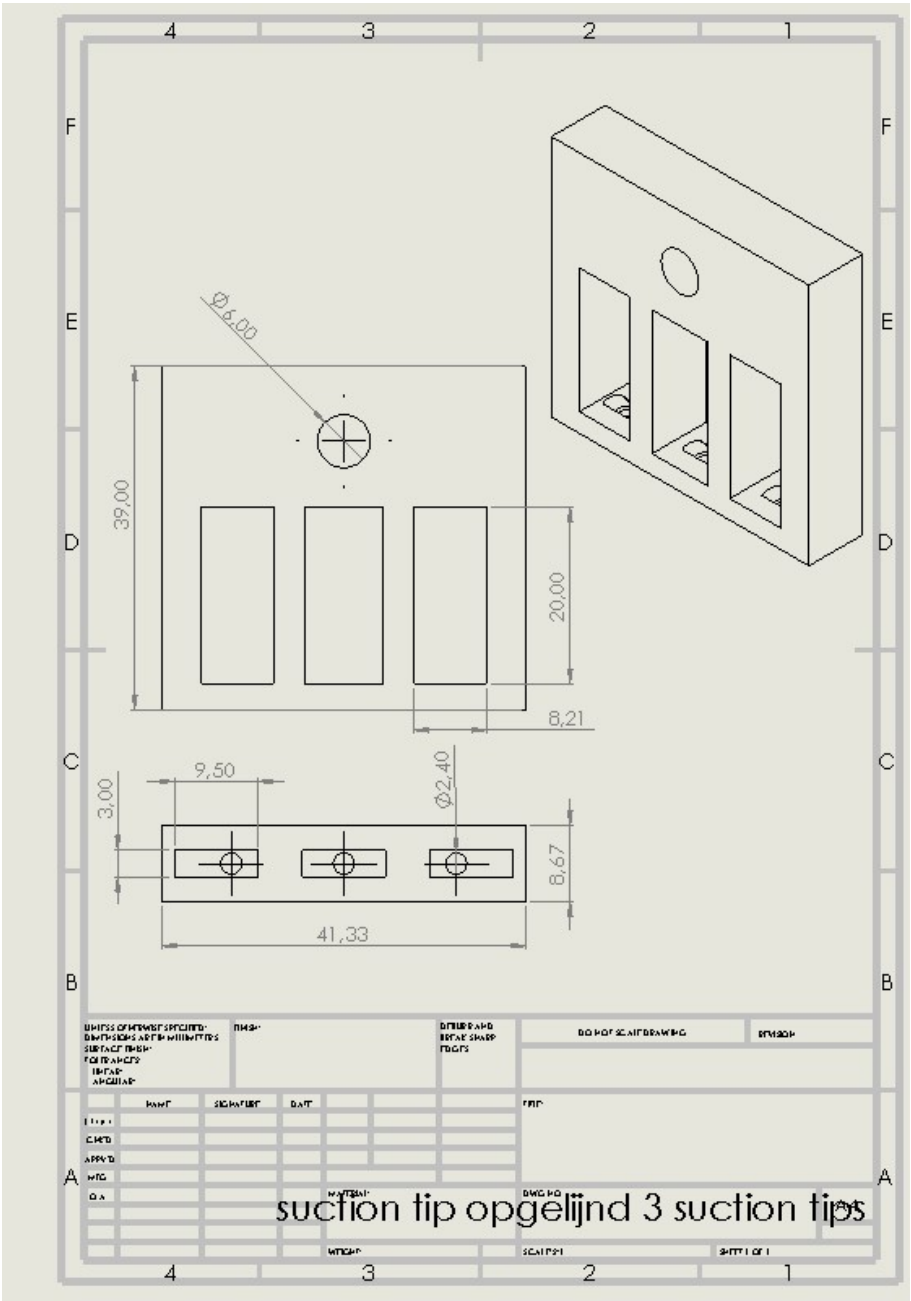

Figure 74: Suction surface designed for experimental testing for the use of 3 suction tips

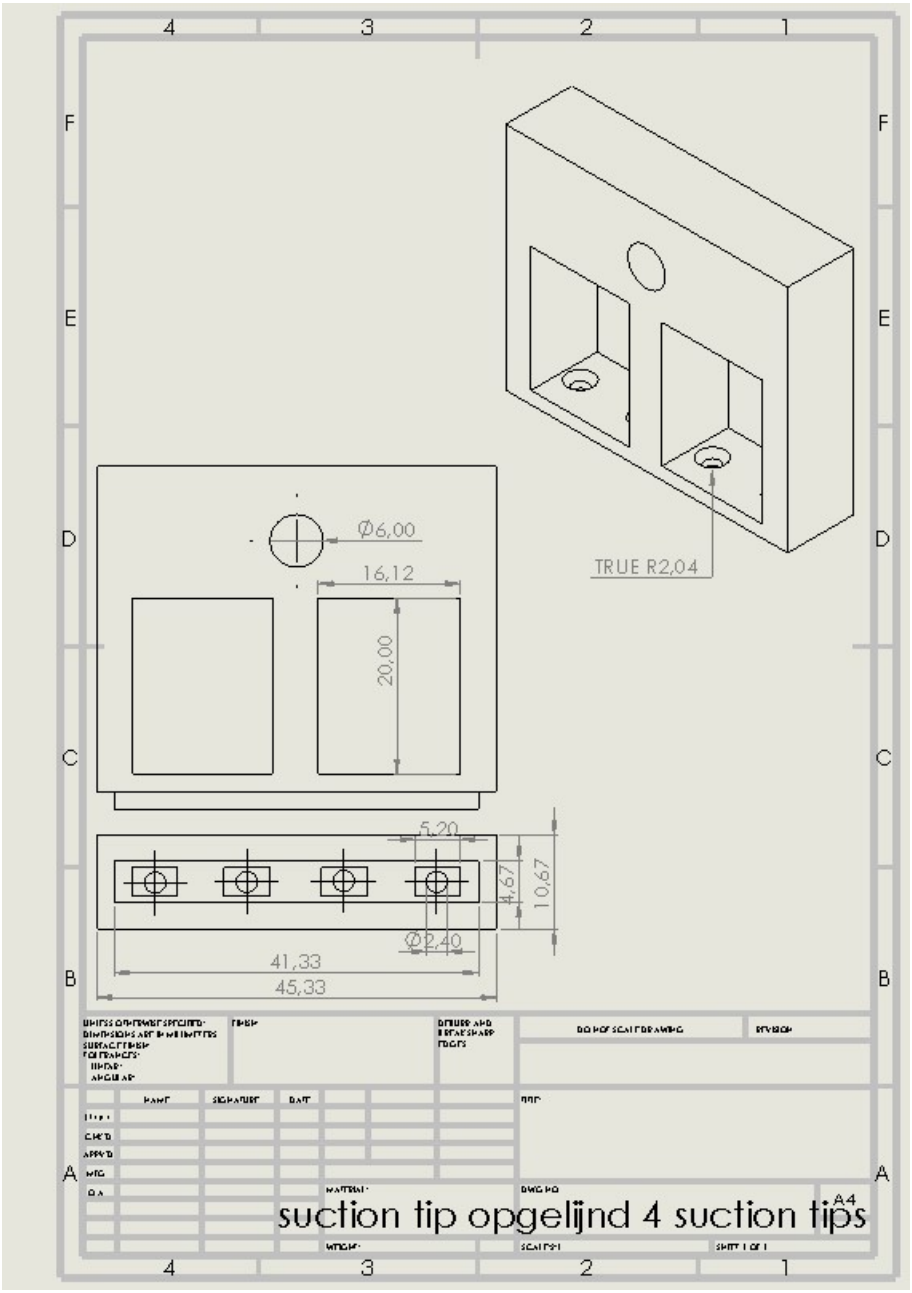

Figure 75: Suction surface designed for experimental testing for the use of 4 suction tips

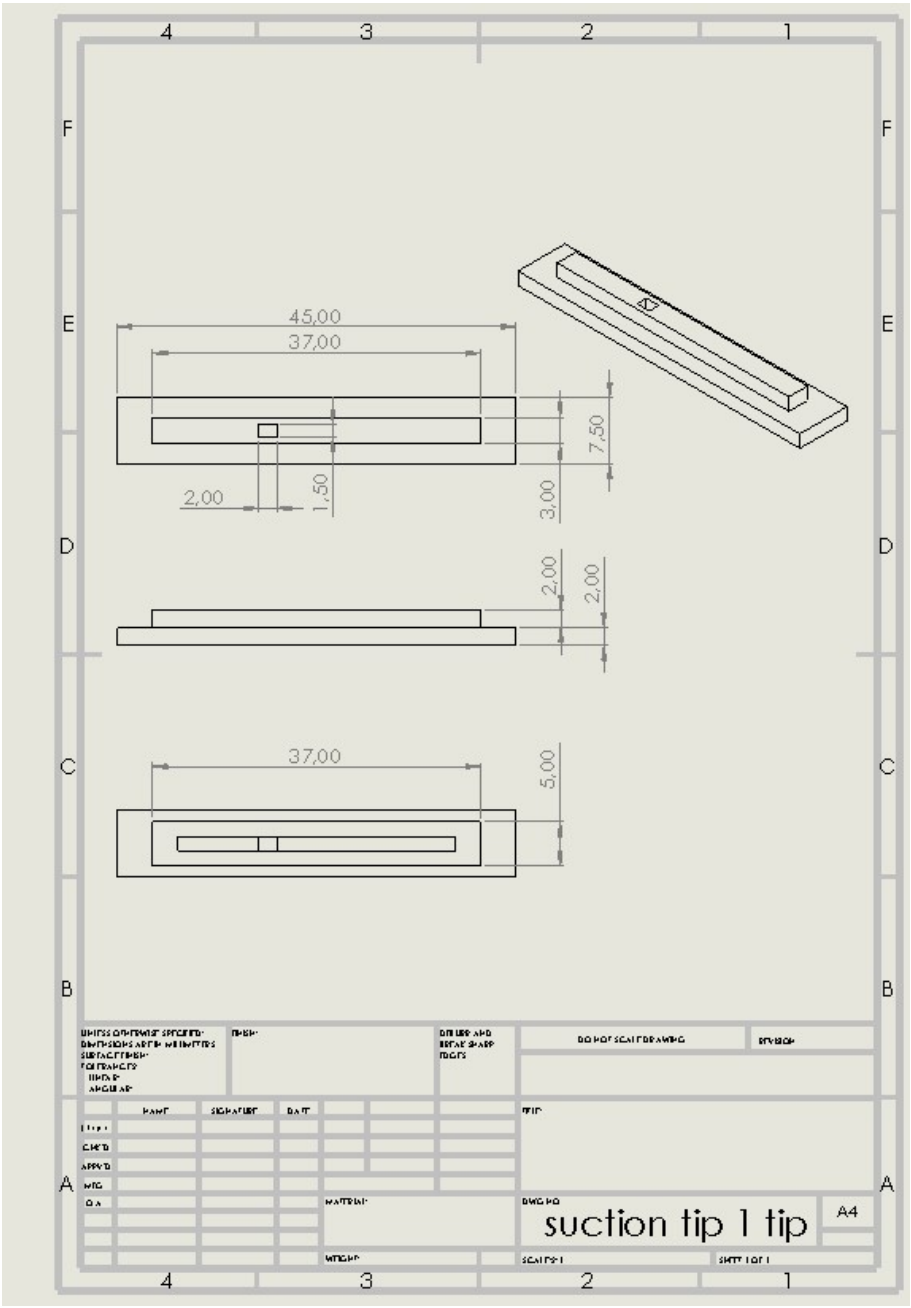

Figure 76: Suction tip for the suction surface with one suction chamber

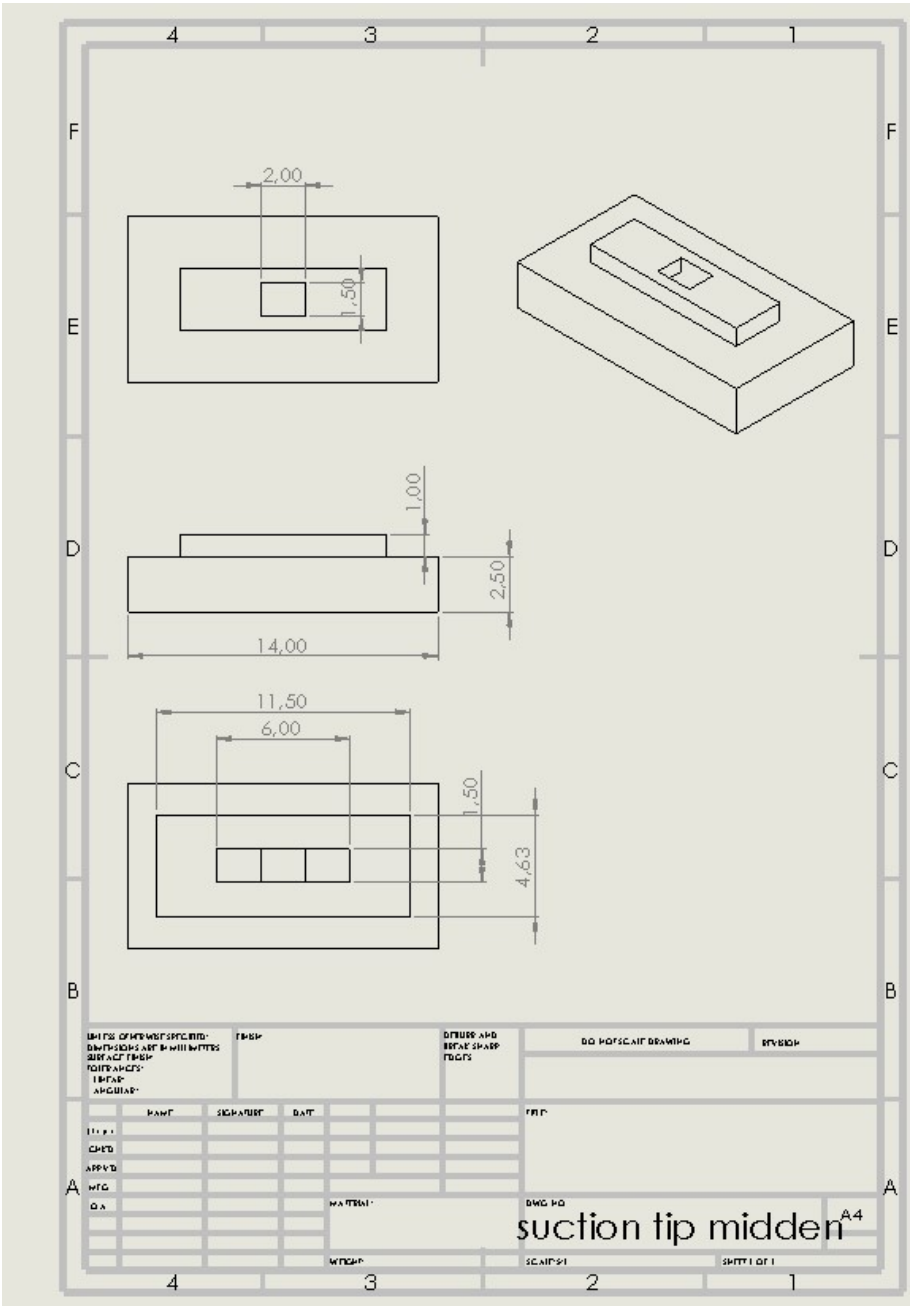

Figure 77: Suction tip for the suction surface with 3 suction chambers

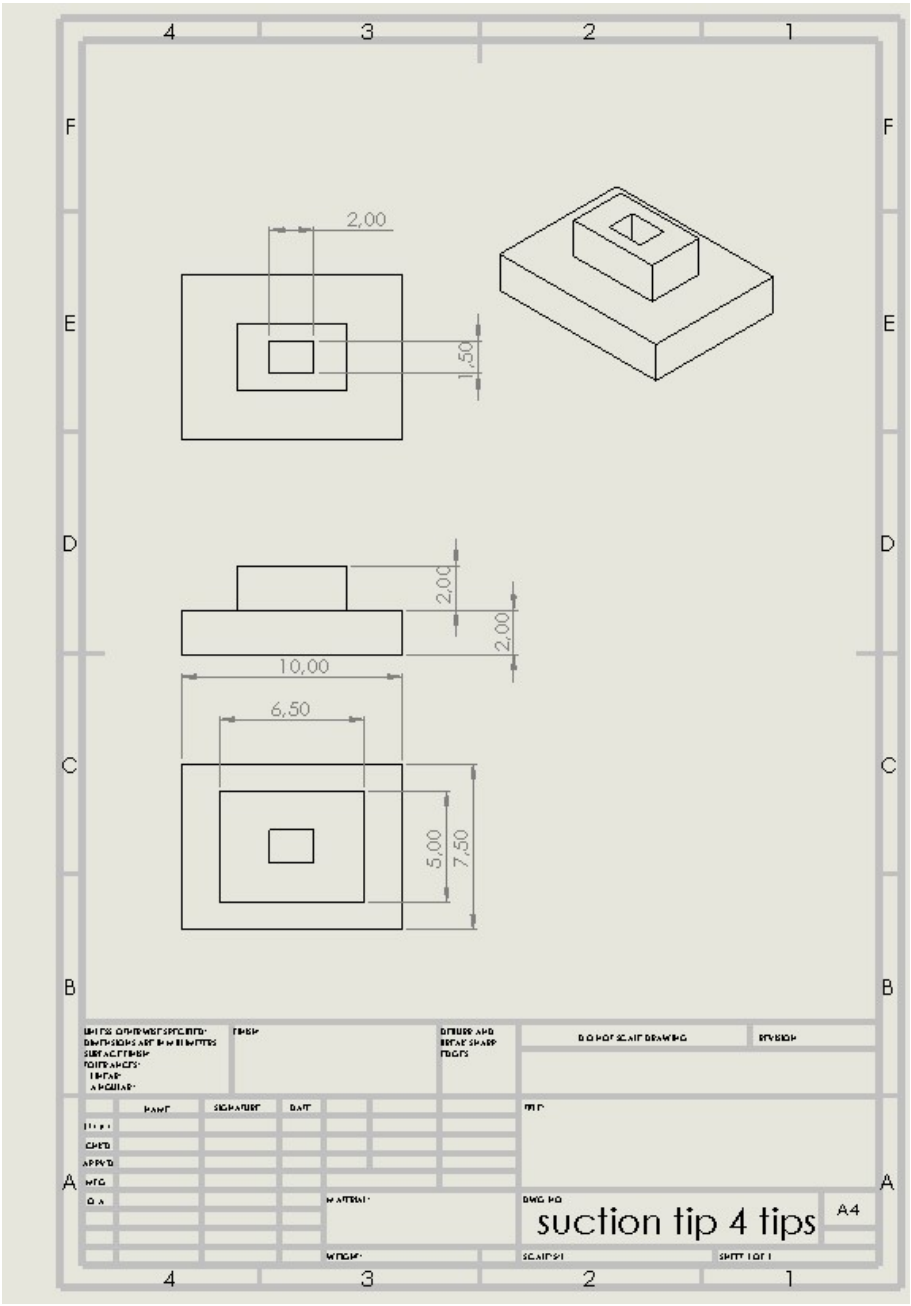

Figure 78: Suction tip for the suction surface with 4 suction chambers

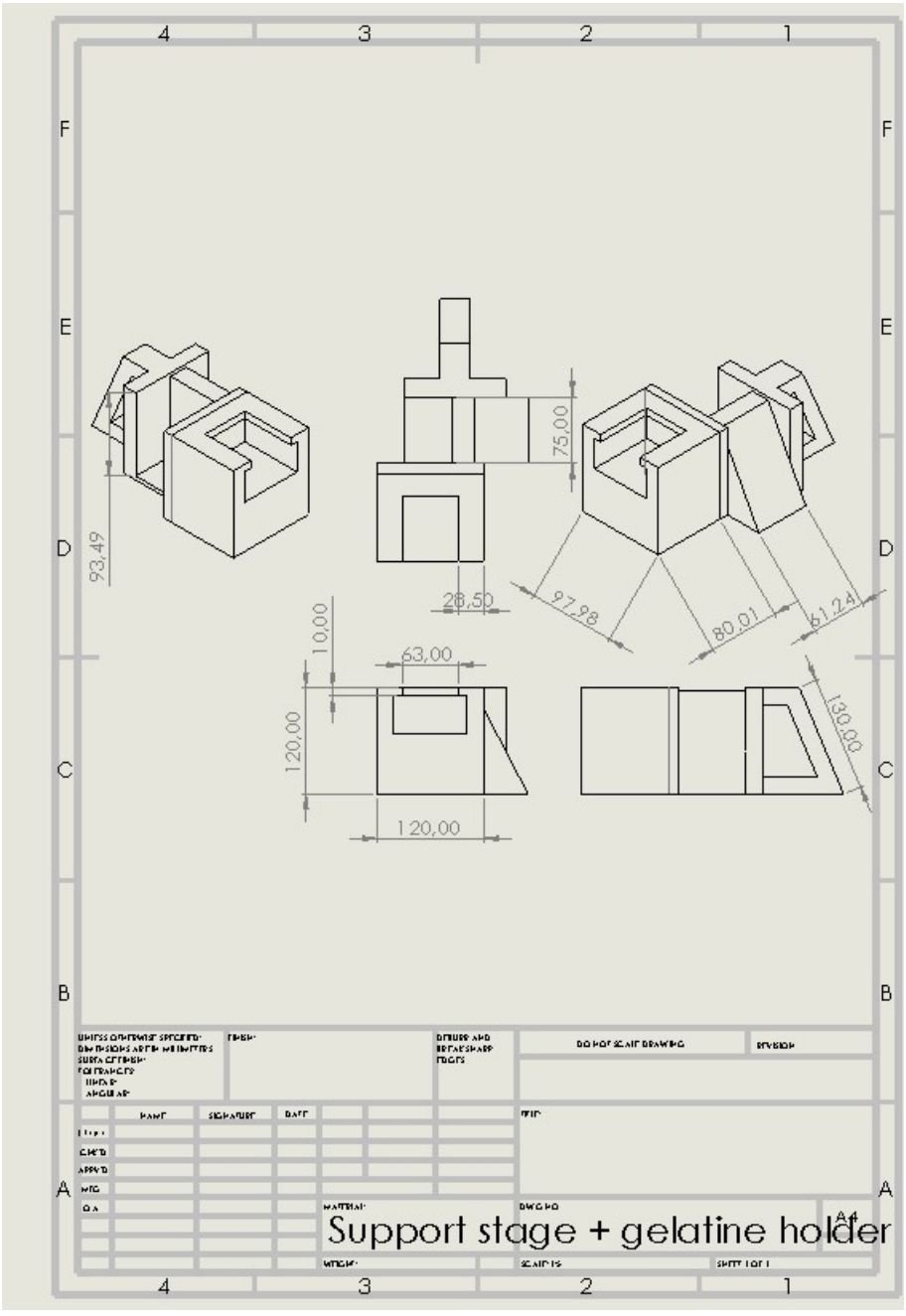

Figure 79: Support of the linear stage that holds it upright

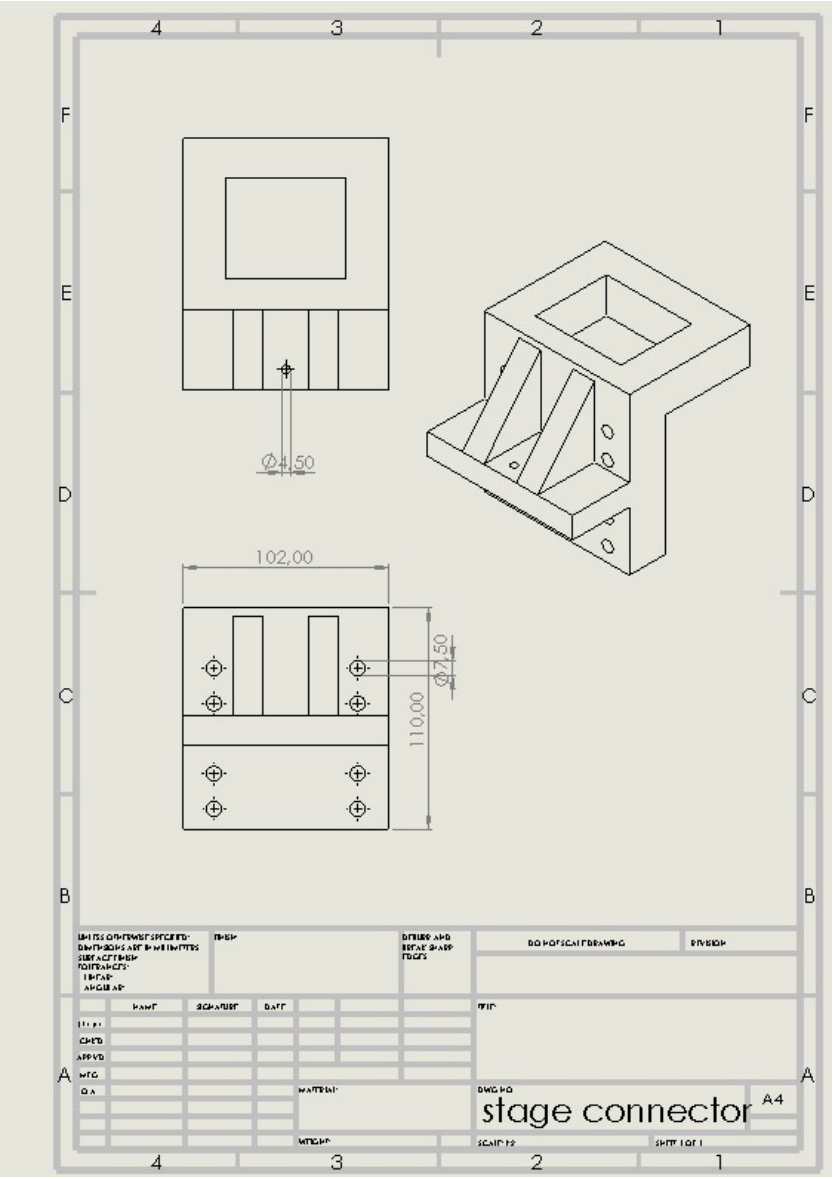

Figure 80: The base plate that is connected to the moving stage. The force sensor is connected to this base.

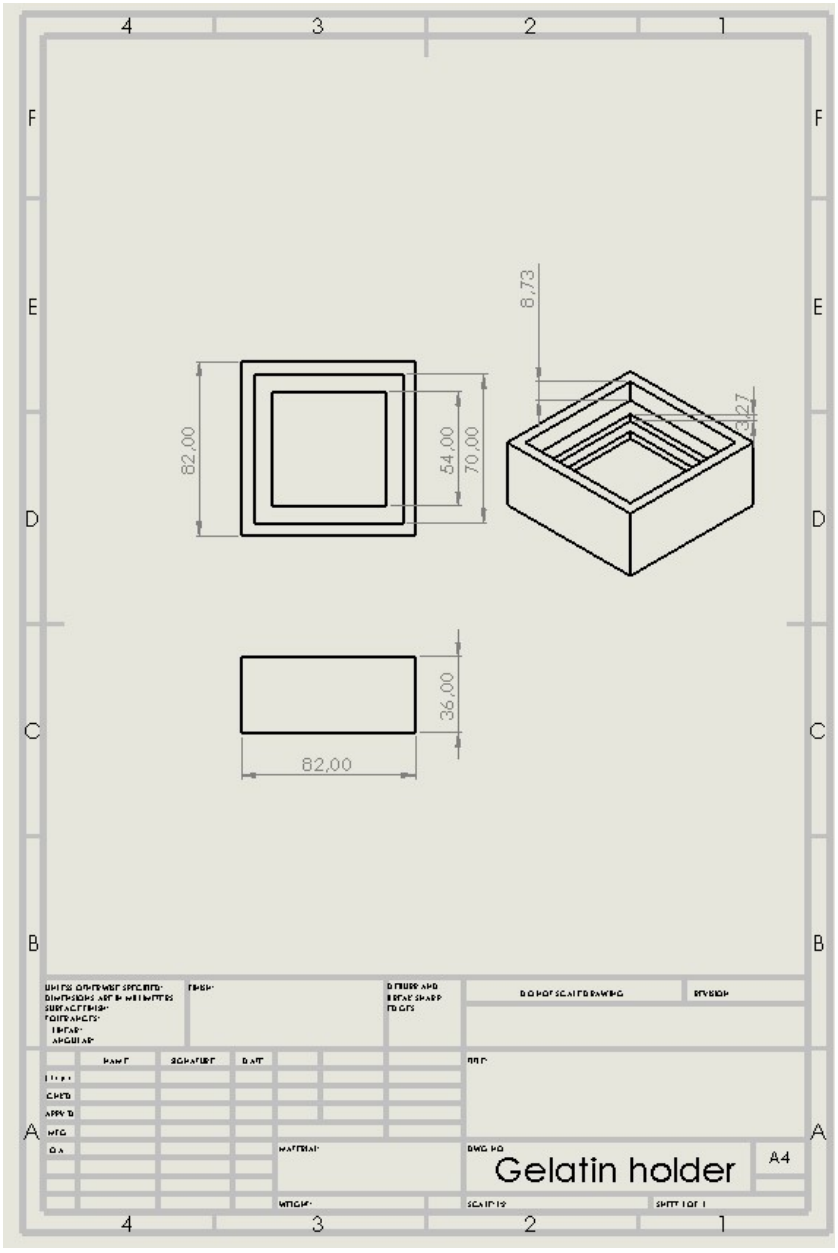

Figure 81: This container holds the gelatine that is used during testing. During curing, a mold is placed on top this container with the correct curvature. This mold is then removed.

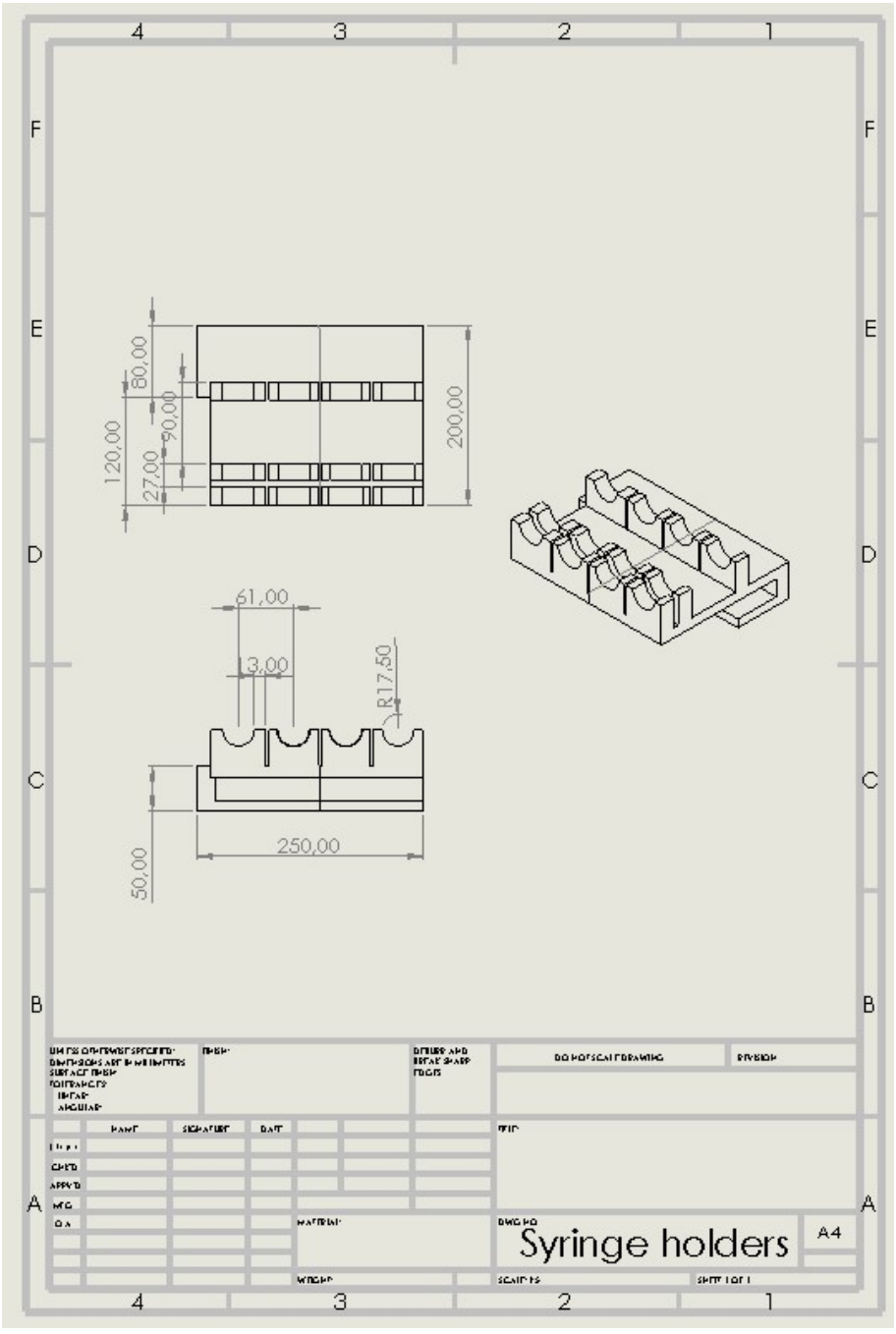

Figure 82: This print functions as holders for the syringes. The syringes fit on the extruded parts. Once the syringe is pulled horizontally, it stays in position. The holders lock onto the desktop

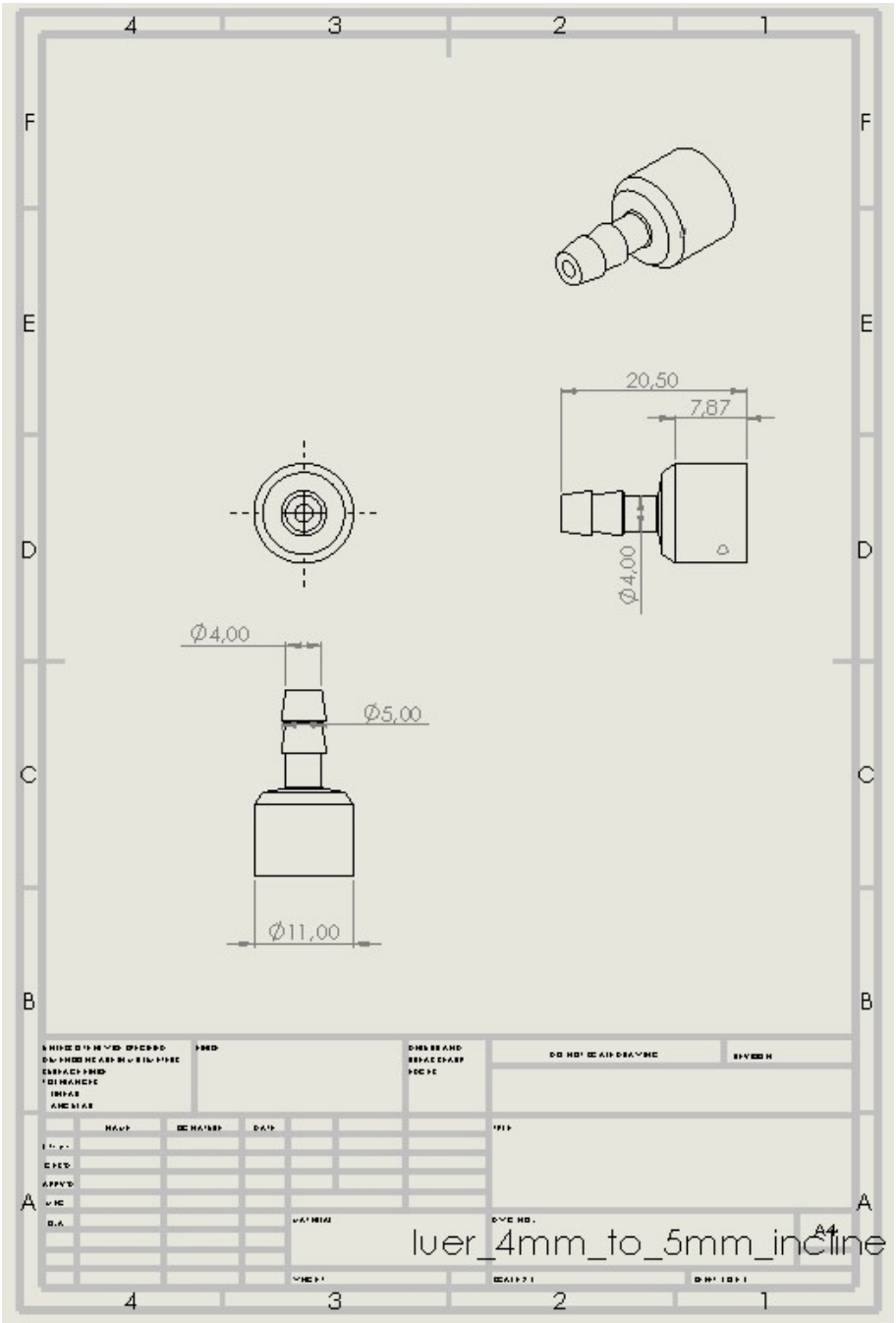

Figure 83: This piece is attached to the 3-way valve using a corresponding female luer lock attachment. A tube with an inner diameter of 4 mm can be placed on the other end.

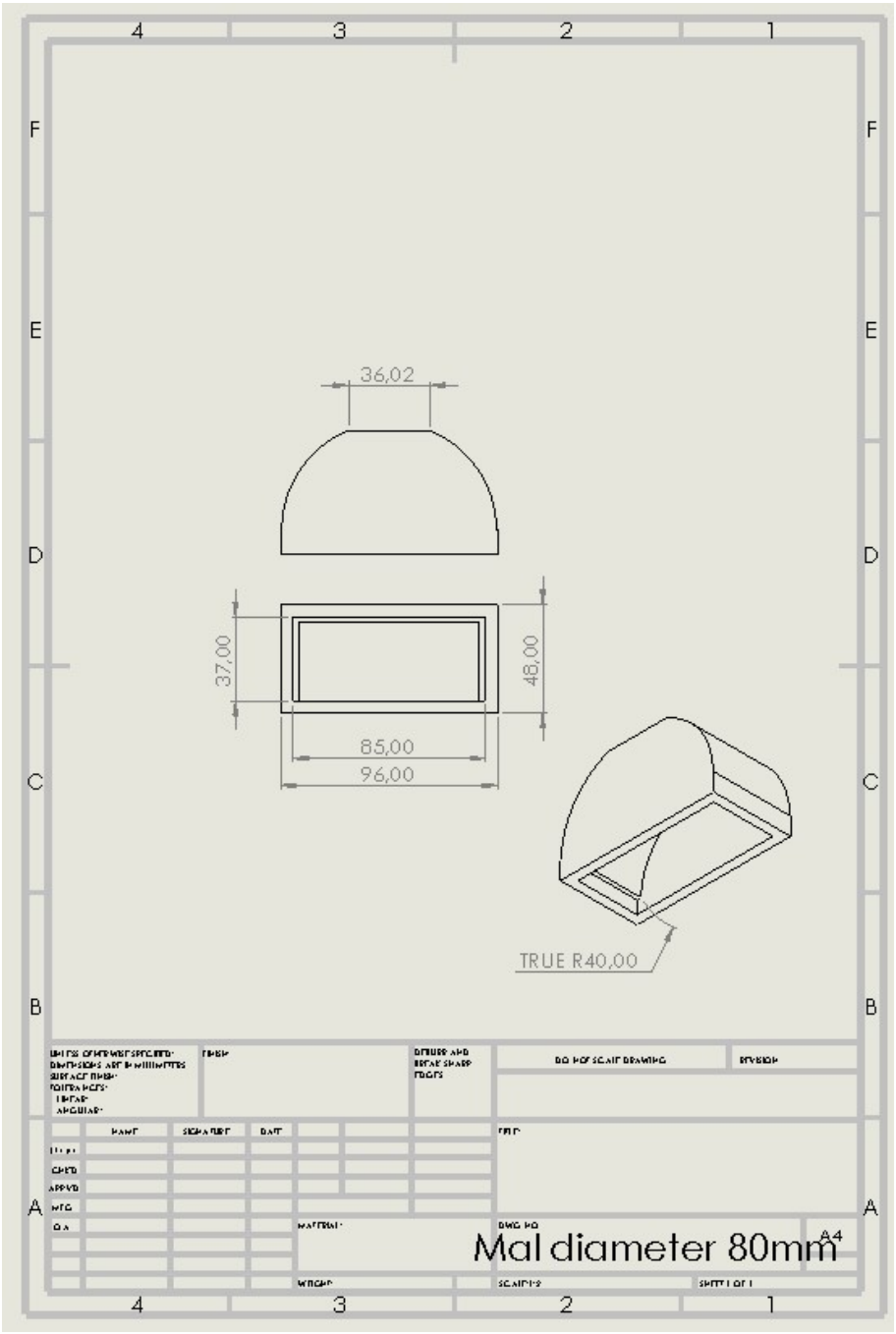

Figure 84: This mold is used to pour in the gelatine to create cured gelatine in a 80 mm diameter curvature

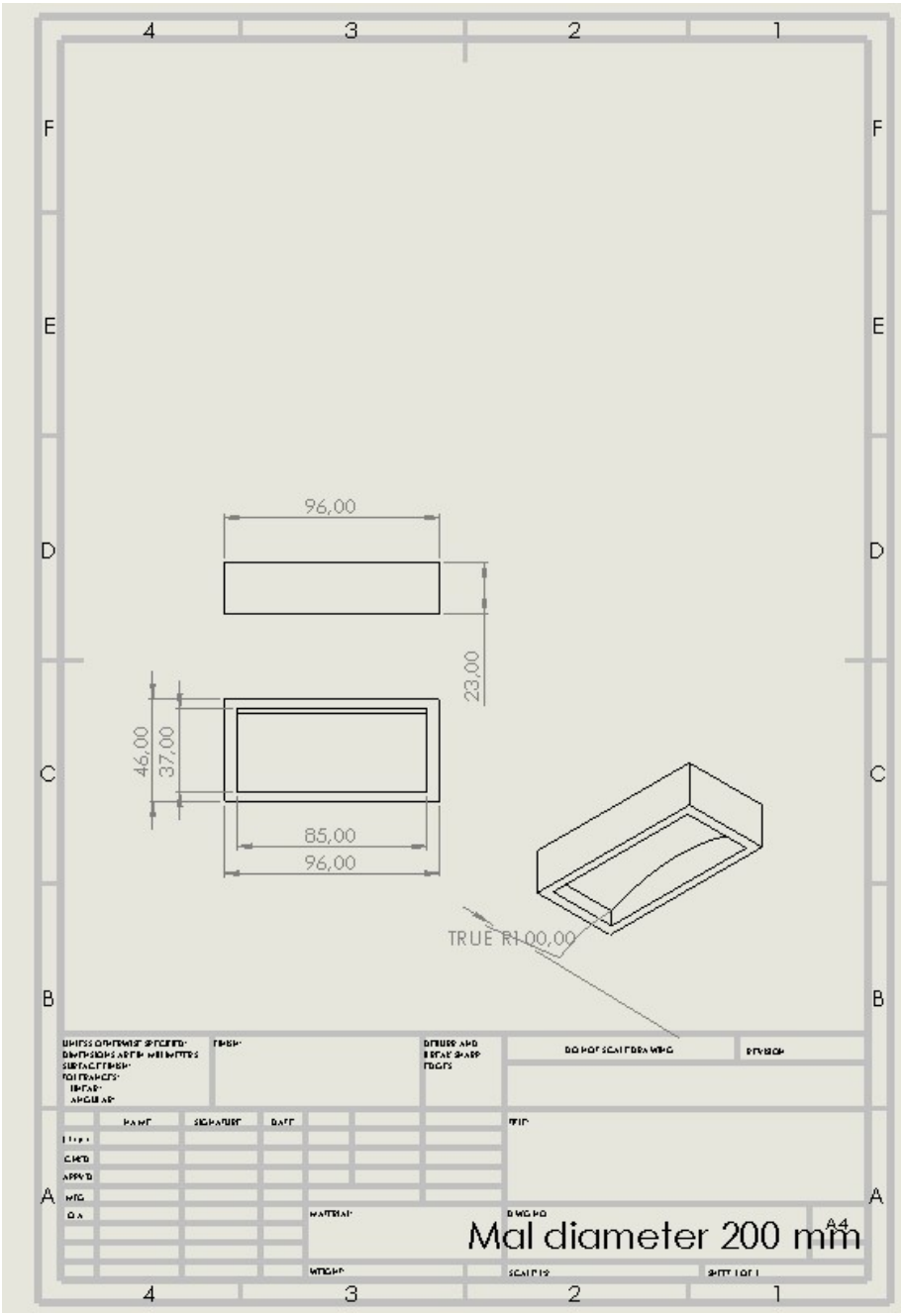

Figure 85: This mold is used to pour in the gelatine to create cured gelatine in a 200 mm diameter curvature

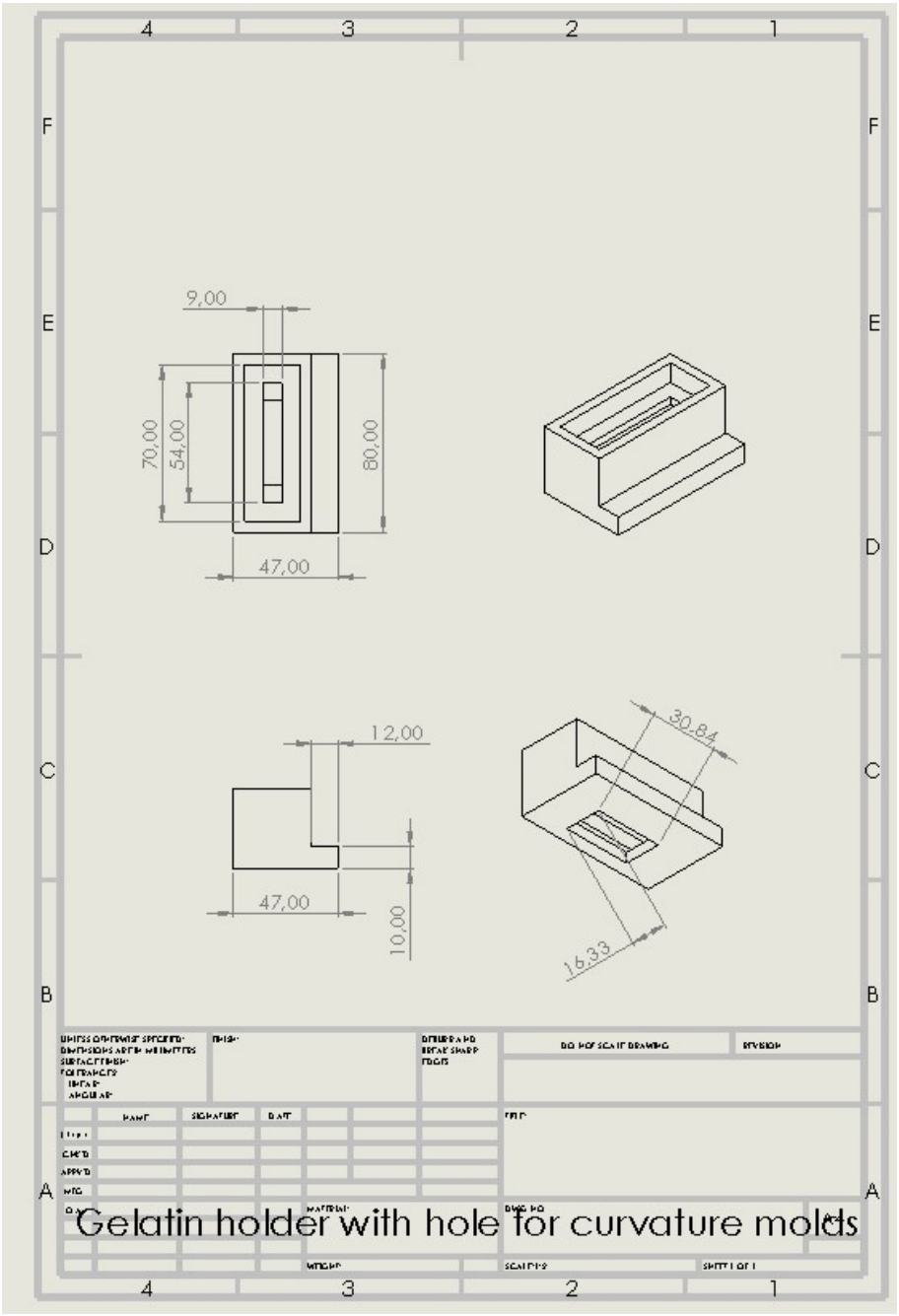

Figure 86: This mold is placed on top of the curvature molds. Gelatine is poured through the hole on the bottom of the mold. The curvature molds are removed after curing and this mold is used during experiments.

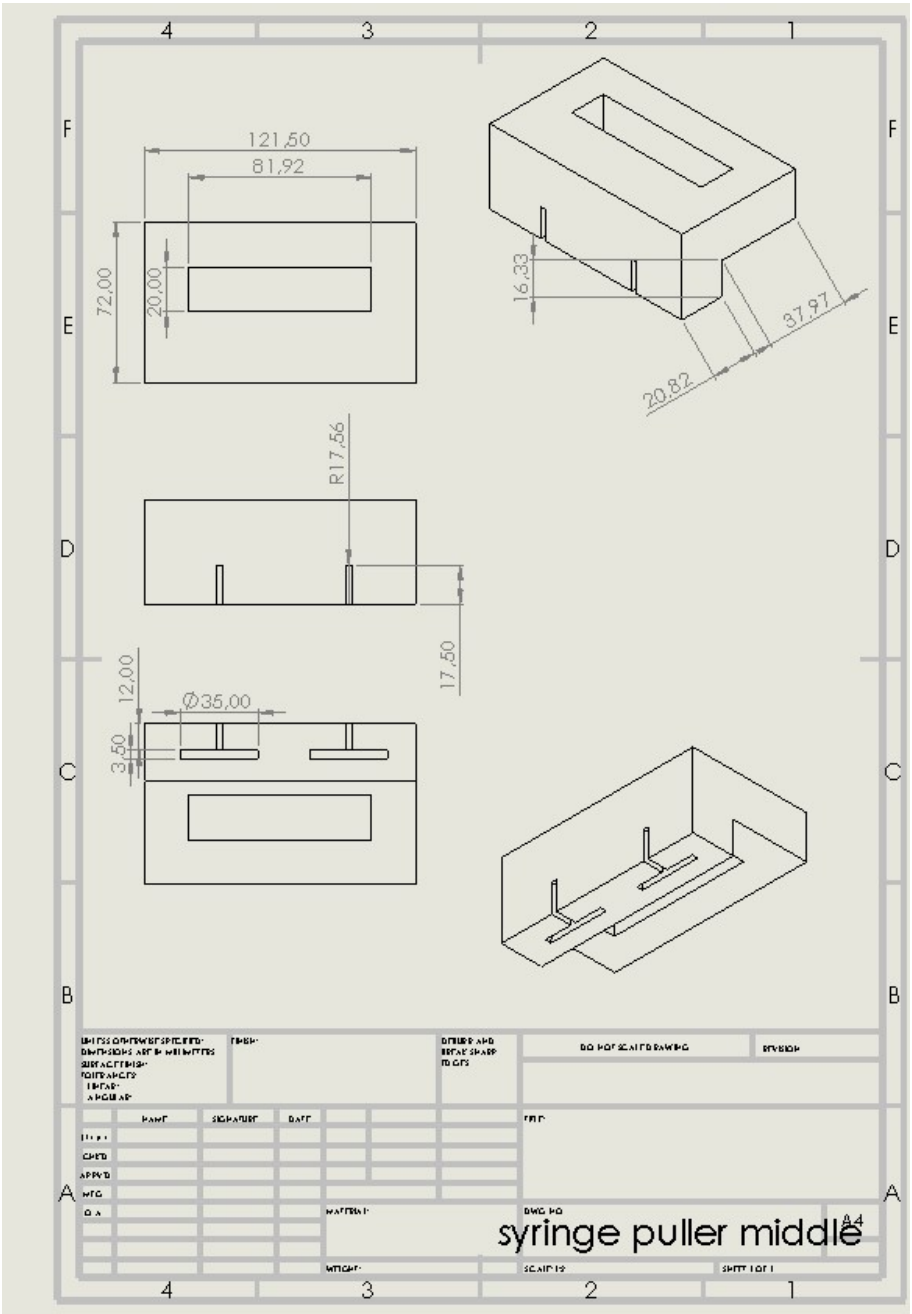

Figure 87: Syringe puller. This 3D-printed part can be placed on top of two syringe handles. Two syringes can be pulled at the same time.

J: Concept alternative for cable actuation

The following surface rotation concept direction is proposed. Instead of using cables, small steel beams (blue) attached to hinges (black). Left: once the surgeon pushes the mechanism, the surface opens. Once the surgeon pulls, the system closes and is able to go through the shaft or the trocar.

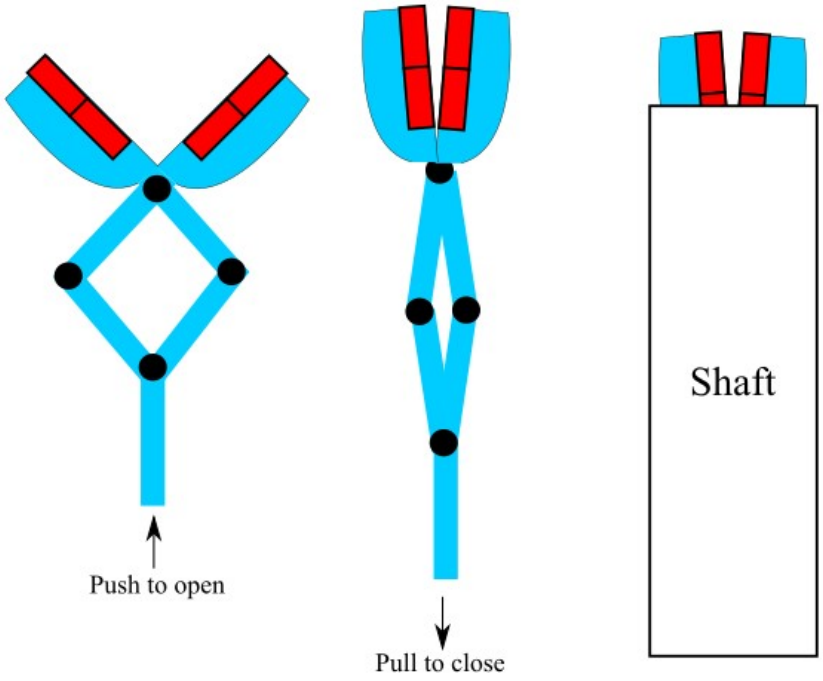

Figure 88: Concept using solid beams instead of cables to rotate the suction surface.

K: Methods on vacuum generation

Manual vacuum pump

A kiwi system can be integrated inside the handle of the instrument. The upper handle can be compressed towards the lower handle. Because of this, air gets squeezed out of the upper handle through the right blue silicone valve. The left silicone valve is connected to the lower handle. This valve is able to let air go from the lower handle to the upper handle only. This way, vacuum pressure of the lower handle can be built up by squeezing the upper handle multiple times. A custom version of this system needs to be designed to be able to use it with multiple suction chambers.

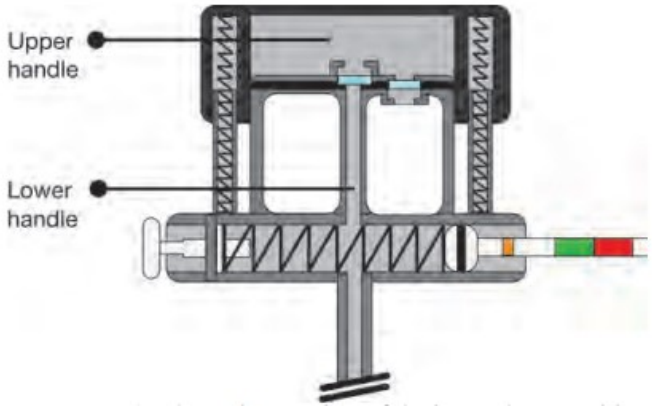

Figure 89: A schematic intersection of the KIWI manual hand pump.

Advantages:

- Handle integration. This means that no external tubes are required.

Disadvantages:

- Since multiple suction chambers are required, the dimensions of these should reduce to still be able to fit the handle inside the palm of the hand. If the surface of the suction chamber reduces, the pressure should increase to still maintain the same suction force (Equation 1). Because of this, the user must squeeze the handle with more force which makes it hard to use and destabilizes the instrument.

Using a vacuum generator

A vacuum generator is a device that uses compressed air to generate a vacuum. It uses the Venturi-effect. Because compressed air travels through the smaller nozzle, the velocity of this air increases (Bernoulli effect). As the compressed air leaves the nozzle and starts to expand, a vacuum is created at the expanded site (white). This draws air molecules from the suction chamber and objects can be lifted.

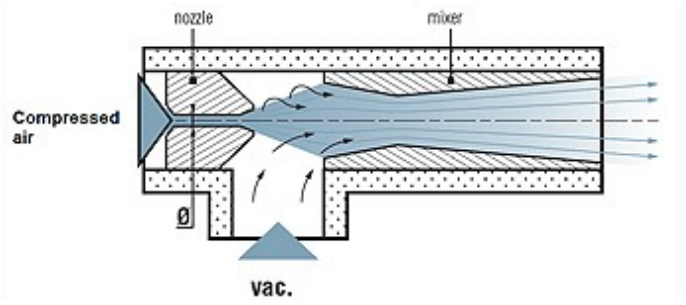

Figure 90: Schematic representation of the working principle of a vacuum generator.

Advantages:

- Small dimensions, can easily be placed in the operating room close to the instrument.
- Low cost

Disadvantages:

- Needs a constant airflow of compressed air to create a negative pressure. For that reason, a compressor is required in the operating room.
- Since a constant airflow is used, air is constantly sucked out of the suction chamber. If the suction tip does not seal correctly, the air gets sucked out of the human body instead. Since MIS depends on a pneumoperotineum, the gasses used for this are also sucked out.
- The constant flow of compressed air generates noise.

Use of an automated vacuum pump

A vacuum pump removes air molecules from the suction chamber. This is done using an eccentrically mounted rotary impeller with blades (A). The size of the suction chamber varies with the rotation of the impeller (B). Up top the volume is larger compared to the lower sections. This causes the pressure to drop creating a partial vacuum. The air is drawn in, compressed and expelled through the outlet at the right.

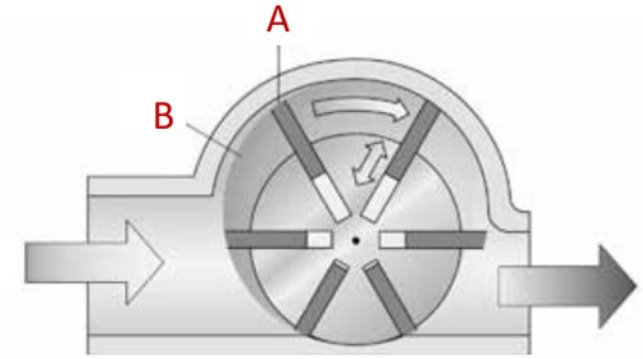

Figure 91: Schematic representation of the working principle of a vacuum pump. Air gets sucked in from the left, travels clockwise inside the suction chamber (B) and leaves the pump through the suction outlet on the right.

Advantages:

- Able to generate high vacuum
- No compressed air is required

Disadvantages:

- Vacuum pumps are large. For that reason it is difficult to place the pump close to the operation table.
- Air and thus the pneumoperitoneum gasses are still sucked away when the suction tip does not seal correctly.

Automated volume expansion mechanism:

An idea that does not depend air that gets sucked away and operates as a closed system is the idea of enlarge the volume of the suction chamber. When this happens, the pressure in the suction chamber and thus the suction tip drops. Because the pressure inside is lower compared to the ambient pressure, a partial vacuum is created. This method is used with octopus suction pads. The octopus uses muscles to enlarge the volume of the chamber (Figure 92). Thus, no air is lost during this process.

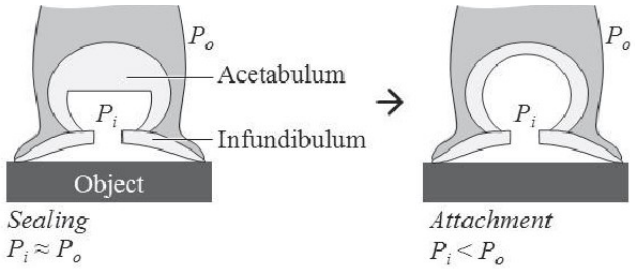

Figure 92: Schematic representation of the working principle of a suction tip of an octopus.

This system can mechanically be build with the use of plungers. This mechanisms works similar compared to the syringes used during this thesis. By pulling the plunger, the volume of the suction chamber enlarges and a negative pressure is created that results in a suction force. Once the suction tip does not seal correctly, the air from the pneumoperitoneum gets sucked into the suction chamber. However, because the system is closed, this air is not exported into ambient air. This minimizes the pressure changes inside the pneumoperitoneum. A motorized system is required that pulls the plungers automatically by only pushing a button to relieve the user from pulling the plungers manually. A mechanical plunger system is represented in Figure 93. A button is placed on the upper handle of the grasper that controls the power output of the system. This motor rotates the gears that translates up and down. A sealed plunger is attached to this system which also translates up and down, enlarging and decreasing the volume of the suction chamber.

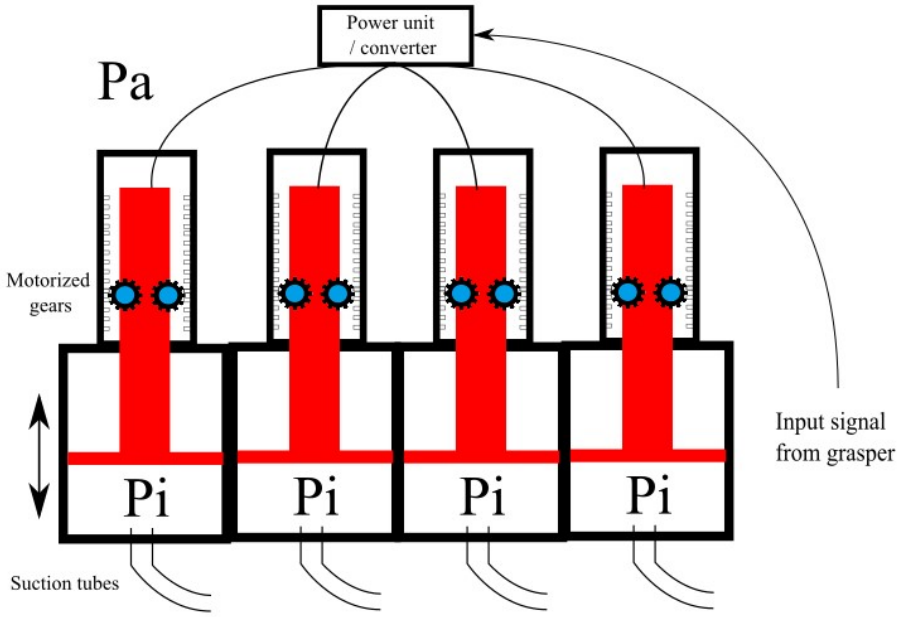

Figure 93: Schematic representation of an example to generate vacuum in a closed system. The suction chamber is able to enlarge in order to reduce the internal pressure (Pi) compared to the atmospheric pressure (Pa).